Adaptive Geometric Numerical Integration of Mechanical Systems

Modin, Klas

2009

Adaptive Geometric Numerical Integration of Mechanical Systems

Klas Modin

LUND UNIVERSITY

Faculty of Engineering
Centre for Mathematical Sciences
Numerical Analysis

Numerical Analysis
Centre for Mathematical Sciences
Lund University
Box 118
SE-221 00 Lund
Sweden

http://www.maths.lth.se/

Doctoral Theses in Mathematical Sciences 2009:3
ISSN 1404-0034

ISBN 978-91-628-7778-1
LUTFNA-1005-2009

Printed in Sweden by MediaTryck, Lund 2009

Acknowledgements

I would like to thank my supervisors Claus Führer and Gustaf Söderlind at Lund University for all the inspiring discussions we have had. I would also like to thank Mathias Persson and Olivier Verdier. Furthermore, I am very grateful for all the help and inspiration I have recieved from Dag Fritzson, Lars–Erik Stacke and the other members of the BEAST–team at SKF. I would also like to thank SKF for support. My friends means a lot to me, as do my relatives. Finally, I am deeply grateful to my wonderful family; mother, father, sister and brother.

Lund, 2009

Klas Modin

Contents

Chapter 1

Introduction

> A journey of a thousand miles must begin with a single step.
>
> *(Lao–Tzu)*

> – You must only concentrate on the next step, the next breath, the next stroke of the broom, and the next, and the next. Nothing else ... That way you enjoy your work, which is important, because then you make a good job of it. And that's how it ought to be.
>
> *(Beppo street–sweeper, "Momo" by Michael Ende)*

1.1 Motivation and Overview

This thesis is about the numerical integration of initial value problems in mechanics. In particular, we are interested in adaptive time-stepping methods for multibody problems in engineering mechanics.

The history of approximate integration of initial value problems is long. Already Newton suggested what is today known as the leap frog method for integrating his equations of celestial motion, see [23]. This was perhaps the first example of a geometric integrator. Almost three centuries later, in the early 1950s, the modern era of numerical computing truly took off. As a consequence, the development and analysis of numerical integration methods for general first order systems of ordinary differential equations (ODEs) was considerably intensified. In 1958 Germund Dahlquist defended his Ph.D. thesis on "Stability and Error Bounds in the Numerical Solution of Ordinary Differential Equations" [13]. Since then Dahlquist's work has had a profound influence. For example, his classic 1963 paper on A–stability [14] is one of the most frequently cited papers in numerical analysis.

In recent years the focal point in the research on numerical integration of ODEs has moved from general-purpose methods toward special-purpose methods. It turns out that by restricting the attention to a specific class of problems (e.g. problems in mechanics), it is possible to achieve more efficient and more accurate integration than with general-purpose methods. The typical approach is to assert that some ge-

ometric structure which is preserved in the exact solution (e.g. symplecticity), also is preserved in the numerical approximation. The following quote is taken from the preface of the influential book on geometric numerical integration by Hairer, Lubich and Wanner [24]:

> The motivation for developing structure preserving algorithms for special classes of problems came independently from such different areas of research as astronomy, molecular dynamics, mechanics, theoretical physics, and numerical analysis as well as from other areas of both applied and pure mathematics. It turned out that preservation of geometric properties of the flow not only produces an improved qualitative behaviour, but also allows for a more accurate long-time integration than with general-purpose methods.

The work in this thesis is part of a collaboration research project between SKF (`www.skf.com`) and the Centre of Mathematical Sciences at Lund University. SKF is developing and maintaining a multibody software package called BEAST (BEAring Simulation Tool), which is used by engineers on a daily basis to analyse the dynamics of rolling bearings and other machine elements under different operating conditions. The mathematical models used in BEAST are complex, mainly due to the necessity of highly accurate force models for describing mechanical impact and contact between bodies. Hence, the right hand side in the resulting ODE is computationally expensive to evaluate. (See Section 1.1.1 below for further information on BEAST.) With this in mind, the industrial need for more efficient integration algorithms, specifically designed for the problem class under study, is easy to understand. The long term objective of the collaboration project is:

- To develop and analyse techniques for special-purpose numerical integration of dynamic multibody problems where impact and contact between bodies occur.

Special-purpose numerical integration methods with structure preserving properties in phase space are designated *geometric integrators* (or sometimes *mechanical integrators* to stress that mechanical problems are considered). This is an active research topic, with a rich theory largely influenced by analytical mechanics. Often the problems under study are conservative, i.e., energy conserving. The typical application fields are celest mechanics, molecular dynamics and theoretical physics. In classical engineering applications, e.g. finite element analysis, rotor dynamics, and in our case rolling bearing simulation, structure preserving integration algorithms have not yet "entered the marked". A main reason is that such problems typically are slightly dissipative, i.e., energy is decreasing slightly during the integration, and originally geometric integrators were considered merely for energy conserving problems. Another is that they typically are non-autonomous due to driving forces. A point made in our work is that structure preserving integration is preferable also for these types

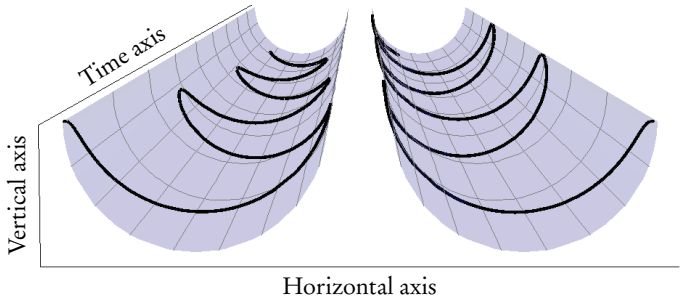

Figure 1.1: Traced position of the non-linear pendulum problem when simulated with a general-purpose integrator (left) and a geometric integrator suitable for the problem (right). The amplitude is decreasing for the general-purpose integrator due to numerical (i.e. non-physical) damping. The geometric integrator gives a physically more correct behaviour, with no numerical damping.

of engineering problems, because the numerical solution will behave in a qualitatively more correct way. Indeed, numerical experiments indicate that geometric integrators are favourable also for dissipative systems, in the sense that energy dissipates at the correct rate, see [33]. The same observations are made in Paper I, where, at least for linear system, this is also analysed theoretically.

To illustrate the benefit of using geometric integrators, consider a non-linear pendulum. The dynamics of the pendulum, when dropped from its horizontal configuration, is simulated using first a general-purpose integrator and then a geometric integrator suitable for the problem.[1] Results are shown in Figure 1.1. The amplitude of the oscillations is decreasing with time for the general-purpose integrator, which is incorrect since the pendulum is undamped. Indeed, after two full periods the energy in the system has decreased to less than 50% of its correct value. In contrast, there is no damping for the geometric integrator, i.e., it gives a physically more correct behaviour. Of course, the results for the general-purpose integrator are improved if the step-size is decreased. However, the point made here is that at the same computational cost the geometric integrator is superior. We return to this problem in Section 2.9.6, where a more detailed study is carried out.

Time-step adaptivity is a well established route to increased efficiency. The idea is to regularise the problem by varying the step-size during the integration process in accordance with the local character of the governing equations. There exist today well written, well tested, well documented solver software for general-purpose state-of-the-art adaptive integration of ODEs, e.g. the SUNDIALS package by Hindmarch

[1] The governing equation is given by $\ddot{\theta} + \sin(\theta) = 0$. Initial conditions are $\theta(0) = \pi/2$ and $\dot{\theta}(0) = 0$. The general-purpose integrator is the implicit Euler method and the geometric integrator is the symplectic Euler method. Both are first order accurate. The step-size $h = 0.1$ is used.

et. al. [27].

During the early development and analysis of geometric integration methods, it was noticed by Gladman et. al. [18] and by Calvo and Sanz-Serna [10] that if standard time-step adaptivity is added to a geometric integrator its "physically correct" behaviour is lost. The reason for this is that the discrete dynamical system constituted by the integrator is altered in such a way that the favourable phase space properties, making it a geometric integrator, are destroyed.

It was soon realised that a feasible path towards adaptive geometric integration is to introduce a time transformation of the original problem, and then to utilise geometric integration of the transformed system, see [52, 49, 21, 29, 9, 44, 12, 28, 42, 8, 26]. This approach, however, is not without difficulties. Indeed, there are still many open problems, in particular on how to construct adaptive geometric integrators that are fully explicit. Much of the work in this thesis is concerned with the problem of combining geometric integration with adaptivity.

We continue with a brief description of the BEAST software, and then the organisation of the thesis and an overview of the contributions.

1.1.1 The BEAST Software Environment

The software environment BEAST, for dynamic multibody simulations and post processing, is developed and maintained at SKF. It is used as a tool for better understanding of the dynamic behaviour of rolling bearings and other machine elements. Contrary to other software packages, such as ADAMS [47] and SIMPACK [19], BEAST is specifically designed for the accurate modelling of contacts between components. Indeed, the mechanical models used are highly complex, and are the result of extensive internal, as well as external, research on tribology [48].

The package essentially contains three parts: a preprocessing tool, a tool for the computation, and a postprocessing tool for the evaluation of the results. The computations are carried out on a high performance computer cluster located at SKF. A typical simulation takes between 5–200 hours to carry out (depending on the number of cluster nodes and complexity of the model).

1.1.2 Composition of Thesis and Contributions

This thesis is compiled out of an integrating part, containing five chapters, and in addition five separate papers. The idea is that the first part should give a concise presentation of the various theories and techniques used in the research, and to make references to the specific papers that contain the actual contributions.

Paper I deals with structure preserving integration of non-autonomous classical engineering problems, such as rotor dynamics. It is shown, both numerically and by backward error analysis, that geometric (structure preserving) integration algorithms

are indeed superior to conventional Runge–Kutta methods. In addition to the specific contributions, this paper can also be seen as a motivation for using geometric integration schemes for engineering problems.

Paper II contains results on how to make the class of variational integrators adaptive for general scaling objectives. Further, a scaling objective suitable for multibody problems with impact force laws is derived. Numerical examples are given.

Paper III concerns the problem of constructing explicit symplectic adaptive integrators. A new approach based on Hamiltonian splitting and Sundman transformations is introduced. Backward error analysis is used to analyze long time energy conservation. Numerical examples validating the energy behavior are given.

Paper IV develops a time transformation technique for Nambu–Poisson systems. Its structural properties are examined. The application in mind is adaptive numerical integration by splitting of Nambu–Poisson Hamiltonians. As an example, a novel integration method for the rigid body problem is presented and analysed.

Paper V sets forth an integration method particularly efficient for multibody problems with contact between bodies. Stability analysis of the proposed method is carried out. Numerical examples are given for a simple test problem and for an industrial rolling bearing problem (using BEAST).

1.2 Preliminaries

Some prerequisites in analytical mechanics and differential geometry are assumed throughout the text. Familiarity with the material in Chapter 1–9 of Arnold's book on classical mechanics [5] is recommended, although parts of it is repeated in Chapter 2 of the thesis. Furthermore, a certain acquaintance with symplectic integrators and their analysis is assumed.

Chapter 2

Dynamics, Geometry and Numerical Integration

> Many modern mathematical theories arose from problems in mechanics and only later acquired that axiomatic-abstract form which makes them so hard to study.
>
> *(V.I. Arnold, [5, p. v])*

> Many of the greatest mathematicians – Euler, Gauss, Lagrange, Riemann, Poincaré, Hilbert, Birkhoff, Atiyah, Arnold, Smale – were well versed in mechanics and many of the greatest advances in mathematics use ideas from mechanics in a fundamental way. Why is it no longer taught as a basic subject to mathematicians?
>
> *(J.E. Marsden, [37, p. iv])*

Summary In this chapter we give a concise exposition of the theory of dynamical systems, phase space geometry and geometric numerical integration. In particular we review some fundamental concepts of analytical mechanics that are needed in order to understand the construction and analysis of geometric methods for mechanical problems. As a general framework for structure preservation, the notion of classifying various types of dynamical systems according to corresponding sub-groups of diffeomorphisms is introduced. This viewpoint is then stressed throughout the remainder of the text.

2.1 Linear Systems

A square matrix $A \in \mathbb{R}^{n\times n}$ determines a linear vector field on $\mathbb{R}^n$ by associating to each $\boldsymbol{x} \in \mathbb{R}^n$ the vector $A\boldsymbol{x} \in \mathbb{R}^n$. Thus, it determines a set of linear (autonomous) ordinary differential equations of the form

$$\frac{\mathrm{d}\boldsymbol{x}}{\mathrm{d}t} = A\boldsymbol{x}\,. \tag{2.1}$$

These are the governing equations for the corresponding linear system: they describe the evolution in time of the coordinate vector $\boldsymbol{x} = (x_1, \ldots, x_n)$. The *flow* of the system is given by the matrix exponential $\exp(tA)$ (see Arnold [6], Chapter 3 for details). That is, the solution curve $\gamma : \mathbb{R} \to \mathbb{R}^n$ with initial data $\boldsymbol{x}$ at $t = 0$ is given by $\gamma(t) = \exp(tA)\boldsymbol{x}$. Recall the following properties of the matrix exponential:

1. $\exp(A)^{-1} = \exp(-A)$,
2. $\dfrac{\mathrm{d}}{\mathrm{d}t}\exp(tA) = A\exp(tA)$,
3. $\exp(\mathrm{diag}(d_1, \ldots, d_n)) = \mathrm{diag}(\mathrm{e}^{d_1}, \ldots, \mathrm{e}^{d_n})$,
4. $\exp((s+t)A) = \exp(sA)\exp(tA)$.

The last property, called the group property, originates from the fact that $\exp(tA)\boldsymbol{x}_0$ is the solution to an autonomous differential equation with initial data $\boldsymbol{x}_0$. Thus, advancing the solution from $\boldsymbol{x}_0$ with time step $s + t$ is the same as first advancing from $\boldsymbol{x}_0$ with time step s landing on $\boldsymbol{x}_1$, and then advancing from there with time step t. This reasoning is valid also for non-linear autonomous initial value problems, which is the basis for generalising the matrix exponential to non-linear vector fields (see Section 2.3).

The problem of constructing a good numerical integration scheme for (2.1) means to find a map $\Phi_h : \mathbb{R}^n \to \mathbb{R}^n$, depending on a step size parameter h, such that Φ_h approximates $\exp(hA) : \mathbb{R}^n \to \mathbb{R}^n$ well. In the classical numerical analysis sense "approximates well" means that $\Phi_h(\boldsymbol{x}) - \exp(hA)\boldsymbol{x}$ should be small, i.e., the *local error* should be small, and that the scheme is stable. In addition, one may also ask that Φ_h shares *structural* properties with $\exp(hA)$. For example that the method is linear, i.e., that it is of the form $\Phi_h(\boldsymbol{x}) = R(hA)\boldsymbol{x}$ for some map $R : \mathbb{R}^{n\times n} \to \mathbb{R}^{n\times n}$ with the property $R(0) = \mathrm{Id}$. Already this allows for some structural analysis of the numerical solution. Indeed, it is well known that the matrix exponential, when seen as a map $\exp : \mathbb{R}^{n\times n} \to \mathbb{R}^{n\times n}$, is invertible in a neighbourhood of the identity, i.e., that the matrix logorithm $\log : \mathbb{R}^{n\times n} \to \mathbb{R}^{n\times n}$ is well defined in a neighbourhood of the identity matrix. Thus, the numerical method may be written $\Phi_h(\boldsymbol{x}) = \exp(\log(R(hA)))\boldsymbol{x}$ (for small enough h). By defining $\tilde{A}_h = \log(R(hA))/h$ we see that Φ_h is the *exact* flow of the *modified* linear differential equation $\dot{\boldsymbol{x}} = \tilde{A}_h\boldsymbol{x}$. That is, $\Phi_h(\boldsymbol{x}) = \exp(h\tilde{A}_h)\boldsymbol{x}$.

This is the notion of *backward error analysis*: to find a modified differential equation whose exact solution reproduces the numerical approximation. It allows for qualitative conclusions about the numerical scheme. For example, from our analysis we can immediately draw the conclusion that structural properties which are true for flows of linear systems also are true for linear numerical methods. Since most numerical integration schemes are linear (e.g. Runge–Kutta methods), this is not a very strong result. As a more delicate example, assume that the matrix A in (2.1) has purely

imaginary eigenvalues. It is then known that the solution is oscillating with constant amplitudes. Thus, for a qualitatively correct behaviour of the numerical solution it is of importance that also the eigenvalues of $\tilde{A}_h$ are purely imaginary. This is certainly not the case in general. For example, not for the explicit and the implicit Euler methods. In order to carry out the analysis in this case one has to find a relation between properties of A and properties of $\exp(hA)$ and then relate this to properties of $R(hA)$. The standard tool at hand, also applicable for non-linear systems, is the theory of Lie groups and Lie algebras which is reviewed in Section 2.4.

2.1.1 Exterior Algebra of a Vector Space

In this section we review some exterior algebra of vector spaces. These results are later generalised to manifolds. For a reference, see Hörmander [30, Sect. 6.2, A1–A2] or Abraham et. al. [2, Ch. 6]. Later on, the results from this section are helpful in the study of Poisson systems and Nambu mechanics.

Let V denote a real vector space of finite dimension n. Its dual space is denoted V^*. Recall that $(\mathsf{V}^*)^*$ is identified with V. Further, the vector space of multilinear alternating maps $(\mathsf{V}^*)^k \to \mathbb{R}$ is denoted $\bigwedge^k \mathsf{V}$. Thus, $\bigwedge^k \mathsf{V}^*$ denotes multilinear alternating maps $\mathsf{V}^k \to \mathbb{R}$. Notice that $\bigwedge^1 \mathsf{V}^* = \mathsf{V}^*$ and $\bigwedge^0 \mathsf{V}^* \equiv \mathbb{R}$. Also, recall that if $\theta \in \bigwedge^k \mathsf{V}^*$ and $\eta \in \bigwedge^l \mathsf{V}^*$, then the exterior product between them is an element $\theta \wedge \eta \in \bigwedge^{k+l} \mathsf{V}^*$. A basis $\varepsilon_1, \ldots, \varepsilon_n$ in V^* induces a basis $\varepsilon_{i_1} \wedge \cdots \wedge \varepsilon_{i_k}$ in $\bigwedge^k \mathsf{V}^*$.

Proposition 2.1.1. *Let W be a real vector space, and let $S : (\mathsf{V}^*)^k \to \mathsf{W}$ be an alternating multilinear map. Then S has a unique representation on the form*

$$S : (\mathsf{V}^*)^k \ni (v_1, \ldots, v_k) \mapsto \tilde{S}(v_1 \wedge \cdots \wedge v_k)$$

where $\tilde{S}$ is a linear map $\bigwedge^k \mathsf{V}^* \to \mathsf{W}$.

Proof. See Hörmander [30]. □

Corollary 2.1.1. *Every linear map $T : \mathsf{V} \to \mathsf{W}$ induces a linear map $\bigwedge^k T : \bigwedge^k \mathsf{V} \to \bigwedge^k \mathsf{W}$.*

Proof. The map

$$\mathsf{V}^k \ni (v_1, \ldots, v_k) \mapsto T(v_1) \wedge \cdots \wedge T(v_k) \in \bigwedge^k \mathsf{W}$$

is alternating and multilinear. Thus, by Proposition 2.1.1 it corresponds to a unique map $\bigwedge^k \mathsf{V} \to \bigwedge^k \mathsf{W}$. □

An immediate consequence of Proposition 2.1.1 is the following generalisation of the fact that $(\mathsf{V}^*)^*$ is identified with V.

Corollary 2.1.2. *The dual space* $(\bigwedge^k \mathsf{V}^*)^*$ *is identified with* $\bigwedge^k \mathsf{V}$.

Proof. An elements $w \in \bigwedge^k \mathsf{V}$ is a multilinear alternating map $(\mathsf{V}^*)^k \to \mathbb{R}$. From Proposition 2.1.1 with $\mathsf{W} = \mathbb{R}$ it follows that w is identified with a unique map $\tilde{w}$: $\bigwedge^k \mathsf{V} \to \mathbb{R}$, i.e., $\tilde{w} \in (\bigwedge^k \mathsf{V}^*)^*$. □

From now on we will not separate $w \in \bigwedge^k \mathsf{V}$ from $\tilde{w} \in (\bigwedge^k \mathsf{V}^*)^*$. Thus, elements in $\bigwedge^k \mathsf{V}^*$ act on elements in $\bigwedge^k \mathsf{V}$ and vice verse by dual pairing, just like elements in V^* act on elements in V.

2.1.2 Non-homogenous and Non-autonomous Systems

A linear system is called non-homogenous if it is of the form

$$\frac{\mathrm{d}\boldsymbol{x}}{\mathrm{d}t} = A\boldsymbol{x} + \boldsymbol{b} \tag{2.2}$$

for some element $\boldsymbol{b} \in \mathbb{R}^n \backslash \{0\}$. Further, a system is called non-autonomous (and non-homogenous) if it is of the form

$$\frac{\mathrm{d}\boldsymbol{x}}{\mathrm{d}t} = A(t)\boldsymbol{x} + \boldsymbol{b}(t) \tag{2.3}$$

where $A : \mathbb{R} \to \mathbb{R}^{n\times n}$ and $\boldsymbol{b} : \mathbb{R} \to \mathbb{R}^n$ are (possibly) time-dependent coefficients of the system.

From a non-autonomous and non-homogenous system of the form (2.3) it is always possible to get an autonomous homogenous system by

$$\frac{\mathrm{d}}{\mathrm{d}t}\begin{pmatrix} \boldsymbol{x} \\ t \\ \xi \end{pmatrix} = \begin{pmatrix} A(t) & 0 & \boldsymbol{b}(t) \\ 0 & 0 & 1 \\ 0 & 0 & 0 \end{pmatrix}\begin{pmatrix} \boldsymbol{x} \\ t \\ \xi \end{pmatrix} \tag{2.4}$$

where ξ is an additional dummy variable with initial value 1.

However, from a structural point of view one has to be careful when doing such transformations. For example, notice that (2.4) is not a linear system. In Paper I a more detailed analysis of non-autonomous systems is carried out in terms of classifying suitable Lie sub-algebras. A typical application for problems of this form is classical rotor dynamics.

2.1.3 Study: Linear Rotor Dynamics

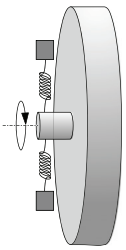

In this study we illustrate the benefit of using geometric integration algorithms for a simple rotor dynamical problem. It consists of a disc attached to a shaft which is rotating with constant angular velocity Ω. The shaft is held by a bearing, which is modelled as a linear spring with stiffness k. (See figure above.) The disc is slightly unbalanced, i.e., its centre of mass does not align with rotational axis. This implies a time-dependent periodic centrifugal force acting on the rotor.

The phase space for this system is given by $\mathbb{R}^4$, with coordinates $\boldsymbol{x} = (q_1, q_2, p_1, p_2)$, which are the horizontal and vertical position of the shaft in a plane perpendicular to the axis of rotation, and their corresponding momenta. The equations of motion are of the form (2.3) with

$$A = \begin{pmatrix} 0 & 0 & m^{-1} & 0 \\ 0 & 0 & 0 & m^{-1} \\ -k & 0 & 0 & 0 \\ 0 & -k & 0 & 0 \end{pmatrix} \qquad \text{and} \qquad \boldsymbol{b}(t) = \varepsilon\Omega^2 \begin{pmatrix} 0 \\ 0 \\ -\cos(\Omega t) \\ \sin(\Omega t) \end{pmatrix}$$

where m is the total mass and ε is the magnitude of the unbalance.

The eigenvalues of A are $\pm \mathrm{i}\sqrt{k/m}$. Thus if Ω is close to a multiple of the eigen frequency $\omega = \sqrt{k/m}$ of the system one can expect resonance effects. From an engineering point of view this corresponds to running the rotor at a rotation speed that triggers the stiffness of the bearing.

As this system is so simple, it is exactly integrable. We compare the exact solution with numerical solutions obtained from four different second order methods; two of them preserve the particular structure of the problem and the other two do not (for details see Paper I).

Method	**Structure preserving?**
Implicit midpoint	Yes
Splitting method	Yes
Implicit extrapolation method	No
Explicit midpoint	No

Results are shown in Figure 2.1. Notice that the geometric methods are superior as they give the qualitatively correct behaviour. This behaviour is explained theoretically in Paper I using backward error analysis.

2.2 Newtonian Mechanics

Newtonian mechanics deals with the dynamics of interacting particles. Each particle "lives" in a four dimensional affine space A^4 equiped with a Galilean space–time structure. Points $\boldsymbol{e} \in \mathsf{A}^4$ are called events. Since A^4 is an affine space, the difference between events is well defined, and the set of all differences between elements in A^4 constitutes the linear space $\mathbb{R}^4$.

The Galilean space–time structure consists of the following:

1. A linear map $\mathsf{t} : \mathbb{R}^4 \to \mathbb{R}$ called time. Two events $\boldsymbol{e}_1$ and $\boldsymbol{e}_2$ are simultaneous if $\mathsf{t}(\boldsymbol{e}_1 - \boldsymbol{e}_2) = 0$.

2. The linear space of simultaneous events, i.e., $\ker(\mathsf{t}) \equiv \mathbb{R}^3$, is equiped with an Euclidean structure $\langle \cdot | \cdot \rangle$. Thus, it is possible to measure the distance between two events in $\ker(\mathsf{t})$. Notice, however, that one cannot measure the distance between non-simultaneous events, unless a coordinate system has been introduced in A^4 as a reference.

Coordinates in A^4 given by $(\boldsymbol{r}, t) = (r^1, r^2, r^3, t)$ are called Galilean coordinates if $\boldsymbol{r}$ are orthogonal coordinates in $\ker(\mathsf{t})$ and $t - \mathsf{t}(\boldsymbol{r}, t) = \text{const}$. A curve in A^4 that appears as the graph of some motion $t \mapsto \boldsymbol{r}(t)$ is called a world line. Thus, the motion of a system of n particles consists of n world lines.

The most fundamental principle in Newtonian mechanics is Newton's equations. These equations describe the motion $t \mapsto (\boldsymbol{r}_1(t), \ldots, \boldsymbol{r}_n(t))$ of n interacting particles. They constitute a system of second order differential equations on the form

$$m_i \frac{\mathrm{d}^2 \boldsymbol{r}_i}{\mathrm{d}t^2} = \boldsymbol{F}_i + \boldsymbol{F}_i^{ext} \,, \qquad i = 1, \ldots, n \,. \tag{2.5}$$

Here, $m_i > 0$ denotes the mass of particle i, $\boldsymbol{F}_i$ the force exerted on particle i by the other particles, and $\boldsymbol{F}_i^{ext}$ the external forces. By introducing coordinates $\boldsymbol{x} = (\boldsymbol{r}_1, \ldots, \boldsymbol{r}_n)$, on the configuration space, i.e., the space of all possible positions the particles can have, the governing equations can be written in the more compact form

$$M \frac{\mathrm{d}^2 \boldsymbol{x}}{\mathrm{d}t^2} = \boldsymbol{F} + \boldsymbol{F}^{ext} \,, \tag{2.6}$$

where $M = \mathrm{diag}(m_1, \ldots, m_n)$, $\boldsymbol{F} = (\boldsymbol{F}_1, \ldots, \boldsymbol{F}_n)$ and $\boldsymbol{F} = (\boldsymbol{F}_1^{ext}, \ldots, \boldsymbol{F}_n^{ext})$.

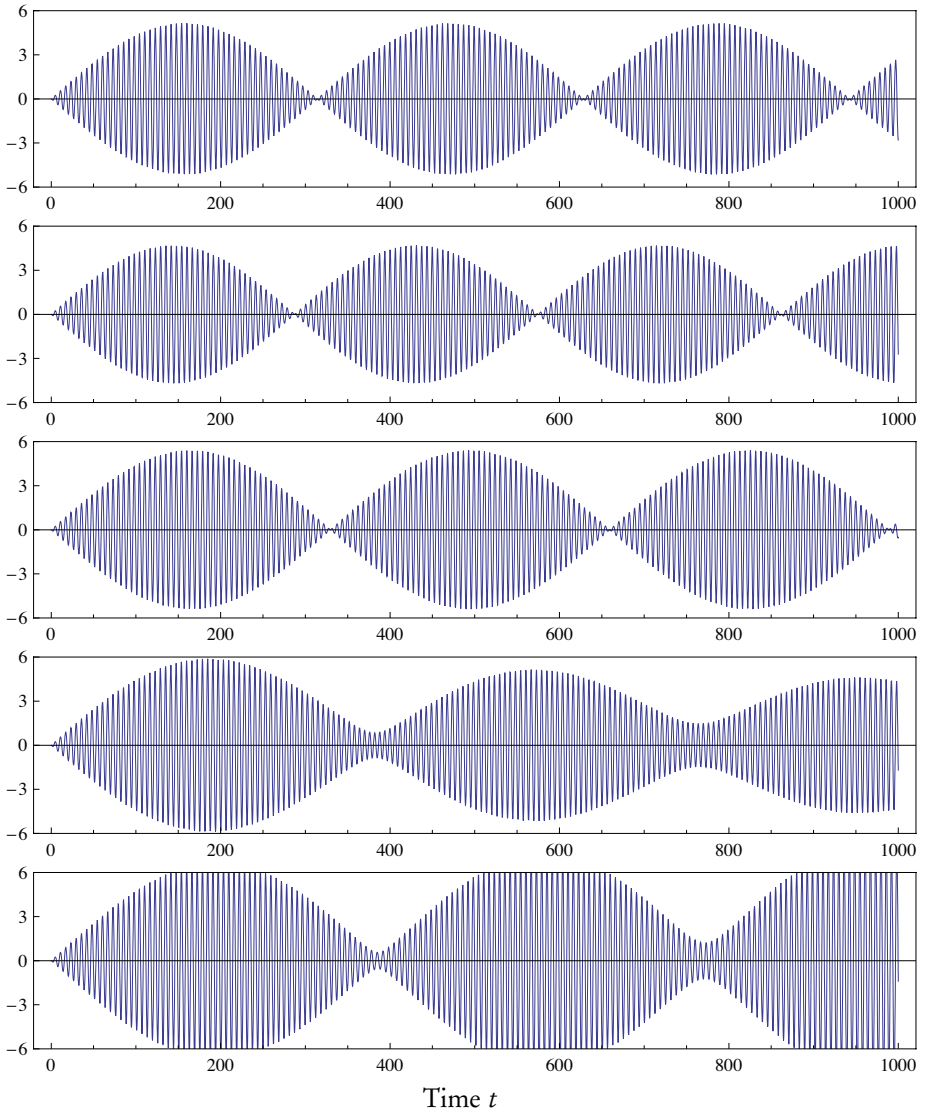

Figure 2.1: Results for q_1 variable for the simple linear rotor study in Section 2.1.3. *From top:* (1) exact solution, (2) implicit midpoint, geometric, (3) Störmer–Verlet, geometric, (4) implicit Runge–Kutta, non-geometric, (5) explicit Runge-Kutta, non-geometric. All methods are second order accurate. Notice the superior qualitative and quantitative behaviour of the geometric methods.

A Galilean transformation is a map $\mathsf{A}^4 \to \mathsf{A}^4$ that preserves the Galilean structure, i.e., affine transformations $(\boldsymbol{r}, t) \mapsto (\boldsymbol{r}', t')$ on the form

$$\begin{aligned} \boldsymbol{r}' &= R\boldsymbol{r} + t\boldsymbol{v} + \boldsymbol{c} \\ t' &= t + c\,, \end{aligned} \tag{2.7}$$

where $c \in \mathbb{R}$, $\boldsymbol{v}, \boldsymbol{c} \in \mathbb{R}^3$ and $R \in \mathrm{O}(3, \mathbb{R})$ is a real orthogonal matrix. The Galilean principle of relativity states that if a system is closed, i.e., if $\boldsymbol{F}^{ext}$ is identically zero, then the equations of motion are preserved under a Galilean transformation of all the world lines. That is, if a Galilean transformation is applied to the world lines of a system then we obtain new world lines of the same system, i.e., the equations of motion (2.5) will have the same form after a Galilean transformation have been applied. This principle imposes restrictions on the force function $\boldsymbol{F}$. For example, due to time–translational invariance any closed Newtonian system must be autonomous.

2.2.1 Conservative Systems

An important type of particle systems are the conservative ones. These are closed Newtonian systems where the forces are derived from a potential function $V : \mathbb{R}^{3n} \to \mathbb{R}$ by

$$\boldsymbol{F} = -\frac{\partial V}{\partial \boldsymbol{x}}\,.$$

Hence, the govering equations have the form

$$M\frac{\mathrm{d}^2\boldsymbol{x}}{\mathrm{d}t^2} = -\frac{\partial V}{\partial \boldsymbol{x}}\,. \tag{2.8}$$

Kinetic energy is a real valued non–negative function of the velocity $\mathrm{d}\boldsymbol{x}/\mathrm{d}t$ of a motion. It is defined by $K(\boldsymbol{v}) = \boldsymbol{v} \cdot M\boldsymbol{v}/2$. The following result holds for any Newtonian potential system:

Theorem 2.2.1 (Conservation of energy)**.** *For any system on the form* (2.8) *the energy*

$$E\Big(\boldsymbol{x}, \frac{\mathrm{d}\boldsymbol{x}}{\mathrm{d}t}\Big) = K\Big(\frac{\mathrm{d}\boldsymbol{x}}{\mathrm{d}t}\Big) + V(\boldsymbol{x})$$

is a first integral.

Proof. Differentiating E with respect to t and then using (2.8) yields

$$\frac{\mathrm{d}}{\mathrm{d}t}E\Big(\boldsymbol{x}, \frac{\mathrm{d}\boldsymbol{x}}{\mathrm{d}t}\Big) = M\frac{\mathrm{d}^2\boldsymbol{x}}{\mathrm{d}t^2}\cdot\frac{\mathrm{d}\boldsymbol{x}}{\mathrm{d}t} + \frac{\partial V}{\partial \boldsymbol{x}}\cdot\frac{\mathrm{d}\boldsymbol{x}}{\mathrm{d}t} = \Big(M\frac{\mathrm{d}^2\boldsymbol{x}}{\mathrm{d}t^2} + \frac{\partial V}{\partial \boldsymbol{x}}\Big)\cdot\frac{\mathrm{d}\boldsymbol{x}}{\mathrm{d}t} = 0\,.$$

□

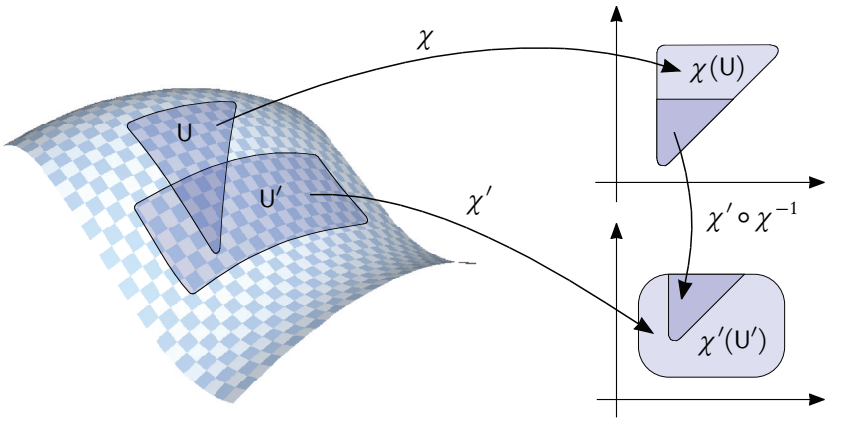

Figure 2.2: Two overlapping coordinate charts for a differentiable manifold. The map $\chi' \circ \chi^{-1} : \chi(U \cap U') \to \chi'(U \cap U')$ between the overlapping parts is smooth.

(The figure is inspired by Abraham and Marsden [1, Figure 1.4-2; p. 32].)

2.3 Manifolds

For many mechanical systems of interest, e.g. rigid bodies and constrained systems, the phase space does not consist of a linear space, but instead of a manifold. Manifolds can be seen as a generalisation of vector spaces. In this section we review the concept of manifolds. Recall the definition:

Definition 2.3.1. A *differentiable manifold* is a set $\mathscr{M}$ equipped with the following structure:

1. A family of *coordinate charts* (called an *atlas*) such that each point $x \in \mathscr{M}$ is represented in a least one chart. A coordinate chart is a subset $U \subset \mathscr{M}$ together with a bijective map $\chi : U \to \chi(U) \subset \mathbb{R}^n$.

2. For every pair of coordinate charts (U, χ) and (U', χ') of the atlas, $\chi(U \cap U')$ and $\chi'(U \cap U')$ are open sets of $\mathbb{R}^n$ and the map

$$\chi' \circ \chi^{-1} : \chi(U \cap U') \to \chi'(U \cap U')$$

is smooth (i.e. C^∞).

(See Figure 2.2 for a visualisation of the concepts.)

Hence, for every point $x \in \mathscr{M}$ there exists a chart (U, χ) in which x is represented by local coordinates $\boldsymbol{x} = (x^1, \ldots, x^n) = \chi(x)$.

Remark 2.3.1. Throughout the rest of the text we sometimes write $\boldsymbol{x} \in \mathscr{M}$ to denote a point in $\mathscr{M}$ represented by local coordinates. This abuse of notation is generally accepted in the literature.

It follows from the definition that transformation between any two different coordinate representations is smooth. This, in turn, implies that the dimension n of $\mathscr{M}$ is well defined. Furthermore, if an assertion about differentiability is made in one coordinate representation, it automatically holds also in other coordinate representations. Hence, ordinary calculus as developed in $\mathbb{R}^n$ may be used also on manifolds.

Remark 2.3.2. Two atlases $\mathfrak{A}$ and $\mathfrak{A}'$ of $\mathscr{M}$ are called equivalent if $\mathfrak{A} \cup \mathfrak{A}'$ is again an atlas of $\mathscr{M}$. The equivalence class of equivalent atlases specifies a *differentiable structure* on $\mathscr{M}$. A differentiable structure may or may not be unique. For example, all differentiable manifolds of dimension 3 or less have unique differentiable structures, whereas S^7 admits 28 differentiable structures, as pointed out by J. Milnor in 1956. Before that it was thought that a topological space admits only one differentiable structure. Throughout the rest of the text, we assume that every manifold is equipped with its *maximal* atlas, i.e., the atlas containing all its equivalent atlases.

Differentiability of maps between manifolds is defined as follows:

Definition 2.3.2. Let $\mathscr{M}$ and $\mathscr{R}$ be two differentiable manifolds of dimension n and m respectively. A map $\varphi : \mathscr{M} \to \mathscr{R}$ is called differentiable at $x \in \mathscr{M}$ if

$$\psi \circ \varphi \circ \chi^{-1} : \mathbb{R}^n \to \mathbb{R}^m$$

is differentiable at $\chi(x)$ for some coordinate charts (U, χ) containing x and (V, ψ) containing $\varphi(x)$.

Notice that the definition of differentiability is independent on the coordinate charts used. Indeed, differentiability is preserved in all coordinate representations, since transformation between coordinates is smooth. The definition of C^r maps follows as in ordinary calculus.

Remark 2.3.3. If $\varphi : \mathscr{M} \to \mathscr{R}$ is smooth and bijective with a smooth inverse, φ is called a *diffeomorphism*. $\mathscr{M}$ and $\mathscr{R}$ are then *diffeomorphic*, meaning that they are essentially the same space (at least when looked upon as manifolds). The set of diffeomorphisms $\mathscr{M} \to \mathscr{M}$ is a group denoted by $\mathrm{Diff}(\mathscr{M})$. Principles in Lagrangian mechanics (see Section 2.6) are invariant with respect to coordinate transformations, and thus, also with respect to this group of transformations. Compare with Newtonian mechanics, where principles are invariant with respect to the Galilean group of transformations.

To specify the equations of motion of a dynamical system it is necessary to consider derivatives of curves in manifolds. The derivative of a curve in a vector space is again

a curve in the vector space. For curves in manifolds this is not the case. Recollect the following concepts, which are needed in order to speak of derivatives of maps between manifolds:

Definition 2.3.3. A *tangent vector* v at a point $x \in \mathscr{M}$ is an equivalence class of differentiable curves $\mathbb{R} \to \mathscr{M}$, where the equivalence relation for two curves γ_1 and γ_2 is given by

$$\gamma_1(0) = \gamma_2(0) = x \quad \text{and} \quad \left.\frac{d(\chi \circ \gamma_1)(t)}{dt}\right|_{t=0} = \left.\frac{d(\chi \circ \gamma_2)(t)}{dt}\right|_{t=0}$$

for some coordinate chart (U, χ) containing x.

Definition 2.3.4. The *tangent space* of $\mathscr{M}$ at x is the set of all tangent vectors at x, and is denoted $T_x\mathscr{M}$. It is a linear space of dimension n, where $\alpha v_1 + \beta v_2$ is defined by the equivalence class of curves γ_3 that fulfils

$$\gamma_3(0) = x \quad \text{and} \quad \left.\frac{d(\chi \circ \gamma_3)(t)}{dt}\right|_{t=0} = \left.\left(\alpha \frac{d(\chi \circ \gamma_1)(t)}{dt} + \beta \frac{d(\chi \circ \gamma_2)(t)}{dt}\right)\right|_{t=0} ,$$

where γ_1 and γ_2 are representatives for v_1 and v_2 respectively.

Definition 2.3.5. The *tangent bundle* of $\mathscr{M}$ is the union of all the tangent spaces, i.e., the set

$$T\mathscr{M} = \bigcup_{x \in \mathscr{M}} T_x\mathscr{M} .$$

An element in $T\mathscr{M}$ which is in $T_x\mathscr{M}$ is denoted v_x. The map $\pi : T\mathscr{M} \to \mathscr{M}$ given by $\pi : v_x \mapsto x$ is called the natural projection. A C^1 map $X : \mathscr{M} \to T\mathscr{M}$ such that $\pi \circ X = \mathrm{Id}$ is called a vector field. Every vector field is intrinsically associated with a differential equation $dx/dt = X(x)$.

Definition 2.3.6. The *cotangent space* of $\mathscr{M}$ at x is the dual space of $T_x\mathscr{M}$, i.e., the space of linear forms on $T_x\mathscr{M}$. It is denoted $T_x^*\mathscr{M}$.

Definition 2.3.7. The *cotangent bundle* of $\mathscr{M}$ is the union of all the cotangent spaces:

$$T^*\mathscr{M} = \bigcup_{x \in \mathscr{M}} T_x^*\mathscr{M} .$$

The natural projection $\pi : T^*\mathscr{M} \to \mathscr{M}$ is defined accordingly.

Remark 2.3.4. The tangent bundle $T\mathscr{M}$ and the cotangent bundle $T^*\mathscr{M}$ both have the structure of differentiable manifolds with dimension $2n$. Below we discuss how coordinate charts in $\mathscr{M}$ naturally introduce coordinate charts in $T\mathscr{M}$ and $T^*\mathscr{M}$.

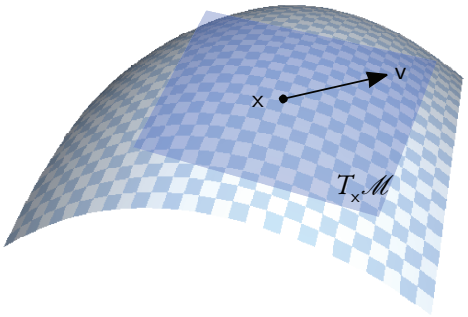

Figure 2.3: A vector v in the tangent space $T_x\mathscr{M}$.

Remark 2.3.5. The set of smooth vector fields on $\mathscr{M}$ is denoted $\mathfrak{X}(\mathscr{M})$. This set is an infinite dimensional vector space (the vector space operations are defined by point-wise operations on each tangent space).

Remark 2.3.6. The set of smooth real valued functions on $\mathscr{M}$ is denoted $\mathcal{F}(\mathscr{M})$. This set is an infinite dimensional vector space (the vector space operations are defined point-wise).

Again, due to the smooth transition between coordinate charts, the definitions above are independent of the choice of coordinate chart (U, χ) (assuming of course that $x \in U$). Hence, if γ is a C^1 curve, its velocity vector at $\gamma(t)$, denoted $\gamma'(t)$ or $(\mathrm{d}\gamma/\mathrm{d}t)(t)$, is a tangent vector in $T_{\gamma(t)}\mathscr{M}$. Consequently, γ' is a map $t \mapsto v_{\gamma(t)} \in T\mathscr{M}$.

Definition 2.3.8. The *derivative* of a differentiable map $\varphi : \mathscr{M} \to \mathscr{R}$ is a map $\varphi_* : T\mathscr{M} \to T\mathscr{R}$ defined by

$$\varphi_*(v_x) = (\varphi \circ \gamma)'(0),$$

where $v_x \in T_x\mathscr{M}$ and γ is a representative for v_x.

Remark 2.3.7. The definition of the derivative is independent of representative γ.

Remark 2.3.8. The derivative φ_* takes a tangent vector in $T_x\mathscr{M}$ and "pushes it forward", by the map φ, to a tangent vector in $T_{\varphi(x)}\mathscr{R}$. Hence, φ_* is sometimes called the push-forward derivative.

Remark 2.3.9. Expressed in coordinates, φ_* constitutes the coordinate representation of φ itself together with the Jacobian, i.e., the matrix valued function that gives the directional derivatives.

A vector in $\mathbb{R}^n$ might be viewed as a first order differential operator that acts on real valued functions on $\mathbb{R}^n$. Hence, the linear space $\mathbb{R}^n$ is equivalent to the linear space of first order differential operators. Pursuing this viewpoint, we may think of $T_x\mathscr{M}$

as the linear space of first order differential operators acting on smooth real valued functions on $\mathscr{M}$ by taking the derivative of them at x in some direction. Indeed, if γ is a representative for $\mathsf{v}_\mathsf{x} \in T_\mathsf{x}\mathscr{M}$ and $f \in \mathcal{F}(\mathscr{M})$, then the differential operator

$$\mathsf{v}_\mathsf{x}[f] = \frac{\mathrm{d}}{\mathrm{d}t}(f \circ \gamma)(t)\bigg|_{t=0}$$

is well defined. Expressed in local coordinates we get

$$\mathsf{v}_\mathsf{x}[f] = \frac{\mathrm{d}}{\mathrm{d}t}(f \circ \chi^{-1} \circ \chi \circ \gamma)(t)\bigg|_{t=0} = \frac{\partial f(\boldsymbol{x})}{\partial \boldsymbol{x}} \cdot \frac{\mathrm{d}(\chi \circ \gamma)(t)}{\mathrm{d}t}\bigg|_{t=0} \tag{2.9}$$

Remark 2.3.10. Notice the abuse of notation: $\partial f(\boldsymbol{x})/\partial \boldsymbol{x}$ really means $\partial(f \circ \chi^{-1})(\boldsymbol{x})/\partial \boldsymbol{x}$.

Remark 2.3.11. The differential operator intrinsically associated with a vector field X on $\mathscr{M}$ (by taking derivatives in the direction of the vector field) is called the *Lie derivative* and is denoted $\pounds_X$. Thus, $\pounds$ acts on $f \in \mathcal{F}(\mathscr{M})$ by $(\pounds_X f)(\mathsf{x}) = X(\mathsf{x})[f]$. The Lie derivative can be extended to act on any geometric object on $\mathscr{M}$ (e.g. vector fields, tensor fields, differential forms) by taking the derivative of them in the direction of X, see [1, Sect. 2.2]

A natural basis in $T_\mathsf{x}\mathscr{M}$ is given by $\partial/\partial x^1, \ldots, \partial/\partial x^n$. Indeed, from (2.9) we see that every element $\mathsf{v} \in T_\mathsf{x}\mathscr{M}$ is uniquely represented in this basis as

$$\mathsf{v}_\mathsf{x} = \sum_{i=1}^{n} \dot{x}^i \frac{\partial}{\partial x^i} = \dot{\boldsymbol{x}} \cdot \frac{\partial}{\partial \boldsymbol{x}},$$

where $\dot{\boldsymbol{x}} = \mathrm{d}(\chi \circ \gamma)(t)/\mathrm{d}t|_{t=0}$. Hence, from coordinates $\boldsymbol{x}$ in $\mathscr{M}$ we have constructed coordinates $\dot{\boldsymbol{x}}$ in $T_\mathsf{x}\mathscr{M}$. Furthermore, the pair $(\boldsymbol{x}, \dot{\boldsymbol{x}})$ constitutes local coordinates for $T\mathscr{M}$, called natural coordinates. The significance of natural coordinates lies in the fact that if the derivative $\gamma'(t)$ of a curve is represented in natural coordinates as $(\boldsymbol{x}(t), \dot{\boldsymbol{x}}(t))$, then it holds that $\mathrm{d}\boldsymbol{x}(t)/\mathrm{d}t = \dot{\boldsymbol{x}}(t)$.

Remark 2.3.12. A basis in a vector space induces a dual basis in the dual vector space. Hence, the basis $\partial/\partial x^1, \ldots, \partial/\partial x^n$ in $T_\mathsf{x}\mathscr{M}$ induces a dual basis $e^1, \ldots, e^n$ in $T^*_\mathsf{x}\mathscr{M}$. Recall that $\langle e^i, \partial/\partial x^j \rangle = \delta_{ij}$. From this we see that $e^i = \mathrm{d}x^i$ (projection of vectors onto the x^i axis). Hence, every element $\mathsf{p} \in T^*_\mathsf{x}\mathscr{M}$ can be written as $\sum_i p_i \, \mathrm{d}x^i = \boldsymbol{p}\,\mathrm{d}\boldsymbol{x}$, and $(\boldsymbol{x}, \boldsymbol{p})$ constitutes a coordinate chart in $T^*\mathscr{M}$. These are called canonical coordinates.

2.3.1 Exterior Algebra of a Manifold

In this section we extend the concept of exterior algebra for vector spaces, reviewed in Section 2.1.1, to manifolds.

Let again $\mathscr{M}$ denote a smooth manifold. The linear spaces $\bigwedge^k T^*_x\mathscr{M}$ are the fibers of a vector bundle $\bigwedge^k T^*\mathscr{M}$. The space of differential k–forms on $\mathscr{M}$ is the space of sections $\mathcal{C}^\infty(\mathscr{M}, \bigwedge^k T^*\mathscr{M})$. It is denoted $\Lambda_k(\mathscr{M})$. Likewise, the space of contravariant totally antisymmetric smooth k–tensor fields, i.e., the space of sections $\mathcal{C}^\infty(\mathscr{M}, \bigwedge^k T\mathscr{M})$, is denoted $\Omega_k(\mathscr{M})$. Notice that $\Lambda_0(\mathscr{M}) = \Omega_0(\mathscr{M}) = \mathcal{F}(\mathscr{M})$, i.e., the space of smooth functions on $\mathscr{M}$. Further, $\Omega_1 = \mathfrak{X}(\mathscr{M})$, which is the space of smooth vector fields on $\mathscr{M}$.

An easily discerned viewpoint for the extension of exterior algebra to manifolds, is to think of the scalar field $\mathbb{R}$ as replaced by the algebra $\mathcal{F}(\mathscr{M})$ of smooth function on $\mathscr{M}$ and the vector space V replace by $\mathfrak{X}(\mathscr{M})$. With this viewpoint, $\Omega_k(\mathscr{M})$ and $\Lambda_k(\mathscr{M})$ are dual to each other, since each pair of corresponding fibers are dual. Thus, all the algebraic operations above for $\bigwedge^k \mathsf{V}^*$ and $\bigwedge^k \mathsf{V}$ carrie over to $\Omega_k(\mathscr{M})$ and $\Lambda_k(\mathscr{M})$. Notice that the pairing between an element in $\Omega_k(\mathscr{M})$ and another in $\Lambda_k(\mathscr{M})$ gives an element in $\mathcal{F}(\mathscr{M})$.

2.4 Lie Groups and Lie Algebras

The theory of Lie groups and Lie algebras is essential in the theory of dynamical systems and geometry of phase space. In our application they appear in several ways:

- For many mechanical systems the configuration space is a Lie group. The most typical example is the rigid body, which evolves on the Lie group of rotations (see Section 2.8).
- Symmetries of mechanical systems, leading to various conservation laws, are described in terms of Lie groups (see Section 2.7).
- In geometric integration, infinite dimensional Lie groups appear as sub-groups of the group of diffeomorphisms on a phase space manifold. This is an important view-point, which is the key to geometric integration and backward error analysis. (see Section 2.5).

Recall that a Lie group is a differentiable manifold $\mathscr{G}$ equipped with a group structure, such that the group multiplication $\mathscr{G} \times \mathscr{G} \ni (g,h) \mapsto gh \in \mathscr{G}$ is smooth. Let e denote the identity element.

A Lie group acts on itself by left and right translation:

$$\begin{aligned} \mathsf{L}_g &: \mathscr{G} \ni h \mapsto gh \in \mathscr{G}\,, \\ \mathsf{R}_g &: \mathscr{G} \ni h \mapsto hg \in \mathscr{G}\,. \end{aligned} \tag{2.10}$$

These maps are, for each g, diffeomorphisms on $\mathscr{G}$. Indeed, the maps

$$\mathsf{L}_g^{-1} = \mathsf{L}_{g^{-1}} \quad \text{and} \quad \mathsf{R}_g^{-1} = \mathsf{R}_{g^{-1}}$$

are smooth, since the group multiplication is smooth. The corresponding push-forward maps L_{g*} and R_{g*} are diffeomorphisms on $T\mathscr{G}$ such that

$$T_h\mathscr{G} \ni \xi_h \mapsto \mathsf{L}_{g*}(\xi_h) \in T_{gh}\mathscr{G}\,,$$

and correspondingly for the right translation.

Each vector $\xi \in T_e\mathscr{G}$ defines a vector field X_ξ on $\mathscr{G}$ by

$$X_\xi(g) = \mathsf{L}_{g*}(\xi)\,. \tag{2.11}$$

Every such vector field is left invariant. That is, the following commutative diagram holds:

$$\begin{array}{ccc} \mathscr{G} & \xrightarrow{\quad\mathsf{L}_g\quad} & \mathscr{G} \\ {\scriptstyle X_\xi}\downarrow & & \downarrow{\scriptstyle X_\xi} \\ T\mathscr{G} & \xrightarrow[\quad\mathsf{L}_{g*}\quad]{} & T\mathscr{G} \end{array} \tag{2.12}$$

The set of left invariant vector fields on $\mathscr{Q}$, denoted $\mathfrak{X}_{\mathsf{L}}(\mathscr{G})$, is a subspace of the linear space $\mathfrak{X}(\mathscr{G})$, i.e., $\mathfrak{X}_{\mathsf{L}}(\mathscr{G})$ is closed under addition and multiplication with scalars. Furthermore, it follows by comparing the upper and the lower branch in the diagram that for any $h \in \mathscr{G}$ the linear space $\mathfrak{X}_{\mathsf{L}}(\mathscr{G})$ is isomorphic to $T_h\mathscr{G}$. Indeed, an isomorphism and its inverse is given by

$$\begin{aligned} &\mathfrak{X}_{\mathsf{L}}(\mathscr{Q}) \ni X \mapsto X(h) \in T_h\mathscr{G}\,,\\ &\quad T_h\mathscr{G} \ni \xi \mapsto X_\xi(\,\cdot\, h^{-1}) \in \mathfrak{X}_{\mathsf{L}}(\mathscr{G})\,. \end{aligned}$$

In particular, we may choose $h = e$, so every left invariant vector field on $\mathscr{G}$ is on the form (2.11) for some unique $\xi \in T_e\mathscr{G}$.

Recall that a vector field on $\mathscr{G}$ acts on the space of smooth real valued functions on $\mathscr{G}$ by differentiation in a direction: $X[f](g) = \langle \mathrm{d}f(g), X(g)\rangle$. Hence, $f \mapsto Y[X[f]]$ acts on f by first differentiating it in the direction of X, and then differentiating once more in the direction of Y, i.e., it is a second order differential operator. However, from the chain rule of differentiation if follows that the "second order parts" of $f \mapsto Y[X[f]]$ and $f \mapsto X[Y[f]]$ are the same, so $f \mapsto Y[X[f]] - X[Y[f]]$ is a first order differential operator. Thus, it corresponds to a new vector field on $\mathscr{G}$ called the commutator of X and Y and denoted $[X, Y]$. The bracket operation

$$[,] : \mathfrak{X}(\mathscr{G}) \times \mathfrak{X}(\mathscr{G}) \to \mathfrak{X}(\mathscr{G}) \tag{2.13}$$

is a bilinear map called the *Poisson bracket of vector fields*, or sometimes the Lie–Jacobi bracket. It fulfils the following properties:

1. skew symmetry, i.e., $[X,Y] = -[Y,X]$;

2. the Jacobi identity, i.e., $[[X,Y],Z] + [[Y,Z],X] + [[Z,X],Y] = 0$.

A vector space equipped with a bilinear map that fulfils 1–2 above is called a *Lie algebra*. Thus, the Poisson bracket of vector fields (2.13) makes $\mathfrak{X}(\mathscr{G})$ into an infinite dimensional Lie algebra.

Remark 2.4.1. The definition of $\mathfrak{X}(\mathscr{G})$ as a Lie algebra is independent of the fact that $\mathscr{G}$ is a Lie group. Indeed, for any manifold $\mathscr{M}$, the commutator makes $\mathfrak{X}(\mathscr{M})$ into a Lie algebra.

Notice that if $X, Y \in \mathfrak{X}_{\mathsf{L}}(\mathscr{G})$ then

$$\mathsf{L}_{g*}\big([X,Y](e)\big) = [X,Y](g)\,,$$

so $[X,Y]$ is left invariant, i.e., it belongs to $\mathfrak{X}_{\mathsf{L}}(\mathscr{G})$. This means that $\mathfrak{X}_{\mathsf{L}}(\mathscr{G})$ is closed under the commutator (2.13), so it is a Lie subalgebra of $\mathfrak{X}(\mathscr{G})$. Furthermore, since $\mathfrak{X}_{\mathsf{L}}(\mathscr{G})$ is isomorphic to $T_e\mathscr{G}$ the commutator also induces a Lie algebra structure in $T_e\mathscr{G}$. Indeed, for $\xi, \eta \in T_e\mathscr{G}$ the bracket operation $[\xi, \eta]$, now called the *Lie bracket*, is defined by

$$[X_\xi, X_\eta] = X_{[\eta,\xi]}\,. \tag{2.14}$$

Definition 2.4.1. Let $\mathscr{G}$ be a Lie group. The vector space $T_e\mathscr{G}$ equipped with the Lie algebra constructed above is called *the Lie algebra of* $\mathscr{G}$ and is denoted $\mathfrak{g}$.

Remark 2.4.2. The concepts developed above are based on left invariant vector fields: the Lie bracket defined by (2.14) is said to be defined by left extension. It is, of course, also possible to use the right invariant vector fields, and define a Lie bracket $[,]^{\mathsf{R}}$ by right extension. The two algebras are then related by $[,] = -[,]^{\mathsf{R}}$.

If $s, t \in \mathbb{R}$ then for any $\xi \in \mathfrak{g}$ we have that $[s\xi, t\xi] = st[\xi,\xi] = 0$, where the last equality is due to skew symmetry of the Lie bracket. From this it follows that the subspace $\xi\mathbb{R} \subset \mathfrak{g}$ is actually a 1–dimensional Lie sub-algebra. It is, in fact, the Lie algebra of the Lie sub-group that is generated by the solution curve through e of the left invariant vector field X_ξ. Indeed, if γ_ξ is a solution curve of X_ξ such that $\gamma_\xi(0) = e$, then $\gamma_\xi(s+t) = \gamma_\xi(s)\gamma_\xi(t)$. $\gamma_\xi(t)$ is called the one parameter subgroup of $\mathscr{G}$ generated by ξ.

Definition 2.4.2. The *exponential map* $\exp : \mathfrak{g} \to \mathscr{G}$ is defined by $\exp(\xi) = \gamma_\xi(1)$.

Since L_{g*} is a linear map, it follows from (2.11) that $sX_\xi = X_{s\xi}$, which implies $\gamma_\xi(t) = \gamma_{t\xi}(1) = \exp(t\xi)$.

Remark 2.4.3. The group of diffeomorphisms Diff($\mathscr{M}$) is an infinite dimensional Lie group. Its Lie algebra is given by $\mathfrak{X}(\mathscr{M})$, with the commutator (2.13) as Lie bracket. Pursuing this viewpoint, it follows that if $X \in \mathfrak{X}(\mathscr{M})$ then the flow of X is given by the exponential map, i.e., $\varphi_X^t = \exp(tX)$.

Remark 2.4.4. The concept of infinite dimensional Lie groups is far more complex than the finite dimensional case, due to the fact that the group operation needs to be smooth. Many assertions made for finite dimensional Lie groups and corresponding Lie algebras are not true in general for infinite dimensional Lie groups. For example, the exponential maps needs not be locally invertible. Throughout the remainder of the text we will formally use infinite dimensional Lie groups in order to classify different classes of maps and corresponding vector fields. We refer to McLachlan and Quispel [40] and Schmid [46] for further issues concerning infinite dimensional Lie groups.

2.5 Geometric Integration and Backward Error Analysis

In this section we review the basic scheme of geometric integration and backward error analysis. Our material is heavily inspired by Reich [45] and by McLachlan and Quispel [40]. See also the references [15, 20, 7, 22] for background.

Throughout this section $\mathscr{M}$ is the phase space manifold. We begin with a rigorous definition of what we mean by "an integrator."

Definition 2.5.1 (One step integrator)**.** A *one step integrator* is a continuous map

$$\Phi : \mathbb{R} \times \mathscr{M} \ni (h, \boldsymbol{x}_0) \mapsto \boldsymbol{x}_1 \in \mathscr{M}$$

such that $\Phi(0, \cdot) = \mathrm{Id}$. The first argument h is called the step size parameter. The numerical solution trajectory corresponding to Φ is the sequence $\boldsymbol{x}_0, \boldsymbol{x}_1, \ldots$ defined recursively by $\boldsymbol{x}_{k+1} = \Phi(h, \boldsymbol{x}_k)$.

Remark 2.5.1. We sometimes write $\Phi_h = \Phi(h, \cdot)$. The parameter h in Φ_h corresponds to t in the exact flow φ_X^t. One important difference, however, is that Φ_h is not (in general) a one parameter group, i.e., $\Phi_h \circ \Phi_s \neq \Phi_{h+s}$. If that had been the case, decreasing the step size parameter would not affect the accuracy of the integration.

Definition 2.5.2 (Order of consistency)**.** The integrator Φ_h is said to be *consistent of order* r relative to a dynamical system with flow φ_X^t for some vector field X on $\mathscr{M}$ if

$$\Phi_h(\boldsymbol{x}) - \varphi_X^h(\boldsymbol{x}) = \mathcal{O}(h^{r+1}) .$$

for each $\boldsymbol{x} \in \mathscr{M}$.

Now to geometry in phase space. A geometric integrator is, somewhat vaguely, a one step integrator that shares some qualitative property with its corresponding exact flow. A standard approach for classifying geometric integrators is obtained through the framework of Lie groups and Lie algebras. Indeed, recall from Section 2.4 that $\mathrm{Diff}(\mathscr{M})$ is an infinite dimensional Lie group corresponding to the infinite dimensional Lie algebra $\mathfrak{X}(\mathscr{M})$. Thus, a natural way to classify integrators is to consider sub-groups of $\mathrm{Diff}(\mathscr{M})$.

Let $\mathfrak{X}_S(\mathscr{M})$ be a sub-algebra of $\mathfrak{X}(\mathscr{M})$, and $\mathrm{Diff}_S(\mathscr{M})$ its corresponding sub-group of $\mathrm{Diff}(\mathscr{M})$. Now, given a vector field $X \in \mathfrak{X}_S(\mathscr{M})$ its flow $t \mapsto \varphi_X^t(\boldsymbol{x})$ is a one-parameter sub-group of $\mathrm{Diff}_S(\mathscr{M})$. In particular, $\varphi_X^t \in \mathrm{Diff}_S(\mathscr{M})$ for each t.

Definition 2.5.3. An integrator Φ_h for $X \in \mathfrak{X}_S(\mathscr{M})$ is called *geometric* (with respect to $\mathrm{Diff}_S(\mathscr{M})$) if it holds that $\Phi_h \in \mathrm{Diff}_S(\mathscr{M})$ for each h small enough.

Remark 2.5.2. Choosing $\mathrm{Diff}_S(\mathscr{M}) = \mathrm{Diff}(\mathscr{M})$ we see that in principle *all* integrators are geometric with respect to $\mathrm{Diff}(\mathscr{M})$. From now on we only denote an integrator geometric when it belongs to a proper sub-group of $\mathrm{Diff}(\mathscr{M})$.

Remark 2.5.3. In Reich [45] the concept of a geometric integrator is somewhat more general in that $\mathfrak{X}_S(\mathscr{M})$ not necessarily needs to be a Lie sub-algebra. This allows also the treatment of reversible integrators within the same framework. (The set of reversible maps does not form a Lie sub-group.) To make the presentation more transparent we consider here only Lie sub-algebras.

The basic principle of backward error analysis is to look for a *modified* vector field $\tilde{X}_h \in \mathfrak{X}_S(\mathscr{M})$ such that $\varphi_{\tilde{X}_h}^h = \Phi_h$. Recall from Section 2.4 that $\varphi_X^t = \exp(tX)$. Thus, the objective is to find $\tilde{X}_h$ such that $\exp(h\tilde{X}_h) = \Phi_h$. A formal solution is given by $\tilde{X}_h = \exp^{-1}(\Phi_h)/h$. Thus, backward error analysis really is the question of whether the exponential map is invertible (at least in a neighbourhood of the identity, i.e., when h is small). If $\mathrm{Diff}_S(\mathscr{M})$ is a finite dimensional sub-group, then it is a well known result that the exponential map is invertible in a neighbourhood of the identity. However, as mentioned above things are much more complex in the infinite dimensional case. In this case one typically have to truncate a power series of $\exp^{-1}(\Phi_h)/h$ about $h = 0$. In conjunction with a result that each term in the power series also is an element in $\mathfrak{X}_S(\mathscr{M})$, this analysis implies that assertions of $\tilde{X}_h$ are valid for exponentially long times, even though the power series does not converge. (See Reich [45] for details.)

By carrying out backward error analysis, i.e., assuring that $\tilde{X}_h \in \mathfrak{X}_S(\mathscr{M})$ (at least formally), one can often draw deep conclusions about Φ_h. For example, if $\mathscr{M}$ is a symplectic manifold (see Section 2.9 below) and $\mathrm{Diff}_S(\mathscr{M})$ is the group of symplectic maps one can assert that $\tilde{X}_h$ is a Hamiltonian vector field. Thus Φ_h will preserve a *modified* Hamiltonian function $\tilde{H}$ (at least locally), which is close to the original Hamiltonian function of X. That is, the Hamiltonian is *nearly* preserved.

2.5.1 Splitting Methods

A simple yet powerful way to derive geometric integrators is by the vector field splitting approach. Let $X \in \mathfrak{X}_S(\mathscr{M})$ and assume that X can be *splitted* into simpler parts $X = X^A + X^B$, where both $X^A, X^B \in \mathfrak{X}_S(\mathscr{M})$. The trick is that X^A and X^B should be explicitly integrable, i.e., that $\varphi^t_{X^A}$ and $\varphi^t_{X^B}$ can be explicitly computed. If that is the case, a geometric integrator for X is obtained by composing $\varphi^t_{X^A}$ and $\varphi^t_{X^B}$ to get a good approximation of φ^t_X. The most popular choice is the *Strang–splitting* obtained by $\Phi_h = \varphi^{h/2}_{X^A} \circ \varphi^h_{X^B} \circ \varphi^{h/2}_{X^A}$. For an extensive treatment of splitting methods and further references see McLachlan and Quispel [41].

2.6 Lagrangian Mechanics

In Newtonian mechanics, the configuration space is a linear space of dimension $3n$, and the basic principle for motion is expressed by Newton's differential equations. For many physical systems, e.g. for constrained systems, this setting is not sufficient and more general configuration spaces must be considered. A particularly important example in our context is the rigid body. Here, the configuration space consists of the set of 3D–rotations, which is not a linear space. We discuss the rigid body and its governing equations further in Section 2.8.

2.6.1 Hamilton's Principle and the Euler–Lagrange Equations

Recall that a Lagrangian mechanical system consists of a configuration space $\mathscr{Q}$, and a Lagrangian function $T\mathscr{M} \times \mathbb{R} \ni (\mathsf{v}_\mathsf{q}, t) \mapsto L(\mathsf{v}_\mathsf{q}, t) \in \mathbb{R}$. Hamilton's principle states that motions of Lagrangian systems extremise the action integral. More precisely, a curve $\gamma : (a, b) \to \mathscr{Q}$ is a motion if

$$A(\gamma) = \int_a^b L\big(\gamma'(t), t\big)\,\mathrm{d}t \tag{2.15}$$

is extremised, i.e., its differential at γ vanishes for variations with fixed endpoints:

$$\langle \mathrm{d}A(\gamma), \delta\gamma \rangle = 0\,, \qquad \forall\ \delta\gamma \in T_\gamma \mathcal{C}(\mathscr{Q}) \tag{2.16}$$

where

$$\mathcal{C}(\mathscr{Q}) = \{C^2 \text{ curves } (a, b) \to \mathscr{Q} \text{ with fixed endpoints } \gamma(a) \text{ and } \gamma(b)\}\,.$$

Remark 2.6.1. The set $\mathcal{C}(\mathscr{Q})$ is an infinite dimensional differentiable manifold. An element $\delta\gamma \in T_\gamma \mathcal{C}(\mathscr{Q})$ is a curve $(a, b) \to T\mathscr{Q}$ such that $\pi \circ \delta\gamma(t) = \gamma(t)$.

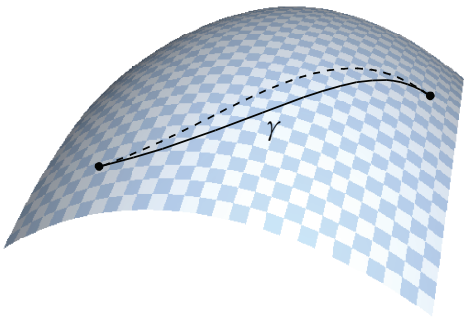

Figure 2.4: Hamilton's principle states that the variation of the action integral vanishes for all variations of motion curves γ with fixed ends.

Hamilton's principle leads to the governing equations. Indeed, differentiation under the integral sign and integration by parts yields a system of second order differential equations for the evolution of $\gamma(t)$ expressed in local coordinates

$$\frac{\mathrm{d}}{\mathrm{d}t}\frac{\partial L}{\partial \dot{\boldsymbol{q}}} - \frac{\partial L}{\partial \boldsymbol{q}} = 0\,. \tag{2.17}$$

These are the well known Euler–Lagrange equations. Together with initial conditions $(\boldsymbol{q}_0, \dot{\boldsymbol{q}}_0)$ they define unique motion curves. The Euler–Lagrange equations have the form (2.17) in all coordinate representations. This reflects the fact that Lagrangian mechanics is invariant under the group $\mathrm{Diff}(\mathscr{Q})$. Compare with Newtonian mechanics, where the basic principles are invariant with respect to the group of Galilean transformations.

The energy of a Lagrangian system, expressed in local coordinates, is given by

$$E = \frac{\partial L}{\partial \dot{\boldsymbol{q}}} \cdot \dot{\boldsymbol{q}} - L\,. \tag{2.18}$$

Taking the derivative of E in the direction of motion curves yields

$$\frac{\mathrm{d}}{\mathrm{d}t}E = \Big(\frac{\mathrm{d}}{\mathrm{d}t}\frac{\partial L}{\partial \dot{\boldsymbol{q}}}\Big) \cdot \dot{\boldsymbol{q}} + \frac{\partial L}{\partial \dot{\boldsymbol{q}}} \cdot \frac{\mathrm{d}\dot{\boldsymbol{q}}}{\mathrm{d}t} - \frac{\partial L}{\partial \boldsymbol{q}} \cdot \frac{\mathrm{d}\boldsymbol{q}}{\mathrm{d}t} - \frac{\partial L}{\partial \dot{\boldsymbol{q}}} \cdot \frac{\mathrm{d}\dot{\boldsymbol{q}}}{\mathrm{d}t} - \frac{\partial L}{\partial t} = -\frac{\partial L}{\partial t}\,,$$

where we in the last equality have used the governing equations (2.17) and the fact that $\mathrm{d}\boldsymbol{q}/\mathrm{d}t = \dot{\boldsymbol{q}}$. Thus, for Lagrangian functions independent of t, i.e., autonomous systems, energy is a first integral.

Remark 2.6.2. Conservation of energy for autonomous Lagrangian system can be understood as a consequence of invariance of the Lagrangian with respect to time translations. We will return to this in Section 2.7.

Example 2.6.1 (Newtonian potential system)**.** A Newtonian potential system is a special case of a Lagrangian system. Here, $\mathscr{Q} = \mathbb{R}^{3n}$ and the Lagrangian function is defined by

$$L(\boldsymbol{x}, \dot{\boldsymbol{x}}) = T(\dot{\boldsymbol{x}}) - V(\boldsymbol{x}) = \frac{\dot{\boldsymbol{x}} \cdot M\dot{\boldsymbol{x}}}{2} - V(\boldsymbol{x}) .$$

The Euler–Lagrange equations (2.17) for this system are exactly Newton's differential equations (2.8).

Remark 2.6.3. As can be seen above, the Lagrangian function for Newtonian potential systems is the difference between kinetic and potential energy. This is in fact a general technique for setting up the equations of motion expressed in general coordinates: derive the potential energy V as a function of $\boldsymbol{q}$ and the kinetic energy T as a function of $\boldsymbol{q}$ and $\dot{\boldsymbol{q}}$, then set $L(\boldsymbol{q}, \dot{\boldsymbol{q}}) = T(\boldsymbol{q}, \dot{\boldsymbol{q}}) - V(\boldsymbol{q})$.

2.6.2 Constrained Systems

Consider a Lagrangian system with configuration space $\mathscr{Q}$ and Lagrangian function L. Often the possible motions are constrained to stay on a submanifold $\mathscr{C} \subset \mathscr{Q}$. Typically, $\mathscr{C} = \boldsymbol{g}^{-1}(0)$ for some vector valued function $\boldsymbol{g} : \mathscr{Q} \to \mathbb{R}^m$.

Example 2.6.2 (Spherical pendulum)**.** Consider a particle of unit mass moving in a gravitational field $\boldsymbol{F}$ which is constant with respect to the coordinates used. This is a Newtonian potential system, so the Lagrangian is given by

$$L(\boldsymbol{r}, \dot{\boldsymbol{r}}) = \frac{|\dot{\boldsymbol{r}}|^2}{2} + \boldsymbol{F} \cdot \boldsymbol{r} .$$

Assume now that the particle is constrained to stay at a constant distance l from the origin. In this case the original configuration space is $\mathscr{Q} = \mathbb{R}^3$ and the constraint manifold is given by $\mathscr{C} = \{\boldsymbol{r} \in \mathscr{Q}; |\boldsymbol{r}| = l\} \equiv S^2$. That is, the particle is constrained to stay on the two–sphere.

The d'Alembert–Lagrange principle states that a motion curve $\gamma : (a, b) \to \mathscr{C}$ of a constrained Lagrangian systems is a conditional extrema of the action A in (2.15). That is, it fulfils

$$\langle \mathrm{d}A(\gamma), \delta\gamma \rangle = 0 , \qquad \forall\ \delta\gamma \in T_\gamma \mathcal{C}(\mathscr{C}) . \tag{2.19}$$

Hence, the action is an extremal under all variations of curves within the constraint manifold $\mathscr{C}$ that vanishes at the endpoints. This, of course, means that the original Euler–Lagrange equations (2.17) will not be fulfilled, i.e.,

$$\boldsymbol{F}^C = \frac{\mathrm{d}}{\mathrm{d}t}\frac{\partial L}{\partial \dot{\boldsymbol{q}}} - \frac{\partial L}{\partial \boldsymbol{q}} \neq 0 .$$

The force vector $\boldsymbol{F}^C$ can be interpreted as a constraint force: it is a force that restricts the motion to $\mathscr{C}$. The principle (2.19) is equivalent to

$$\langle \boldsymbol{F}^C, \xi \rangle = 0 , \qquad \forall\ \xi \in T_q\mathscr{C} . \tag{2.20}$$

Remark 2.6.4. In Lagrangian mechanics a force acting at a point $\mathsf{q} \in \mathscr{Q}$ is a 1–form on $T_{\mathsf{q}}\mathscr{Q}$, i.e., an element in $T^*_{\mathsf{q}}\mathscr{Q}$. The work exerted by a force $\mathsf{F} \in T^*_{\mathsf{q}}\mathscr{Q}$ on a vector $\mathsf{v} \in T_{\mathsf{q}}\mathscr{Q}$ is given by $\langle \mathsf{F}, \mathsf{v} \rangle$.

Remark 2.6.5. The elements ξ in (2.20) are sometimes called virtual variations: it is a variation of the motion in an admissible direction as defined by the tangent space $T_q\mathscr{C}$. Hence, the d'Alembert–Lagrange principle states that the work of the constraint force on any virtual variation is zero.

Remark 2.6.6. To separate the two equivalent formulations (2.19) and (2.20), the former is sometimes referred to as the integral d'Alembert–Lagrange principle and the latter the local d'Alembert–Lagrange principle.

There are different ways of obtaining governing equations for constrained systems. The most straightforward way is to introduce local coordinates $\boldsymbol{c} = (c^1, \ldots, c^{n-m})$ in $\mathscr{C}$ and then set

$$L^C(\boldsymbol{c}, \dot{\boldsymbol{c}}) = L|_{T\mathscr{C}} \left(\boldsymbol{q}(\boldsymbol{c}), \dot{\boldsymbol{q}}(\boldsymbol{c}, \dot{\boldsymbol{c}}) \right) .$$

Obviously, when working in coordinates $\boldsymbol{c}$ the principle (2.19) is Hamilton's principle (2.16) for the system on $\mathscr{C}$ with Lagrangian function L^C. Hence, the governing equations become

$$\frac{\mathrm{d}}{\mathrm{d}t} \frac{\partial L^C}{\partial \dot{\boldsymbol{c}}} - \frac{\partial L^C}{\partial \boldsymbol{c}} = 0 . \tag{2.21}$$

In this approach, the configuration space has been reduced.

Another approach is based on augmenting the configuration space to $\mathscr{Q} \times \mathbb{R}^m$. Coordinates in the augmented configuration space are given by $(\boldsymbol{q}, \boldsymbol{\lambda})$, where $\boldsymbol{\lambda} = (\lambda^1, \ldots, \lambda^m)$ are Lagrangian multipliers. An augmented Lagrangian function on $T(\mathscr{Q} \times \mathbb{R}^m)$ is given by

$$L^{aug}(\boldsymbol{q}, \boldsymbol{\lambda}, \dot{\boldsymbol{q}}, \dot{\boldsymbol{\lambda}}) = L(\boldsymbol{q}, \dot{\boldsymbol{q}}) + \boldsymbol{\lambda} \cdot \boldsymbol{g}(\boldsymbol{q}) .$$

The Lagrange multiplier theorem (see e.g. [1]) asserts that the following two statements are equivalent:

1. $\gamma : (a, b) \to \mathscr{C}$ is a conditional extremal curve of A, i.e., it fulfils (2.19) ;

2. $(\gamma, \boldsymbol{\lambda}) : (a, b) \to \mathscr{Q} \times \mathbb{R}^m$ is an extremal curve of $A^{aug} = \int_a^b L^{aug}$.

Thus, governing equations for the constrained system are obtained from the Euler–Lagrange equations for L^{aug}:

$$\begin{aligned} \frac{\mathrm{d}}{\mathrm{d}t}\frac{\partial L}{\partial \dot{\boldsymbol{q}}} - \frac{\partial L}{\partial \boldsymbol{q}} &= \frac{\partial(\lambda\cdot \boldsymbol{g})}{\partial \boldsymbol{q}} \ , \\ \boldsymbol{g}(\boldsymbol{q}) &= 0 \ . \end{aligned} \tag{2.22}$$

Remark 2.6.7. Notice that $\partial(\lambda\cdot\boldsymbol{g})/\partial\boldsymbol{q}$ is perpendicular to $\mathscr{C}$, i.e., $\langle \partial(\lambda\cdot\boldsymbol{g})/\partial\boldsymbol{q}, \xi\rangle = 0$ for all virtual variations ξ, so the constraint forces are given by $\boldsymbol{F}^C = \partial(\lambda\cdot\boldsymbol{g})/\partial\boldsymbol{q}$.

Example 2.6.3 (Spherical pendulum, continued)**.** Consider Problem 2.6.2. Local coordinates on $\mathscr{C} \equiv S^2$ are given by two spherical coordinates (θ, ϕ). These are related to the original Cartesian coordinates by

$$r^1 = l\cos\theta\sin\phi \ , \quad r^2 = -l\sin\theta\sin\phi \ , \quad r^3 = l\cos\phi \ .$$

Thus, the reduced Lagrangian function is given by

$$L^C(\theta,\phi,\dot\theta,\dot\phi) = L(\boldsymbol{r}(\theta,\phi), \dot{\boldsymbol{r}}(\theta,\phi,\dot\theta,\dot\phi)) \, .$$

The motion of the constrained particle is obtained by solving the Euler–Lagrange equations for L^C. Notice, however, that the equations of motion become rather complicated when expressed in the local coordinates (θ, ϕ). Furthermore, this coordinate chart does not cover all of S^2 (for topological reasons the manifold S^2 can not be equipped with global coordinates, as is well known).

By using the augmented approach instead, i.e., setting

$$L^{aug}(\boldsymbol{r},\lambda,\dot{\boldsymbol{r}},\dot\lambda) = |\dot{\boldsymbol{r}}|^2/2 + \boldsymbol{F}\cdot\boldsymbol{r} + \lambda(|\boldsymbol{r}|^2 - l^2) \, ,$$

the augmented Euler–Lagrange equations become

$$\begin{aligned} \frac{\mathrm{d}^2\boldsymbol{r}}{\mathrm{d}t^2} &= \boldsymbol{F} + 2\lambda\boldsymbol{r} \ , \\ |\boldsymbol{r}|^2 &= l^2 \, . \end{aligned}$$

Notice that $2\lambda\boldsymbol{r}\cdot\dot{\boldsymbol{r}} = 0$ for all $\dot{\boldsymbol{r}} \in T_r\mathscr{C}$, in accordance with the theory.

2.6.3 Dissipative Systems

The original setting of Lagrangian mechanics (the one described above) does not include all Newtonian systems. This is due to the fact that the forces in a Newtonian mechanical system need not be conservative. Indeed, dissipative systems, such as the damped harmonic oscillator, do not fit into standard Lagrangian mechanics. For this reason, an extension is often made in order to cover also dissipative systems.

Definition 2.6.1. A *Lagrangian force field* is a map $\mathsf{F} : T\mathscr{Q} \to T^*\mathscr{Q}$, which is fibre preserving, i.e., $\pi(\mathsf{F}(\mathsf{v}_\mathsf{q})) = \mathsf{q}$ for all $\mathsf{v}_\mathsf{q} \in T\mathscr{Q}$.

In order to be able to study also forced system within the framework of Lagrangian mechanics, Hamilton's principle is modified: given a Lagrangian function L and a Lagrangian force field F every motion curve γ satisfies Hamilton's forced principle

$$\langle \mathrm{d}A(\gamma), \delta\gamma\rangle + \int_a^b \langle \mathsf{F}(\gamma'(t)), \delta\gamma(t)\rangle \,\mathrm{d}t = 0\,, \qquad \forall\ \delta\gamma \in T_\gamma \mathcal{C}(\mathscr{Q})\,. \tag{2.23}$$

By introducing local coordinates and using integration by parts, just as in the ordinary case (2.16), we get the forced Euler–Lagrange equations

$$\frac{\mathrm{d}}{\mathrm{d}t}\frac{\partial L}{\partial \dot{\boldsymbol{q}}} - \frac{\partial L}{\partial \boldsymbol{q}} = \boldsymbol{F}\,. \tag{2.24}$$

A particularly important case is when $\langle \mathsf{F}(\mathsf{v}_\mathsf{q}), \mathsf{v}_\mathsf{q}\rangle < 0$. Such forces are called strongly dissipative (weakly if $<$ is replaced with $\leq$). The name is motivated by the following observation concerning the time evolution of the energy:

$$\frac{\mathrm{d}}{\mathrm{d}t}E = -\frac{\partial L}{\partial t} + \boldsymbol{F}\cdot\dot{\boldsymbol{q}}\,.$$

So, for autonomous systems, a dissipative force asserts that the total energy of the system is decreasing with time.

2.6.4 Variational Integrators

Variational integrators are designed for problems described in the framework of Lagrangian mechanics.

The classical approach for deriving integrators for problems in mechanics is to discretise the governing differential equations with some scheme. In contrast, the key point in variational integrators is to directly discretise Hamilton's principle. This approach leads to the formulation of discrete mechanical systems. For an extensive treatment of the theory, and for an account of its origin, see [39] and references therein. In short, discretisation of the action integral (2.15) leads to the concept of an action sum

$$A_d(\boldsymbol{q}_0, \ldots, \boldsymbol{q}_{n-1}) = \sum_{k=1}^{n-1} L_d(\boldsymbol{q}_{k-1}, \boldsymbol{q}_k)\,, \tag{2.25}$$

where $L_d : \mathscr{Q} \times \mathscr{Q} \to \mathbb{R}$ is an approximation of L called the discrete Lagrangian. Hence, the phase space in the discrete setting is $\mathscr{Q} \times \mathscr{Q}$. An intuitive motivation for this is that two points close to each other correspond approximately to the same information as one point and a velocity vector. The discrete Hamilton's principle states

that if the sequence $(q_0,\dots,q_{n-1})$ is a solution trajectory of the discrete mechanical system then it extremises the action sum:

$$\mathrm{d}A_d(q_0,\dots,q_{n-1})=0\,. \tag{2.26}$$

By differentiation and rearranging of the terms (rearranging corresponds to partial integration in the continuous case), the *discrete Euler-Lagrange* (DEL) equations are obtained:

$$D_2L_d(q_{k-1},q_k)+D_1L_d(q_k,q_{k+1})=0\,, \tag{2.27}$$

where D_1, D_2 denote differentiation with respect to the first and second arguments respectively. The DEL equations define a discrete flow $\Phi:(q_{k-1},q_k)\mapsto(q_k,q_{k+1})$ called a *variational integrator*. Due to the variational approach, Φ possesses qualitative properties similar to those in continuous mechanics. Indeed, Φ can, through the discrete Legendre transform, be given as a symplectic map on $T^*\mathcal{Q}$. Furthermore, if $\mathcal{G}$ is a Lie group with Lie algebra $\mathfrak{g}$, and L_d is invariant under an action $\phi:\mathcal{G}\times\mathcal{Q}\to\mathcal{Q}$, then there is a discrete version of Noether's theorem which states that Φ conserves a corresponding momentum map $I_d:\mathcal{Q}\times\mathcal{Q}\to\mathfrak{g}$.

The construction of L_d from L depends on a discretisation step size parameter h. We write $L_d(q_0,q_1;h)$ when the dependence needs to be expressed. L_d is said to be of order r relative to L if

$$L_d\big(\gamma(0),\gamma(h);h\big)-\int_0^h L\big(\gamma(u),\gamma'(u)\big)\,\mathrm{d}u=\mathcal{O}(h^{r+1}) \tag{2.28}$$

for solution curves γ of the Euler–Lagrange equations (2.17). It is shown in [39, Part 2] that if L_d is of order r relative to L then the order of accuracy of the corresponding variational integrator is r.

If $\mathcal{Q}$ is a linear space, a class of low order discretisations is given by

$$L_d^\alpha(q_0,q_1;h)=hL\Big((1-\alpha)q_0+\alpha q_1,\frac{q_1-q_0}{h}\Big)\,,\quad 0\le\alpha\le 1\,, \tag{2.29}$$

and by the symmetric version

$$L_d^{\mathrm{sym},\alpha}=\frac{1}{2}\big(L_d^\alpha+L_d^{1-\alpha}\big)\,. \tag{2.30}$$

Often L is in the standard form

$$L(q,\dot q)=\frac{1}{2}\dot q\cdot M\dot q-V(q)\,,\qquad q\in\mathcal{Q}=\mathbb{R}^m, \tag{2.31}$$

where M is a mass matrix and V a potential function. In this case, the variational integrator given by (2.29) with $\alpha=1/2$ turns out to be the classical implicit midpoint

rule. Further, the choice $\alpha = 0$ gives the symplectic Euler method. The discretisation (2.30) with $\alpha = 0$ or $\alpha = 1$ gives the Störmer–Verlet method, which is explicit and of second order. See [39, Part 2] for other well known integrators that can be interpreted as variational integrators.

As described above, variational integrators are derived for constant step sizes. In Paper I of the thesis the framework of variational integrators is extended to allow variable steps. The approach is based on time transformation techniques, that are reviewed in the next section.

2.7 Symmetries

In closed Newtonian systems, total linear and angular momentum are preserved. Mathematically, this means that the governing differential equations have first integrals.

The concepts of linear and angular momentum are generalised in analytical mechanics by means of symmetries and momentum maps. Indeed, the celebrated theorem by Noether states that if a Lagrangian function is invariant with respect to a group of transformations, i.e., it has a symmetry, then the system has a corresponding first integral, called a momentum map. The same holds also for Hamiltonian systems. In this section we review these concepts.

2.7.1 Symmetry Groups

A Lie group $\mathcal{G}$ acts on another manifold $\mathcal{Q}$ by actions.

Definition 2.7.1. A *Lie group action* is a map $\phi : \mathcal{G} \times \mathcal{Q} \to \mathcal{Q}$ such that

$$\begin{aligned} \phi(e, \boldsymbol{q}) &= \boldsymbol{q}\,, & &\forall\, \boldsymbol{q} \in \mathcal{Q}\,, \\ \phi(g, \phi(h, \boldsymbol{q})) &= \phi(gh, \boldsymbol{q})\,, & &\forall\, g, h \in \mathcal{G} \text{ and } \boldsymbol{q} \in \mathcal{Q}\,. \end{aligned} \tag{2.32}$$

Sometimes it is convenient to write $\phi^g = \phi(g, \cdot)$. The last equality in (2.32) means that ϕ preserves the group structure: applying ϕ^h and then ϕ^g is the same as applying ϕ^{gh}.

Remark 2.7.1. If $\mathcal{G} = \mathbb{R}$, with addition as group multiplication, then ϕ^s is a flow on $\mathcal{Q}$, i.e., it gives the solution curves to the differential equation with vector field $X(\boldsymbol{q}) = \mathrm{d}\phi^s(\boldsymbol{q})/\mathrm{d}s|_{s=0}$. So, the concept of Lie group actions is a generalisation of the concept of flows of vector fields.

Remark 2.7.2. For every $\xi \in \mathfrak{g}$ a group action induces a vector field $\xi_{\mathcal{Q}}$ on $\mathcal{Q}$ by

$$\xi_{\mathcal{Q}}(\boldsymbol{q}) = \left.\frac{\mathrm{d}}{\mathrm{d}t}\right|_{t=0} \phi^{\exp(t\xi)}(\boldsymbol{q})\,. \tag{2.33}$$

Thus, $\xi_{\mathscr{Q}}$ is the representation on $\mathscr{Q}$ of the left invariant vector field on $\mathscr{G}$ corresponding to $\xi \in \mathfrak{g}$. $\xi_{\mathscr{Q}}$ is called the *infinitesimal generator* of the group action $\phi^{\exp(t\xi)}$.

Invariance of a map with respect to a group action is called a symmetry of the map. For Lagrangian function, a symmetry is given by invariance with respect to the push-forward of an action group on $\mathscr{Q}$, whereas for Hamiltonian functions a symmetry means invariance with respect to a canonical group action on $\mathscr{P}$. More precisely we have the following definitions for Lagrangian functions, Lagrangian force fields, and Hamiltonian functions respectively.

Definition 2.7.2. A group action ϕ on $\mathscr{Q}$ is said to be a *symmetry* of a Lagrangian function L if

$$L \circ \phi_*^g = L\,, \qquad \forall\, g \in \mathscr{G}\,.$$

Definition 2.7.3. A group action ϕ on $\mathscr{Q}$ is said to be a *symmetry* of a Lagrangian force field F if

$$\langle \mathsf{F}(\boldsymbol{q}), \xi_{\mathscr{Q}}(\boldsymbol{q}) \rangle = 0\,, \qquad \forall\, \xi \in \mathfrak{g}\,,\ \boldsymbol{q} \in \mathscr{Q}\,,$$

where $\xi_{\mathscr{Q}}(\boldsymbol{q})$ is given by (2.33).

Definition 2.7.4. Let ϕ be a group action on $\mathscr{P}$, such that for each $g \in \mathscr{G}$, the map ϕ^g is canonical. Then ϕ is called a *symmetry* of a Hamiltonian function H if

$$H \circ \phi^g = H\,, \qquad \forall\, g \in \mathscr{G}\,.$$

If a curve γ fulfils the Euler–Lagrange equations (2.17), and L has a symmetry ϕ, then the curve $t \mapsto \phi^g(\gamma(t))$ also fulfils the same Euler–Lagrange equations. The same holds also for Hamiltonian systems. Thus, a symmetry takes solution curves to solution curves.

2.7.2 Noether's Theorem and Momentum Maps

Consider a Lagrangian system with a symmetry ϕ. From Definition 2.7.2 it follows that

$$\left\langle \left.\frac{\partial (L \circ \phi_*^g)}{\partial g}\right|_{g=e}, \xi \right\rangle = 0\,, \qquad \forall\, \xi \in \mathfrak{g}\,. \tag{2.34}$$

Notice that (2.34) defines a map from the tangent bundle $T\mathscr{Q}$ to the dual of the Lie algebra of $\mathscr{G}$, i.e., a map $T\mathscr{Q} \to \mathfrak{g}^*$. Written in coordinates we have

$$(L \circ \phi_*^g)(\boldsymbol{q}, \dot{\boldsymbol{q}}) = L\Big(\phi^g(\boldsymbol{q}), \frac{\partial \phi^g(\boldsymbol{q})}{\partial \boldsymbol{q}} \dot{\boldsymbol{q}}\Big)\,,$$

so (2.34) reads

$$\frac{\partial L(\boldsymbol{q}, \dot{\boldsymbol{q}})}{\partial \boldsymbol{q}} \left.\frac{\partial \phi^g(\boldsymbol{q})}{\partial g}\right|_{g=e} + \frac{\partial L(\boldsymbol{q}, \dot{\boldsymbol{q}})}{\partial \dot{\boldsymbol{q}}} \left.\frac{\partial^2 \phi^g(\boldsymbol{q})}{\partial g \partial \boldsymbol{q}} \dot{\boldsymbol{q}}\right|_{g=e} = 0$$

where we have used that $\phi^e = \mathrm{Id}$. Now, by using the equations of motion (2.17) and commutation of derivatives ($\partial/\partial g \partial \boldsymbol{q} = \partial/\partial \boldsymbol{q} \partial g$) we get

$$\Big(\frac{\mathrm{d}}{\mathrm{d}t}\frac{\partial L(\boldsymbol{q},\dot{\boldsymbol{q}})}{\partial \dot{\boldsymbol{q}}}\Big)\frac{\partial \phi^g(\boldsymbol{q})}{\partial g}\Big|_{g=e} + \frac{\partial L(\boldsymbol{q},\dot{\boldsymbol{q}})}{\partial \dot{\boldsymbol{q}}}\Big(\frac{\mathrm{d}}{\mathrm{d}t}\frac{\partial \phi^g(\boldsymbol{q})}{\partial g}\Big)\Big|_{g=e} = 0\,.$$

Notice that this is the time derivative of a function on $T\mathcal{Q}$ in the direction of motion curves. Hence the following famous theorem by Emmy Noether:

Theorem 2.7.1 (Noether)**.** *If a Lagrangian system has a symmetry group ϕ, then there is a corresponding first integral given by the* momentum map

$$I : T\mathcal{Q} \ni (\boldsymbol{q},\dot{\boldsymbol{q}}) \mapsto \frac{\partial L(\boldsymbol{q},\dot{\boldsymbol{q}})}{\partial \dot{\boldsymbol{q}}}\frac{\partial \phi^g(\boldsymbol{q})}{\partial g}\Big|_{g=e} \in \mathfrak{g}^*\,.$$

That is, if γ is a motion curve, then $I \circ \gamma' = const.$

Remark 2.7.3. Emmy Noether herself did not consider symmetries under general Lie groups, but under one–parameter groups, i.e., the case where $\mathcal{G} = \mathbb{R}$ with addition as group multiplication. Later on, her result was generalised to the version stated above.

Remark 2.7.4. It is straightforward to check that Noether's theorem also applies to forced Lagrangian systems, where the Lagrangian function and the force field share the same symmetry. Indeed, using the governing equations for such systems we get

$$\frac{\partial L(\boldsymbol{q},\dot{\boldsymbol{q}})}{\partial \boldsymbol{q}}\xi_{\mathcal{Q}}(\boldsymbol{q}) = \Big(\frac{\mathrm{d}}{\mathrm{d}t}\frac{\partial L(\boldsymbol{q},\dot{\boldsymbol{q}})}{\partial \dot{\boldsymbol{q}}} - \boldsymbol{F}(\boldsymbol{q},\dot{\boldsymbol{q}})\Big)\xi_{\mathcal{Q}}(\boldsymbol{q}) = \Big(\frac{\mathrm{d}}{\mathrm{d}t}\frac{\partial L(\boldsymbol{q},\dot{\boldsymbol{q}})}{\partial \dot{\boldsymbol{q}}}\Big)\xi_{\mathcal{Q}}(\boldsymbol{q})\,.$$

So the momentum map I given above is a first integral also for such systems.

Remark 2.7.5. Noether's theorem is easily extended to Hamiltonian systems with canonical symmetry actions. For details on this generalisation, see [38, Ch. 11].

2.8 The Rigid Body

As mentioned previously, the equations of motion of the rigid body are of fundamental importance in this thesis. In this section the governing equations for free and forced rigid bodies are derived. The presentation is inspired by Arnold's fundamental paper [4] where mechanical systems on Lie groups with left invariant Lagrangians are analysed. See also [5, App. 2] and [38, Ch. 15].

Definition 2.8.1. A *reference configuration* of a body is a compact subset $\mathcal{B} \subset \mathbb{R}^3$ such that its boundary is integrable.

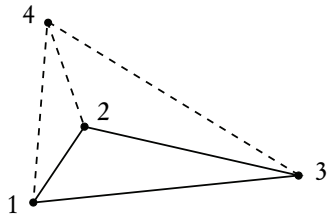

Figure 2.5: The dimension of the configuration space of the particles 1,2,3 constrained to stay at fixed distances from each other is $3\cdot 3-3=6$. If a fourth particle is added to the system, then the number of degrees of freedom increases by 3, but at the same time 3 additional constraints are needed (the dotted lines), so the dimension of the configuration space of the particles $1,2,3,4$ is still 6.

Thus, a rigid body consists of an infinite number of points in $\mathbb{R}^3$. However, there are also an infinite number of constraints on the motion of these points: the distance between any two points is preserved during the motion of the body. Consider a system consisting of 3 particles and assume that the distance between them is fixed. This is a constrained system, where the number of constraints are 3 and the original dimension is $3\cdot 3=9$, so the dimension of the constraint manifold is $9-3=6$. Now, assume we add another particle to the system. The dimension of the system then increases by 3, but at the same time 3 additional constraints are needed in order to "hold the particle fixed" in relation to the other particles. Thus, no matter how many particles we add to the system, the dimension of the constraint manifold will still be 6 (see Figure 2.5). Hence, the dimension of the configuration space for a rigid body is 6. Furthermore, since a motion is a continuous curve, we need only consider connected parts of the constraint manifold, i.e., we rule out reflections. All in all, this implies that the configuration space of a rigid body is the space of translations and rotations, i.e., $\mathscr{Q}=\mathbb{R}^3\times \mathrm{SO}(3)$. A motion curve $t\mapsto (\boldsymbol{r}(t),A(t))$ thus takes a point $\boldsymbol{X}\in\mathcal{B}$ into $A(t)\boldsymbol{X}+\boldsymbol{r}(t)$, as is illustrated in Figure 2.6.

Remark 2.8.1. The space of rotation matrices SO(3) is called the *special orthogonal group*. It is a three dimensional Lie group, with group multiplication given by $(A,B)\mapsto AB$.

Remark 2.8.2. The space of translations and rotations $\mathbb{R}^3\times\mathrm{SO}(3)$ is called the *special Euclidean group* and is denoted SE(3). It is a six dimensional Lie group, with group multiplication given by $((\boldsymbol{a},A),(\boldsymbol{b},B))\mapsto(\boldsymbol{a}+\boldsymbol{b},AB)$.

The free rigid body can be described as a system in Lagrangian mechanics, with configuration space $\mathscr{Q}=\mathrm{SE}(3)$. Its Lagrangian is given by the total kinetic energy

$$L(\boldsymbol{r},A,\dot{\boldsymbol{r}},\dot{A})=\frac{1}{2}\int_{\mathcal{B}}\rho(\boldsymbol{X})|\dot{A}\boldsymbol{X}+\dot{\boldsymbol{r}}|^2\,\mathrm{d}\boldsymbol{X}\,, \tag{2.35}$$

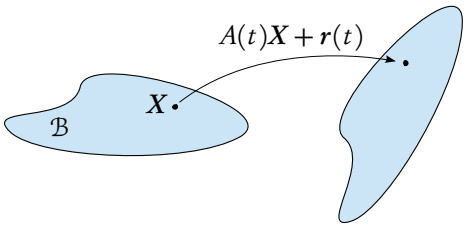

Figure 2.6: A motion curve $t \mapsto (r(t), A(t)) \in \mathbb{R}^3 \times \mathrm{SO}(3)$ of a rigid body takes points $X \in \mathcal{B}$ into points $A(t)X + r(t) \in \mathbb{R}^3$.

where $\rho(X)$ is the mass density of the body at X. If the origin $X = 0$ is placed at the centre of mass of the body we have

$$L(r, A, \dot{r}, \dot{A}) = \frac{1}{2}\int_{\mathcal{B}} \rho(X)\left(|\dot{A}X|^2 + 2\dot{A}X \cdot \dot{r} + |\dot{r}|^2\right) \mathrm{d}X = \frac{1}{2}\int_{\mathcal{B}} \rho(X)|\dot{A}X|^2 \,\mathrm{d}X + \frac{m}{2}|\dot{r}|^2 \,, \quad (2.36)$$

where m is the total mass of the body. Thus, the translational motion and the rotational motion of the centre of mass are decoupled and can be solved for independent of each other.

Remark 2.8.3. Due to translational and rotational invariance, the action $\phi : \mathrm{SE}(3) \times \mathcal{Q} \to \mathcal{Q}$ given by $\phi^{(d,D)}(r, A) = (Dr + d, DA)$ is a symmetry for the rigid body Lagran-gian (2.35). The corresponding conserved momentum map consists of linear and angular momentum.

Remark 2.8.4. Notice that the symmetry group for the free rigid body Lagrangian (2.35) is its entire configuration space, since $\mathcal{Q} = \mathrm{SE}(3)$. As we will see below, this fact can be utilised to reduce the phase space to $\mathfrak{se}(3)$.

By introducing coordinates in $\mathcal{Q}$ (typically three Cartesian coordinates and three angles), the governing equations for the free rigid body are obtained by the Euler–Lagrange equations (2.17). However, since the SO(3) part of the configuration space is a true manifold, i.e., it can not be equipped with a global coordinate system, the resulting differential equations contain singularities, i.e., they are not everywhere well defined. If the motion of the body stays only on a small portion of the phase space, e.g. close to a stable equilibrium, this is not a problem as the singularities then can be avoided. On the other hand, if all types of rotations occur in the motion, this matter has to be taken into account. We give a list of possible options:

1. To reparametrise the SO(3)–part of the configuration space during the integration of the governing equations. That is, to alternate between different coordinate charts.

2. To embed the SO(3)–part in a larger dimensional vector space $\mathbb{R}^n$, where $n > 3$, and consider a corresponding constrained system. For example, by using quaternions SO(3) may be embedded in $\mathbb{R}^4$. An embedding $\eta : \mathrm{SO}(3) \to \mathbb{R}^n$ defines a submanifold $\mathscr{C} \subset \mathbb{R}^n$ to which the solution is constrained. Thus, a constrained Lagrangian system is obtained.

3. To utilise the fact that SO(3) is *parallelisable* (as is any Lie group). That is, its tangent bundle $T\mathrm{SO}(3)$ is isomorphic as a manifold to $\mathrm{SO}(3) \times \mathfrak{so}(3)$. Indeed, an isomorphism is given by left translation of $\dot{A}$ to $\mathfrak{so}(3)$

$$T\mathrm{SO}(3) \ni (A, \dot{A}) \mapsto (A, \mathsf{L}_{A^{-1}*}\dot{A}) = (A, A^{-1}\dot{A}) = (A, \hat{\mathbf{\Omega}}) \in \mathrm{SO}(3) \times \mathfrak{so}(3)\,,$$

where $\hat{\mathbf{\Omega}}$ is the *body angular velocity*, i.e., the angular velocity as seen from the body frame of reference. Alternatively one may use right translation

$$T\mathrm{SO}(3) \ni (A, \dot{A}) \mapsto (A, \mathsf{R}_{A^{-1}*}\dot{A}) = (A, \dot{A}A^{-1}) = (A, \hat{\boldsymbol{\omega}}) \in \mathrm{SO}(3) \times \mathfrak{so}(3)\,,$$

where $\hat{\boldsymbol{\omega}}$ is the *spatial angular velocity*, i.e., the angular velocity as seen from the spatial frame of reference.

Remark 2.8.5. The Lie algebra $\mathfrak{so}(3)$ is the space of skew symmetric 3×3–matrices. Hence, it is isomorphic to $\mathbb{R}^3$. In accordance with standard notation, elements in $\mathfrak{so}(3)$ are denoted with a hat, e.g. $\hat{\boldsymbol{\omega}}$, and its corresponding element in $\mathbb{R}^3$ without the hat, e.g. $\boldsymbol{\omega}$. As $\mathfrak{so}(3)$ is a matrix subgroup its Lie bracket is given by the matrix commutator $[\hat{\boldsymbol{\omega}}_1, \hat{\boldsymbol{\omega}}_2] = \hat{\boldsymbol{\omega}}_1\hat{\boldsymbol{\omega}}_2 - \hat{\boldsymbol{\omega}}_2\hat{\boldsymbol{\omega}}_1$. The corresponding operation in $\mathbb{R}^3$ is given by the cross product $\boldsymbol{\omega}_1 \times \boldsymbol{\omega}_2$. Furthermore, it holds that $\hat{\boldsymbol{\omega}}_1\boldsymbol{\omega}_2 = \boldsymbol{\omega}_1 \times \boldsymbol{\omega}_2$.

Thus, elements $(\boldsymbol{r}, A, \dot{\boldsymbol{r}}, \dot{A})$ in the phase space $T\mathrm{SE}(3)$ are isomorphic to elements $(\boldsymbol{r}, \dot{\boldsymbol{r}}, A, \hat{\mathbf{\Omega}})$ in $\mathbb{R}^3 \times \mathbb{R}^3 \times \mathrm{SO}(3) \times \mathfrak{so}(3)$ (or to elements $(\boldsymbol{r}, \dot{\boldsymbol{r}}, A, \hat{\boldsymbol{\omega}})$). The whole idea with the transformation is that $\mathfrak{so}(3)$ is a vector space, so it can be equipped with global coordinates.

We now have to work out how the governing equations of motion look like expressed in these elements. They will not have the Euler–Lagrange form due to the fact that the relation between A and $\mathbf{\Omega}$ is not that of natural coordinates, i.e., in general $(\mathrm{d}A/\mathrm{d}t)(t) \neq \mathbf{\Omega}(t)$. For simplicity we only consider the rotational term in the Lagrangian, as the translational term is trivial.

Due to the fact that the length of a vector is invariant under rotation and that the Lagrangian is independent of A it holds that

$$L(A, \dot{A}) = L(\dot{A}) = L(B\dot{A})\,, \quad \forall B \in \mathrm{SO}(3).$$

This means that the kinetic rotational energy L is *left invariant*, i.e., it is invariant under left translation L_{B*}. In turn, this implies that $\partial L/\partial \dot{A}$ is left invariant, so that

$$\frac{\partial L}{\partial \dot{A}}(\dot{A}) = \mathsf{L}_{A*}\Big(\frac{\partial L}{\partial \hat{\boldsymbol{\Omega}}}(\hat{\boldsymbol{\Omega}})\Big) = A\frac{\partial L}{\partial \hat{\boldsymbol{\Omega}}}(\hat{\boldsymbol{\Omega}})\,. \tag{2.37}$$

Due to (2.37) the Euler–Lagrange equations expressed in $(A,\hat{\boldsymbol{\Omega}})$ instead of $(A,\dot{A})$ transform according to

$$\begin{aligned}\frac{\mathrm{d}}{\mathrm{d}t}\frac{\partial L}{\partial \dot{A}}(\dot{A}) = \frac{\partial L}{\partial A}(\dot{A}) = 0 \quad &\Longleftrightarrow \quad \frac{\mathrm{d}}{\mathrm{d}t}\Big(A\frac{\partial L}{\partial \hat{\boldsymbol{\Omega}}}(\hat{\boldsymbol{\Omega}})\Big) = 0 \\ &\Longleftrightarrow \quad A\frac{\mathrm{d}}{\mathrm{d}t}\frac{\partial L}{\partial \hat{\boldsymbol{\Omega}}}(\hat{\boldsymbol{\Omega}}) + \dot{A}\frac{\partial L}{\partial \hat{\boldsymbol{\Omega}}}(\hat{\boldsymbol{\Omega}}) = 0\end{aligned} \tag{2.38}$$

Since $\mathsf{L}_{A^{-1}*}$ is an isomorphism $T_A\mathrm{SO}(3) \to \mathfrak{so}(3)$ we may apply it to the rightmost equation in (2.38), which gives

$$\frac{\mathrm{d}}{\mathrm{d}t}\frac{\partial L}{\partial \hat{\boldsymbol{\Omega}}}(\hat{\boldsymbol{\Omega}}) + A^{-1}\dot{A}\frac{\partial L}{\partial \hat{\boldsymbol{\Omega}}}(\hat{\boldsymbol{\Omega}}) = 0 \quad \Longleftrightarrow \quad \frac{\mathrm{d}}{\mathrm{d}t}\frac{\partial L}{\partial \hat{\boldsymbol{\Omega}}}(\hat{\boldsymbol{\Omega}}) + \hat{\boldsymbol{\Omega}}\frac{\partial L}{\partial \hat{\boldsymbol{\Omega}}}(\hat{\boldsymbol{\Omega}}) = 0\,. \tag{2.39}$$

Notice that these equations involve $\hat{\boldsymbol{\Omega}}$, but not A. Thus, the phase space has been *reduced* from $T\mathrm{SO}(3)$ to $\mathfrak{so}(3)$. The equations (2.39) are actually the Euler equations for the free rotating rigid body.

From (2.36) it follows that $L(\hat{\boldsymbol{\Omega}})$ is a positive definite quadratic form on $\mathfrak{so}(3)$. Thus, it holds that $\hat{\mathbb{I}} = \partial L/\partial \hat{\boldsymbol{\Omega}}$ is a linear invertible map $\mathfrak{so}(3) \to \mathfrak{so}(3)^*$ (its corresponding representation on $\mathbb{R}^3$ is a symmetric positive definite matrix denoted $\mathbb{I}$). In fact, it is the *inertia tensor* of the rigid body. Expressed on $\mathbb{R}^3$ (i.e. transforming $\hat{\boldsymbol{\Omega}} \mapsto \boldsymbol{\Omega}$) the governing equations (2.39) become

$$\mathbb{I}\dot{\boldsymbol{\Omega}} = \mathbb{I}\boldsymbol{\Omega} \times \boldsymbol{\Omega}\,. \tag{2.40}$$

This is the classical form of the Euler equations. (We have used that $\hat{\boldsymbol{\Omega}}\frac{\partial L}{\partial \hat{\boldsymbol{\Omega}}}(\hat{\boldsymbol{\Omega}}) = \hat{\boldsymbol{\Omega}}\mathbb{I}\boldsymbol{\Omega} = -\mathbb{I}\boldsymbol{\Omega} \times \boldsymbol{\Omega}$.)

When $\boldsymbol{\Omega}(t)$ has been computed then $A(t)$, i.e., the solution path on SO(3), is reconstructed by the non-autonomous system $\dot{A}(t) = A(t)\hat{\boldsymbol{\Omega}}(t)$.

Remark 2.8.6. From the second step in (2.38) it follows that

$$A\frac{\partial L}{\partial \hat{\boldsymbol{\Omega}}}(\hat{\boldsymbol{\Omega}}) \quad \text{(which expressed on } \mathbb{R}^3 \text{ is } A\mathbb{I}\boldsymbol{\Omega}\text{)}$$

is conserved by the flow. From a Noether's theorem point of view, this is the conserved momentum map (angular momentum) due to invariance of the Lagrangian with respect to left action of the symmetry group SO(3).

Remark 2.8.7. The inertia tensor $\hat{\mathbb{I}}$ induces an Euclidean structure on $\mathfrak{so}(3)$ by

$$(\hat{\omega}_1, \hat{\omega}_2) \mapsto \langle \hat{\mathbb{I}}(\hat{\omega}_1), \hat{\omega}_2 \rangle.$$

In turn, this structure induces a left invariant Riemannian metric on SO(3) by left translation. Arnold pointed out in his ground breaking paper [4] that motions of the free rigid body correspond to geodesics on SO(3) with respect to this induced Riemannian metric. The results were also generalised to infinite dimensional Lie groups, with a particular application to the hydrodynamics of ideal fluids. Arnold's paper was the starting point for the theory of mechanics on Lie groups and topological fluid dynamics, see [34].

So far we have derived the governing equations for the free rigid body. In presence of orientation and translation dependent forces and moments, the full set of governing equations (expressed using $\boldsymbol{\Omega}$) take the form

$$\begin{aligned} m\ddot{\boldsymbol{r}} &= \boldsymbol{F} \\ \mathbb{I}\dot{\boldsymbol{\Omega}} &= \mathbb{I}\boldsymbol{\Omega} \times \boldsymbol{\Omega} + \boldsymbol{M} \\ \dot{A} &= A\hat{\boldsymbol{\Omega}}\,, \end{aligned} \tag{2.41}$$

where $\boldsymbol{F}$ and $\boldsymbol{M}$ are the forces and moments respectively acting on the body. These equations are sometimes called the *Newton–Euler equations*.

2.9 Hamiltonian Mechanics

A Lagrangian mechanical system is defined by a configuration manifold $\mathscr{Q}$ and Lagrangian function. As we have seen, the principles and the form of the governing equations in Lagrangian mechanics are invariant with respect to transformations between local coordinates in $\mathscr{Q}$, or, if one likes, with respect to the group of diffeomorphisms on $\mathscr{Q}$. We are not, however, free to choose any coordinates on $T\mathscr{Q}$: they must be the induced natural coordinates.

In Hamiltonian mechanics, a system is defined by a symplectic manifold $\mathscr{P}$ of dimension $2n$ and a function $H : \mathscr{P} \to \mathbb{R}$ on it. The principles and the governing equations in Hamiltonian mechanics are invariant with respect to all diffeomorphisms on $\mathscr{P}$ that preserve the symplectic structure. Notably, this group of transformations is larger than Diff($\mathscr{Q}$).

2.9.1 Symplectic Manifolds

Definition 2.9.1. A *symplectic manifold* is a differential manifold $\mathscr{P}$ together with a non-degenerate closed differential 2–form Ω on it.

Recall that a differential 2–form on a manifold is a field of skew symmetric bilinear forms (one on each tangent space). That is, to each tangent space $T_z\mathscr{P}$, a bilinear skew symmetric form $\Omega(z) : T_z\mathscr{P} \times T_z\mathscr{P} \to \mathbb{R}$ is associated. Just as an inner product on a vector space E induces an isomorphism $E \to E^*$, the form $\Omega(z)$, being non-degenerate, induces an isomorphism $J(z) : T_z\mathscr{P} \to T_z^*\mathscr{P}$ by

$$J(z) : v \mapsto \Omega(z)[\cdot, v] . \tag{2.42}$$

Definition 2.9.2. A map $\varphi : \mathscr{P} \to \mathscr{P}$ is called *symplectic* (or sometimes *canonical*) if it preserves the symplectic form Ω. That is $\varphi^*\Omega = \Omega$.

Remark 2.9.1. Recall that the pullback $\varphi^*\Omega$ of differential 2–forms is defined by

$$(\varphi^*\Omega)(z)[v, w] = \Omega(\varphi(z))[\varphi_*(z)v, \varphi_*(z)w] .$$

Remark 2.9.2. Recall that a 2–form is called closed if its exterior derivative is zero, i.e., $d\omega = 0$. Due to Poincaré's lemma and Darboux's theorem, the symplectic form being closed implies that locally there exists a coordinate chart in which Ω has the canonical representation $\Omega = d\boldsymbol{q} \wedge d\boldsymbol{p}$. See [38, Ch. 5] for details.

Remark 2.9.3. From standard properties of the determinant one gets

$$\det(J(z)) = \det(J(z)^*) = \det(-J(z)) = (-1)^m \det(J(z)),$$

where m is the dimension of $\mathscr{P}$. Since $J(z)$ is non-singular, this implies that a symplectic manifold must be even dimensional, i.e., $m = 2n$ for some positive integer n.

2.9.2 Hamiltonian Vector Fields and Phase Flows

A Hamiltonian system is defined by a symplectic manifold $\mathscr{P}$, called the phase space, and a real valued function H on it. The corresponding Hamiltonian vector field is given by

$$X_H(z) = J(z)^{-1} dH(z) .$$

Thus, the governing equations of motion for a Hamiltonian system are given by

$$\frac{dz}{dt} = X_H(z) . \tag{2.43}$$

The solution curves as a function of the initial data is a map $\varphi^t : \mathscr{P} \to \mathscr{P}$ called the phase flow. Notice that φ indeed is a flow, i.e., it fulfils $\varphi^t \circ \varphi^s = \varphi^{t+s}$.

Remark 2.9.4. As in Lagrangian mechanics, the Hamiltonian function may also depend explicitly on time t, so non-autonomous systems may also be treated. In the following, we will assume that every system is autonomous. This is not actually a restriction, as the phase space may be extended to include also time and a corresponding momentum variable, see [50]

Recall the following properties of Hamiltonian systems:

1. The Hamiltonian function H is a first integral, i.e., energy is conserved. Indeed,

$$\frac{\mathrm{d}H(\mathsf{z})}{\mathrm{d}t} = \langle \mathrm{d}H(\mathsf{z}), \frac{\mathrm{d}\mathsf{z}}{\mathrm{d}t} \rangle = \langle \mathsf{J}(\mathsf{z}) X_H(\mathsf{z}), X_H(\mathsf{z}) \rangle = \Omega(\mathsf{z})[X_H(\mathsf{z}), X_H(\mathsf{z})] = 0\,,$$

   where the last equality follows from the skew symmetry of Ω. As a straightforward generalisation of this result, notice that any real valued function I on $\mathscr{P}$ such that $\Omega[X_I, X_H] = 0$ is a first integral of (2.43).

2. The phase flow φ^t, with fixed t, is a symplectic map $\mathscr{P} \to \mathscr{P}$. See Arnold [5, Ch. 8] for a proof.

Remark 2.9.5. The symplectic form induces a bilinear map $\mathcal{F}(\mathscr{P}) \times \mathcal{F}(\mathscr{P}) \to \mathcal{F}(\mathscr{P})$ by

$$\{H, I\}(\mathsf{z}) = \Omega(\mathsf{z})[X_I(\mathsf{z}), X_H(\mathsf{z})] \tag{2.44}$$

called the *Poisson bracket*. Thus, I is a first integral of the Hamiltonian system with Hamiltonian function H if and only if $\{H, I\} = 0$.

Due to the fact that Ω is closed, it holds that $X_{\{H,I\}} = [X_H, X_I]$. Thus, the Poisson bracket (2.44) gives $\mathcal{F}(\mathscr{P})$ the structure of a Lie algebra. By the homomorphism $F \mapsto X_F$ this algebra defines a Lie subalgebra of $\mathfrak{X}(\mathscr{P})$ called the Lie algebra of Hamiltonian vector fields and denoted $\mathfrak{X}_\Omega(\mathscr{P})$. The corresponding infinite dimensional sub-group of $\mathrm{Diff}(\mathscr{P})$ is the group of symplectic transformation and is denoted $\mathrm{Diff}_\Omega(\mathscr{P})$.

2.9.3 Canonical Symplectic Structure on $T^*\mathscr{Q}$ and the Legendre Transformation

As mentioned before, coordinates $\boldsymbol{q}$ on $\mathscr{Q}$ induce canonical coordinates $\boldsymbol{z} = (\boldsymbol{q}, \boldsymbol{p})$ on $T^*\mathscr{Q}$, such that an element in $T^*_{\boldsymbol{q}}\mathscr{Q}$ is represented by $\boldsymbol{p}\,\mathrm{d}\boldsymbol{q}$. Now, notice that $\boldsymbol{p}\,\mathrm{d}\boldsymbol{q}$ can be interpreted as a differential 1–form θ on $T^*\mathscr{Q}$, i.e., a field of forms $T_{\boldsymbol{z}}T^*\mathscr{Q} \to \mathbb{R}$. θ is called the canonical 1–form on $T^*\mathscr{Q}$. Its exterior derivative $\omega = \mathrm{d}\theta$ defines a non-degenerate 2–form on $T^*\mathscr{Q}$ called the canonical symplectic form. In coordinates we have that $\omega = \mathrm{d}\boldsymbol{p} \wedge \mathrm{d}\boldsymbol{q}$. Hence, the manifold $T^*\mathscr{Q}$ equipped with ω is a symplectic manifold.

Expressed in canonical coordinates, the map (2.42) is given by

$$J = \begin{pmatrix} 0 & -\mathrm{Id} \\ \mathrm{Id} & 0 \end{pmatrix}\,.$$

Thus, the governing equations $\mathrm{d}\boldsymbol{z}/\mathrm{d}t = \boldsymbol{J}^{-1}\nabla H(\boldsymbol{z})$ expressed in canonical coordinates for a Hamiltonian system on $T^*\mathscr{Q}$ have the form

$$\begin{aligned} \frac{\mathrm{d}\boldsymbol{q}}{\mathrm{d}t} &= \frac{\partial H(\boldsymbol{q},\boldsymbol{p})}{\partial \boldsymbol{p}} \\ \frac{\mathrm{d}\boldsymbol{p}}{\mathrm{d}t} &= -\frac{\partial H(\boldsymbol{q},\boldsymbol{p})}{\partial \boldsymbol{q}} \,. \end{aligned} \tag{2.45}$$

The relation between Lagrangian and Hamiltonian mechanics is via the Legendre transformation, which takes a Lagrangian system on $T\mathscr{Q}$ and transforms it into a Hamiltonian system on $T^*\mathscr{Q}$. It is defined by the map

$$T\mathscr{Q} \ni \mathsf{v}_\mathsf{q} \mapsto \frac{\mathrm{d}}{\mathrm{d}\epsilon}\bigg|_{\epsilon=0} L(\mathsf{v}_\mathsf{q} + \epsilon\,\cdot\,) \in T^*\mathscr{Q} \,. \tag{2.46}$$

In natural coordinates on $T\mathscr{Q}$ and corresponding canonical coordinates on $T^*\mathscr{Q}$ it takes the form

$$(\boldsymbol{q},\dot{\boldsymbol{q}}) \mapsto \Big(\boldsymbol{q}, \frac{\partial L(\boldsymbol{q},\dot{\boldsymbol{q}})}{\partial \dot{\boldsymbol{q}}}\Big) = (\boldsymbol{q},\boldsymbol{p}) \,. \tag{2.47}$$

Notice that this is an isomorphism if and only if $\dot{\boldsymbol{q}}$ is a well defined function of $(\boldsymbol{q},\boldsymbol{p})$, i.e., if $\partial L(\boldsymbol{q},\dot{\boldsymbol{q}})/\partial \dot{\boldsymbol{q}}$ as a map $T_q\mathscr{Q} \to T_q^*\mathscr{Q}$ is invertible. Such Lagrangians are called regular.

For a Lagrangian system with a regular Lagrangian function, the Legendre transformation takes the Euler–Lagrange equations (2.17) into a Hamiltonian system with Hamiltonian function $H(\boldsymbol{q},\boldsymbol{p}) = \boldsymbol{p}\cdot\dot{\boldsymbol{q}} - L(\boldsymbol{q},\dot{\boldsymbol{q}})$.

2.9.4 Poisson Dynamics

Poisson dynamics is a generalisation of symplectic dynamics. The idea is to start directly with Poisson bracket which is not necessarily of the form (2.44). Instead, $\mathscr{P}$ is called a *Poisson manifold* if it is equipped with a Poisson bracket, which is a bilinear map $\{\cdot_1,\cdot_2\} : \mathcal{F}(\mathscr{P}) \times \mathcal{F}(\mathscr{P}) \to \mathcal{F}(\mathscr{P})$ that fulfils

$$\{F,G\} = -\{G,F\} \qquad \text{(skew-symmetry)} \tag{2.48a}$$

$$\{FG,H\} = F\{G,H\} + G\{F,H\} \qquad \text{(Leibniz rule)} \tag{2.48b}$$

$$\{\{F,G\},H\} + \{\{H,F\},G\} + \{\{G,H\},F\} = 0 \qquad \text{(Jacobi identity)} \,. \tag{2.48c}$$

A *Poisson system* is a dynamical system determined by the Poisson structure and a Hamiltonian function $H \in \mathcal{F}(\mathscr{P})$. The equations of motion are given by

$$\frac{\mathrm{d}F}{\mathrm{d}t} = \{H,F\} \,, \quad \forall\, F \in \mathcal{F}(\mathscr{P}) \,. \tag{2.49}$$

The corresponding vector field X_H on $\mathscr{P}$ is defined by $\mathcal{L}_{X_H} F = \{H, F\}$. Using local coordinates $\boldsymbol{z} = (z_1, \ldots, z_n)$, we may write (2.49) in the more conventional form

$$\frac{\mathrm{d}\boldsymbol{z}}{\mathrm{d}t} = X_H(\boldsymbol{z})\,. \tag{2.50}$$

Remark 2.9.6. From (2.49) it follows that $I \in \mathcal{F}(\mathscr{P})$ is a first integral if and only if $\{H, I\} = 0$. Due to skew symmetry, H itself is always a first integral.

Remark 2.9.7. Symplectic manifolds are special cases of Poisson manifolds. Indeed, if Ω is a symplectic form then the corresponding Poisson bracket is given by $\{F, G\}(\boldsymbol{z}) = \Omega(\boldsymbol{z})[\,\mathrm{d}F(\boldsymbol{z}), \mathrm{d}G(\boldsymbol{z})]$.

Example 2.9.1 (Free rigid body, Poisson formulation)**.** It is well known that the Euler equations describing the motion of a free rigid body (see Section 2.8) admits a Poisson structure. Here, the phase space is $\mathscr{P} = \mathbb{R}^3$ with coordinates $\boldsymbol{\Pi} = (\Pi_1, \Pi_2, \Pi_3)$ (corresponding to angular momentum) and bracket given by

$$\{F, G\}(\boldsymbol{\Pi}) = \nabla G(\boldsymbol{\Pi}) \cdot B(\boldsymbol{\Pi}) \cdot \nabla F(\boldsymbol{\Pi})\,,$$

where

$$B(\boldsymbol{\Pi}) = \begin{pmatrix} 0 & \Pi_3 & -\Pi_2 \\ -\Pi_3 & 0 & \Pi_1 \\ \Pi_2 & -\Pi_1 & 0 \end{pmatrix}\,.$$

The Hamiltonian is given by the kinetic energy $H(\boldsymbol{\Pi}) = \sum_i \Pi_i^2 / I_i$, where I_1, I_2, I_3 are the principle moments of inertia. Thus, the governing equations of motion are given by

$$\frac{\mathrm{d}\boldsymbol{\Pi}}{\mathrm{d}t} = X_H(\boldsymbol{\Pi}) = B(\boldsymbol{\Pi}) \cdot \nabla H(\boldsymbol{\Pi})\,. \tag{2.51}$$

(This is exactly equation (2.39) derived above, but expressed in angular momentum $\boldsymbol{\Pi} = \mathbb{I}\boldsymbol{\Omega}$ instead of angular velocity $\boldsymbol{\Omega}$, and assuming a diagonal inertia tensor $\mathbb{I}$.)

Total angular momentum is given by $G(\boldsymbol{\Pi}) = \sum \Pi_i^2$. It is straightforward to check that $\{H, G\} = 0$, so both H and G are first integrals of the system.

2.9.5 Integrators for Hamiltonian problems

It is a well known result by Ge and Marsden [53] that exact conservation of both the symplectic form and energy (i.e. the Hamiltonian function) in a numerical method in general implies that the method actually reproduces the exact flow up to a time reparametrisation. Thus, the field of numerical integration of Hamiltonian problems is naturally divided into two classes: *symplectic integrators* and *energy conserving integrators*. The question of which class that is favourable over the other for different types of problems is currently an active research topic with many open questions.

Of the two classes, the former has been most thoroughly examined. For example, as mentioned above it is known that symplectic methods "nearly" conserves energy for exponentially long time-intervals, which is theoretically explained using backward error analysis, see Hairer et. al. [24]. Further, using KAM theory (cf. Hairer et. al. [24]) on can show that the invariant tori of integrable systems is nearly preserved with symplectic integrators.

2.9.6 Study: Non-linear Pendulum

We now return to the non-linear pendulum problem described in Chapter 1. It can be expressed as a Hamiltonian system on the phase space $\mathscr{P} = \mathbb{R}^2$ with canonical coordinates (q, p). The Hamiltonian function is

$$H(q,p) = \frac{p^2}{2} - \cos(q)\,. \tag{2.52}$$

Recall that the problem (2.52) was integrated with two different methods. One non-geometric method with none of the mentioned geometric properties. One geometric method which is symplectic. Both are first order accurate. A phase diagram of the results are shown in Figure 2.7. Notice that the non-geometric trajectory quickly drifts away from the exact phase curve, whereas the geometric trajectory stays close to it without any sign of drift-off. Geometrically the exact phase diagram of (2.52) is the energy level set $\{(q,p) \in \mathscr{P}\,;\, H(q,p) = H_0\}$. Thus, Figure 2.7 suggests that the energy is nearly conserved for the geometric method, which indeed is the case as is illustrated in Figure 2.8. In addition, we see in Figure 2.9 that the global error grows significantly slower for the geometric method.

The classical approach for error analysis of numerical integrators is based on the propagation of local errors (see e.g. the classical volume [25, Sect. II.3]). However, the estimates used in this type of analysis are not sufficiently elaborate to explain the superiority of the geometric method. Indeed, the Euclidean norm of the local error map $\Phi_h - \varphi^h$ along the trajectory of each of the methods are of the same magnitude, as is shown in Figure 2.10. Thus, the superiority of the geometric integrator must be due to cancellation of local errors. This cancellation is not taken into account in the classical error analysis.

Instead, the right tool to understand the beneficial behaviour of the geometric method is backward error analysis.

Notice that the phase space trajectory $\{z_0, z_1, \ldots\}$ for the geometric method (in Figure 2.7) seems to stay on a perturbed level set, close to the correct level set. This observation suggests that there exists a modified Hamiltonian function $\widetilde{H}$ such that $\{z_0, z_1, \ldots\}$ stays on its level set $\{z \in \mathscr{P}\,;\, \widetilde{H}(z) = H_0\}$. Indeed, since the numerical method is symplectic, i.e., an element in the Lie sub-group $\mathrm{Diff}_\Omega(\mathbb{R}^2)$, it corresponds (at least formally) to the exact integral of a modified vector field $\tilde{X}$ in the corresponding Lie

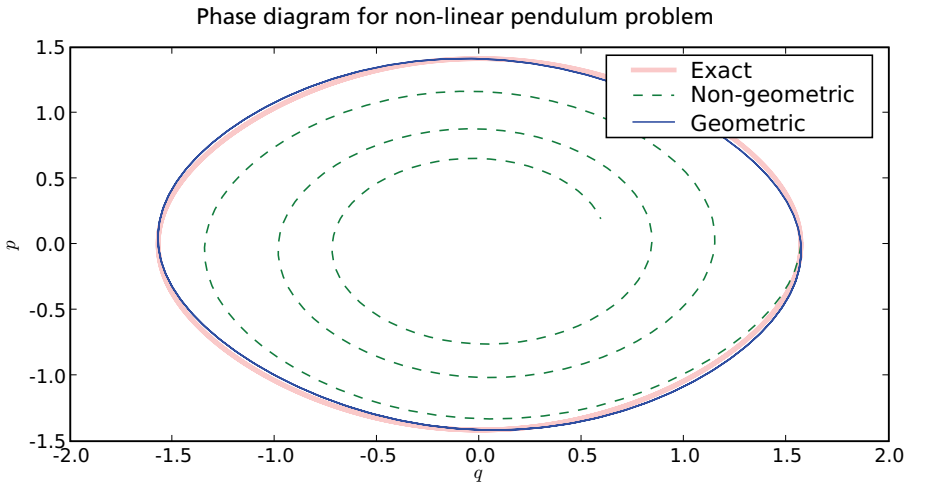

Figure 2.7: Phase diagram for non-linear pendulum problem integrated with a non-geometric and a geometric (symplectic) method. The geometric method stays close to the exact curve, whereas the non-geometric method drifts away from it.

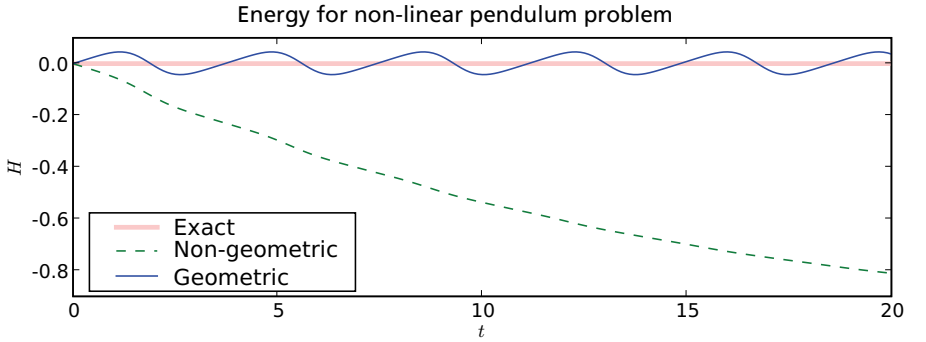

Figure 2.8: Energy behaviour for the non-geometric and geometric method. The geometric method nearly conserves the energy, whereas the non-geometric method introduces a significant numerical dissipation.

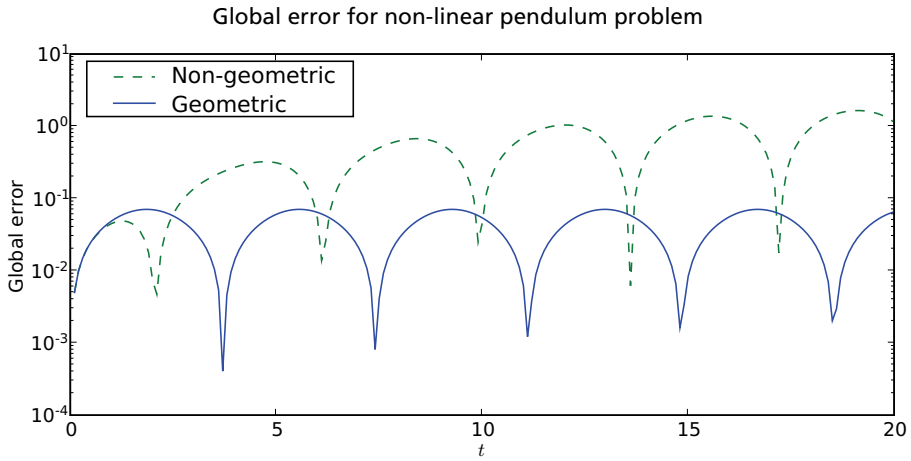

Figure 2.9: Euclidean norm of global error for the non-geometric and geometric method. The error grows considerably slower for the geometric method.

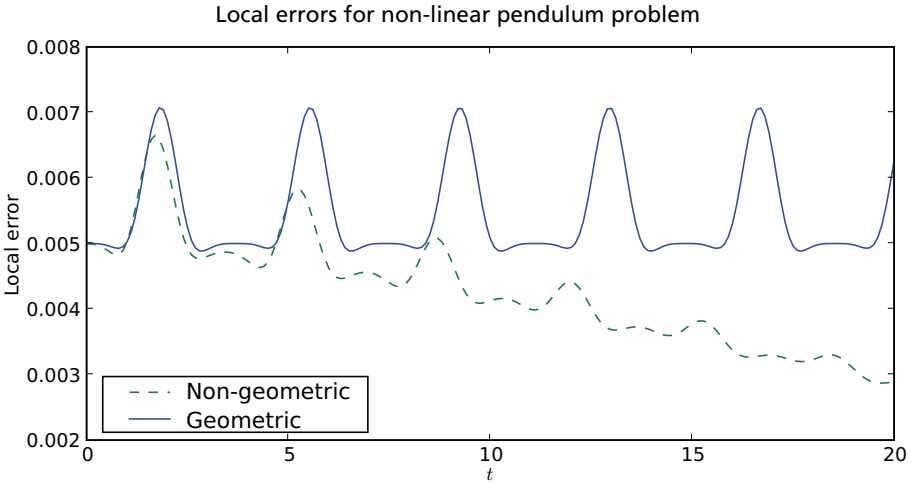

Figure 2.10: Euclidean norm of the local error at each step for the non-geometric and geometric method. The errors are of the same magnitude. Thus, standard numerical error analysis can not be used to explain the superiority of the geometric method.

sub-algebra $\mathfrak{X}_\Omega(\mathbb{R}^2)$. Since $\mathfrak{X}_\Omega(\mathbb{R}^2)$ is isomorphic as a Lie algebra, up to a constant, to $\mathcal{F}(\mathbb{R}^2)$ equipped with the Poisson bracket, it holds that every vector field in $\mathfrak{X}_\Omega(\mathbb{R}^2)$ is generated by corresponding Hamiltonian function in $\mathcal{F}(\mathbb{R}^2)$. Thus, $\dot{z} = \tilde{X}(z)$ is a Hamiltonian system for a modified Hamiltonian function $\tilde{H}$.

2.10 Nambu Mechanics

In Hamiltonian mechanics, the phase space manifold $\mathscr{P}$ is equipped with a Poisson structure, defined by a bracket operation $\{\cdot_1,\cdot_2\} : \mathcal{F}(\mathscr{P}) \times \mathcal{F}(\mathscr{P}) \to \mathcal{F}(\mathscr{P})$ that is skew-symmetric, fulfils the Leibniz rule and the Jacobi identity. Nambu–Poisson mechanics is a generalisation.

Definition 2.10.1. A Nambu–Poisson manifold of order k consists of a smooth manifold $\mathscr{P}$ together with a multilinear map

$$\{\cdot_1,\ldots,\cdot_k\} : \underbrace{\mathcal{F}(\mathscr{P}) \times \ldots \times \mathcal{F}(\mathscr{P})}_{k \text{ times}} \to \mathcal{F}(\mathscr{P})$$

that fulfils:

- total skew-symmetry

$$\{H_1,\ldots,H_k\} = \operatorname{sgn}(\sigma)\{H_{\sigma_1},\ldots,H_{\sigma_k}\} \tag{2.53a}$$

- Leibniz rule

$$\{GH_1,\ldots,H_k\} = G\{H_1,\ldots,H_k\} + H_1\{G,H_2,\ldots,H_k\} \tag{2.53b}$$

- fundamental identity

$$\begin{aligned}\{H_1,\ldots,H_{k-1},\{G_1,\ldots,G_k\}\} = \{\{H_1,\ldots,H_{k-1},G_1\},G_2,\ldots,G_k\} \\ + \{G_1,\{H_1,\ldots,H_{k-1},G_2\},G_3,\ldots,G_k\} + \ldots \\ + \{G_1,\ldots,G_{k-1},\{H_1,\ldots,H_{k-1},G_k\}\}.\end{aligned} \tag{2.53c}$$

Remark 2.10.1. The case $k = 2$ coincides with ordinary Poisson manifolds.

The first two conditions, total skew-symmetry (2.53a) and Leibniz rule (2.53b), are straightforward: they imply that the bracket is of the form

$$\{H_1,\ldots,H_k\} = \eta(\mathrm{d}H_1,\ldots,\mathrm{d}H_k)$$

for some totally skew-symmetric contravariant k–tensor η [51]. The third condition, the fundamental identity (2.53c), is more intricate. The range of possible Poisson–Nambu brackets is heavily restricted by this condition [51].

A Nambu–Poisson system on a Nambu–Poisson manifold of order k is determined by $k-1$ Hamiltonian function $H_1,\dots,H_{k-1}\in\mathcal{F}(\mathscr{P})$. The governing equations are

$$\frac{\mathrm{d}F}{\mathrm{d}t}=\{H_1,\dots,H_{k-1},F\}\qquad\forall\, F\in\mathcal{F}(\mathscr{P}),\tag{2.54a}$$

which may also be written

$$\frac{\mathrm{d}\boldsymbol{x}}{\mathrm{d}t}=X_{H_1,\dots,H_{k-1}}(\boldsymbol{x}),\tag{2.54b}$$

where $X_{H_1,\dots,H_{k-1}}\in\mathfrak{X}(\mathscr{P})$ is defined by $\pounds X_{H_1,\dots,H_{k-1}}F=\{H_1,\dots,H_{k-1},F\}$. The corresponding flow map is denoted $\varphi^t_{H_1,\dots,H_{k-1}}$. Notice that due to skew symmetry of the bracket, all the Hamiltonians $H_1,\dots,H_{k-1}$ are first integrals, which follows from equation (2.54a).

Due to the fundamental identity (2.53c), Nambu–Poisson systems fulfil certain properties which have direct counterparts in Hamiltonian mechanics (the case $k=2$).

Theorem 2.10.1 (Takhtajan [51])**.** *The set of first integrals of system* (2.54) *is closed under the Nambu–Poisson bracket. That is, if $G_1,\dots,G_k$ are first integrals, then $\{G_1,\dots,G_k\}$ is again a first integral.*

Theorem 2.10.2 (Takhtajan [51])**.** *The flow of system* (2.54) *preserves the Nambu–Poisson structure. That is,*

$$\{G_1,\dots,G_k\}\circ\varphi^t_{H_1,\dots,H_{k-1}}=\{G_1\circ\varphi^t_{H_1,\dots,H_{k-1}},\dots,G_n\circ\varphi^t_{H_1,\dots,H_{k-1}}\}\qquad\forall\, G_1,\dots,G_k\in\mathcal{F}(\mathscr{P}),$$

or equivalently

$$\pounds X_{H_1,\dots,H_{k-1}}\eta=0.\tag{2.55}$$

Remark 2.10.2. The set of vector fields that fulfils equation (2.55) is denoted $\mathfrak{X}_\eta(\mathscr{P})$. Clearly $\mathfrak{X}_\eta(\mathscr{P})$ is closed under linear combinations, so it is a sub-space of $\mathfrak{X}(\mathscr{P})$. Further, since $\pounds[X,Y]\eta=\pounds X(\pounds Y\eta)-\pounds Y(\pounds X\eta)$ it is also closed under the commutator. Thus, $\mathfrak{X}_\eta(\mathscr{P})$ is a Lie sub-algebra of $\mathfrak{X}(\mathscr{P})$. Correspondingly, $\mathrm{Diff}_\eta(\mathscr{P})$ denotes the Lie sub-group of $\mathrm{Diff}(\mathscr{P})$ that preserves the Nambu–Poisson structure. An element $\Phi\in\mathrm{Diff}_\eta(\mathscr{P})$ is called an η–map.

Remark 2.10.3. It is important to point out that in general not every $X\in\mathfrak{X}_\eta(\mathscr{P})$ corresponds to a Nambu–Poisson system, i.e., a system of the form of equation (2.54). The reason is that the set of vector fields of the form of equation (2.54) is not closed under linear combinations.

There are also fundamental differences between Hamiltonian and Nambu–Poisson mechanics, i.e., between $k=2$ and $k\geq 3$. In particular there is the following result, conjectured by Chatterjee and Takhtajan [11] and later proved by several authors.

Theorem 2.10.3 ([17], [3], [43], [31], [36]). *A totally skew-symmetric contravariant tensor of order $k \geq 3$ is a Nambu–Poisson tensor if and only if it is locally decomposable about any regular point. That is, about any point $\mathbf{x} \in \mathscr{P}$ such that $\eta(\mathbf{x}) \neq 0$ there exist local coordinates $(x_1, \ldots, x_k, x_{k+1}, \ldots, x_n)$ such that*

$$\eta = \frac{\partial}{\partial x_1} \wedge \cdots \wedge \frac{\partial}{\partial x_k}.$$

Thus, every Nambu–Poisson tensor with $k \geq 3$ is in essence a determinant on a sub-manifold of dimension k. It is not so for Poisson tensors.

In Paper IV geometric Nambu–Poisson integrators are obtained by splitting of each if the Nambu Hamiltonians. Thus, these integrators have the geometric property that they preserve the Nambu–Poisson tensor.

Chapter 3

Time Transformation and Adaptivity

> Time is no law of nature. It is a plan. When you look at it with awareness, or start to touch it, then it starts to disintegrate.
>
> *(Peter Høeg, "Borderliners")*

As mentioned in the introduction, the approach to adaptivity for geometric integrators is to introduce a time reparametrisation $t \longleftrightarrow \tau$ in the governing equations such that the flow ψ^τ of the transformed system corresponds to the flow φ^t of the original system by

$$\psi^\tau(\boldsymbol{z}) = \varphi^{\sigma(\tau,\boldsymbol{z})}(\boldsymbol{z}),$$

where $\sigma(\cdot,\boldsymbol{z})$ is a bijective function $\mathbb{R} \to \mathbb{R}$ for each $\boldsymbol{z}$ in the phase space. The idea is then to discretise the time transformed governing equations with a geometric integrator, using equidistant steps ϵ in τ, which correspond to variable steps in t.

Different types of time transformation techniques have been used. Below we review them, and point out how they are used to construct adaptive integrators with geometric properties.

3.1 Sundman Transformation

Consider a dynamical system with phase space $\mathscr{P}$ on the form

$$\frac{\mathrm{d}\boldsymbol{z}}{\mathrm{d}t} = X(\boldsymbol{z}). \tag{3.1}$$

Reparametrisation of time $t \longleftrightarrow \tau$ in (3.1) yields an equivalent time transformed system

$$\frac{\mathrm{d}\boldsymbol{z}}{\mathrm{d}\tau} = \frac{\mathrm{d}t}{\mathrm{d}\tau} X(\boldsymbol{z}). \tag{3.2}$$

A *Sundman transformation* is a time transformation where the relation between t and τ is determined dynamically by a relation on the form $\mathrm{d}t/\mathrm{d}\tau = G(\boldsymbol{z})$. The real valued function G is called the *scaling function* of the time transformation, and is

assumed to be strictly positive, thus making the transformation bijective. Altogether, a new dynamical system is obtained

$$\frac{\mathrm{d}\boldsymbol{z}}{\mathrm{d}\tau} = G(\boldsymbol{z})X(\boldsymbol{z}) \tag{3.3a}$$

$$\frac{\mathrm{d}t}{\mathrm{d}\tau} = G(\boldsymbol{z})\,. \tag{3.3b}$$

Notice that it is an autonomous system on the extended phase space $\mathscr{P} \times \mathbb{R}$ with coordinates $(\boldsymbol{z}, t)$. Since the original system is autonomous (3.3b) does not alter (3.3a), so dynamics is restricted to $\mathscr{P}$. Reconstruction of time (3.3b) is merely quadrature.

Sundman transformations have been used to construct reversible/symmetric adaptive integrators, see [49, 29, 9]. However, if X is symplectic, the transformed vector field $G(\boldsymbol{z})X(\boldsymbol{z})$ is not in general symplectic. For this reason the Sundman transformation has not been used to construct adaptive symplectic methods. Nevertheless, it turns out that by using a splitting technique in conjunction with Sundman transformations, it is possible to preserve symplecticity. This approach is investigated in Paper II of the thesis.

3.2 Extended Phase Space Approach

In this section we review the explicit reversible step size control suggested in [26].

Consider a reversible Hamiltonian system on a symplectic phase space $\mathscr{P}$ with canonical coordinates $\boldsymbol{z} = (\boldsymbol{q}, \boldsymbol{p})$. That is, a system on the form

$$\frac{\mathrm{d}\boldsymbol{z}}{\mathrm{d}t} = X_H(\boldsymbol{z}) \tag{3.4}$$

where the Hamiltonian vector field X_H is reversible with respect to the linear map

$$R : (\boldsymbol{q}, \boldsymbol{p}) \mapsto (\boldsymbol{q}, -\boldsymbol{p})\,.$$

That is,

$$R \circ X_H = -X_H \circ R.$$

Due to the reversibility condition the flow $\varphi^t_{X_H}$ is reversible, i.e., $R \circ \varphi^t_{X_H} = \varphi^{-t}_{X_H} \circ R$.

In order to obtain time step adaptivity, the time variable t is considered as a function of a new independent variable τ. Let the step density ρ be defined by $\mathrm{d}t/\mathrm{d}\tau = 1/\rho$. Hence we have $\mathrm{d}/\mathrm{d}t = \rho\,\mathrm{d}/\mathrm{d}\tau$. The idea is now to determine the step size control by specifying an equation on the form $\mathrm{d}\rho/\mathrm{d}\tau = \xi(\boldsymbol{z})$ for the step density. Here, $\xi : \mathscr{P} \to \mathbb{R}$ determines the dynamics of the step size control. Substituting

$\mathrm{d}/\mathrm{d}t = \rho\,\mathrm{d}/\mathrm{d}\tau$ in (3.4) and adding the equation for ρ we end up with an augmented dynamical system

$$\begin{aligned}\frac{\mathrm{d}\boldsymbol{z}}{\mathrm{d}\tau} &= X_H(\boldsymbol{z})/\rho \\ \frac{\mathrm{d}\rho}{\mathrm{d}\tau} &= \xi(\boldsymbol{z})\end{aligned} \tag{3.5}$$

on the extended phase space $\bar{\mathscr{P}} = \mathscr{P} \times \mathbb{R}$ with coordinates $\bar{\boldsymbol{z}} = (\boldsymbol{z}, \rho)$. Just as for Sundman transformations, notice that the time variable t does not alter the dynamics of (3.5); it is recovered by a mere quadrature process. If ξ fulfils $\xi = -\xi \circ R$ then the augmented system (3.5) is reversible with respect to the map $\bar{R} : (\boldsymbol{z}, \rho) = (R(\boldsymbol{z}), \rho)$.

Typical adaptivity aims at keeping the step size times a positive function $Q : \mathscr{P} \to \mathbb{R}^+$, called a control objective, constant. That is, $Q(\boldsymbol{z})/\rho = \text{const}$. By differentiating that objective we are lead to

$$\xi(\boldsymbol{z}) = \{Q, H\}(\boldsymbol{z})/Q(\boldsymbol{z}). \tag{3.6}$$

This choice fulfils the reversibility condition on ξ whenever $Q = Q \circ R$.

In [26] the following algorithm is suggested.

Algorithm 3.2.1. Let Φ_h be a reversible one-step method for (3.4). Further, let $\rho_0 = 1$, and let $\epsilon > 0$ be a constant. Define $\boldsymbol{z}_0, \boldsymbol{z}_1, \ldots$ by

$$\begin{aligned}\rho_{k+1/2} &= \rho_k + \epsilon\xi(\boldsymbol{z}_k)/2, \\ \boldsymbol{z}_{k+1} &= \Phi_{\epsilon/\rho_{k+1/2}}(\boldsymbol{z}_k), \\ \rho_{k+1} &= \rho_{k+1/2} + \epsilon\xi(\boldsymbol{z}_k)/2,\end{aligned} \tag{3.7}$$

where $\boldsymbol{z}_k$ approximates $\boldsymbol{z}(t_k)$ and time is reconstructed by $t_{k+1} = t_k + \epsilon/\rho_{k+1/2}$.

This defines a reversible (with respect to $\bar{R}$) one-step method $\bar{\Phi}_\epsilon$ for (3.5). In particular, if the Hamiltonian is separable $H(\boldsymbol{z}) = T(\boldsymbol{p}) + V(\boldsymbol{q})$ and Φ_h is the Störmer–Verlet method, then $\bar{\Phi}_\epsilon$ gives a fully explicit adaptive reversible integrator of order 2.

Just as in the Sundman transformation case, symplecticity is not preserved by step density transformations, so $\bar{\Phi}_\epsilon$ is not a symplectic integrator although Φ_h is.

3.3 Nambu Mechanics and Time Transformation

In this section we review the time transformation technique for Nambu–Poisson systems developed in Paper IV. By splitting of the individual Nambu Hamiltonians, this technique can be used to construct adaptive integrators that preserve the Nambu–Poisson structure.

Let $\mathscr{P}$ be a Nambu–Poisson manifold of order k and η its Nambu–Poisson tensor. Consider again the extended phase space $\bar{\mathscr{P}} = \mathscr{P} \times \mathbb{R}$. Our first goal is to introduce a Nambu–Poisson structure on $\bar{\mathscr{P}}$. The most natural extension of the Nambu–Poisson tensor η is given by

$$\bar{\eta} = \eta \wedge \frac{\partial}{\partial \xi}. \tag{3.8}$$

It is not obvious that the bracket corresponding to $\bar{\eta}$ will fulfil the fundamental identity (2.53c). For example, in the canonical Poisson case, i.e., $k = 2$, it is not so if $n \geq 3$.

Lemma 3.3.1. *If $k \geq 3$ or $k = n = 2$, then $\bar{\eta}$ given by equation* (3.8) *defines a Nambu–Poisson structure of order $k+1$ on $\bar{\mathscr{P}}$.*

Proof. If $k \geq 3$ then it follows from Theorem 2.10.3 that η is decomposable about its regular points, and when $k = n = 2$ it is obviously so. Thus, $\eta \wedge \frac{\partial}{\partial \xi}$ is also decomposable about its regular points, so the assertion follows from Theorem 2.10.3. □

The bracket associated with $\bar{\eta}$ is denoted $\bar{\{}\cdot,\ldots,\cdot\bar{\}}$.

Let $H_1, \ldots, H_{k-1} \in \mathcal{F}(\mathscr{P})$ be the Hamiltonians for a Nambu–Poisson system on $\mathscr{P}$, i.e., of the form of system (2.54). Further, let $G \in \mathcal{F}(\bar{\mathscr{P}})$ and consider the system on $\bar{\mathscr{P}}$ given by

$$\frac{\mathrm{d}F}{\mathrm{d}\tau} = \bar{\{}H_1, \ldots, H_{k-1}, G, F\bar{\}} \qquad \forall\, F \in \mathcal{F}(\bar{\mathscr{P}}). \tag{3.9}$$

Remark 3.3.1. A functions $H \in \mathcal{F}(\mathscr{P})$ is considered to belong to $\mathcal{F}(\bar{\mathscr{P}})$ by the natural extension $\bar{\boldsymbol{x}} \mapsto H(\boldsymbol{x})$. Likewise, $\bar{H} \in \mathcal{F}(\bar{\mathscr{P}})$ is considered to be a function in $\mathcal{F}(\mathscr{P})$ depending on the parameter ξ. Thus, $\bar{\{}\cdot,\ldots,\cdot\bar{\}}$ is defined also for elements in $\mathcal{F}(\mathscr{P})$ and vice versa.

The following is a main result in Paper IV. It states that time transformation of a Nambu–Poisson system can be realised as an extended Nambu–Poisson system.

Theorem 3.3.1. *Let $G \in \mathcal{F}(\bar{\mathscr{P}})$ and assume the conditions in Lemma 3.3.1 are valid. Then:*

1. *The extended system* (3.9) *is a Nambu–Poisson system.*
2. *Its flow restricted to $\mathscr{P}$ is a time transformation, determined by the additional first integral G, of the flow of system* (2.54)*. That is,*

$$\Pi \varphi^{\tau}_{H_1,\ldots,H_{k-1},G}(\bar{\boldsymbol{x}}) = \varphi^{\sigma(\tau,\bar{\boldsymbol{x}})}_{H_1,\ldots,H_{k-1}}(\boldsymbol{x}) \qquad \forall\, \bar{\boldsymbol{x}} \in \bar{\mathscr{P}}, \tau \in \mathbb{R},$$

where

$$\sigma(\tau,\bar{\boldsymbol{x}}) \equiv \int_0^\tau \frac{\partial G}{\partial \xi}\left(\varphi^s_{H_1,\ldots,H_{k-1},G}(\bar{\boldsymbol{x}})\right) \mathrm{d}s.$$

Proof. The first assertion follows directly from Lemma 3.3.1, since $\bar{\eta}$ is a Nambu–Poisson tensor. Since H_i for $i = 1,\ldots,k-1$ are independent of ξ, it follows from the definition (3.8) of $\bar{\eta}$ that

$$\bar{\{}H_1,\ldots,H_{k-1},G,F\bar{\}} = \frac{\partial G}{\partial \xi}\{H_1,\ldots,H_{k-1},F\} - \frac{\partial F}{\partial \xi}\{H_1,\ldots,H_{k-1},G\}.$$

Thus, for $F = x_1,\ldots,x_n$, the governing equations (3.9) are parallel with those of system (2.54a), i.e., $\Pi\varphi^\tau_{H_1,\ldots,H_{k-1},G}$ and $\varphi^t_{H_1,\ldots,H_{k-1}}$ defined the same phase diagram. The relation between τ and t is given by $\mathrm{d}t/\mathrm{d}\tau = \partial G/\partial\xi$, which, after integration, gives the desired form of $\sigma(\tau,\bar{\boldsymbol{x}})$. □

It is straightforward to check the following corollary, which shows that the technique used by Hairer and Söderlind [26], reviewed in Section 3.2, is a special case.

Corollary 3.3.1. *The case* $G(\bar{\boldsymbol{x}}) = \log(\xi/Q(\boldsymbol{x}))$ *coincides with the transformation* (3.5) *applied to system* (2.54).

Chapter 4

Implementation

Things should be made as simple as possible, but not any simpler.

(Albert Einstein)

4.1 Multibody Problems

In this section we discuss numerical issues that are specific to multibody problems with contact force laws between bodies.

Consider a system of N bodies. We assume that the configuration space for body i has the form

$$\mathscr{Q}_i = \mathrm{SE}(3) \times \mathsf{V}_i \,. \tag{4.1}$$

- SE(3) is the natural configuration space for a rigid body (recall Section 2.8). It describes the position and orientation of the centre of mass of the body.

- V_i is a vector space that describes additional degrees of freedom for the body, e.g. elasticity and/or thermal distribution. If body i is rigid, then V_i is the empty set.

In practical numerical computations some coordinate representation must be used for the phase space $T\mathscr{Q}_i$. Recall from Section 2.8 that there are various ways of doing this. The approach we consider here is to use parallelisability of SE(3). Thus, the phase space for body i is $\mathscr{P}_i = \mathrm{SE}(3) \times \mathfrak{se}(3) \times \mathsf{V}_i \times \mathsf{V}_i$ (since V_i is a vector space). Global coordinates may be introduced in the $\mathfrak{se}(3) \times \mathsf{V}_i \times \mathsf{V}_i$ part of the phase space (the vector space part). However, we also need to represent elements in SE(3), which is not a vector space since it contains SO(3). As mentioned in Section 2.8 quaternions may be used to embed SO(3) in $\mathbb{R}^4$. It is essential that the numerical solution stays at the sub-manifold induced by the embedding. A natural way of achieving this is to use so called *Lie group integrators*. These integrators are based on the fact that SO(3) is closed under matrix multiplication. For an extensive treatment of the theory, see [32].

The governing differential equations for a system of N bodies are on the form

$$\frac{\mathrm{d}\boldsymbol{z}^i}{\mathrm{d}t} = X_i(\boldsymbol{z}^i) + \sum_{j \neq i} X_{ij}(\boldsymbol{z}^i, \boldsymbol{z}^j), \tag{4.2}$$

where

- $\boldsymbol{z}^i \in \mathscr{P}_i$ are state variables for body i,
- $X_i : \mathscr{P}_i \to T\mathscr{P}_i$ describes the internal dynamics of body i,
- $X_{ij} : \mathscr{P}_i \times \mathscr{P}_j \to T\mathscr{P}_i$ describes the dynamics due to interaction between body i and body j.

4.1.1 Constraints and impact force laws

In computational multibody mechanics the treatment of constraints is a crucial issue, although not the main focus in this thesis. In addition to the obvious possibility of reducing the dynamics to the constraint manifold in accordance with (2.21), there are two main principles:

1. To solve the augmented set of governing equations (2.22), which has the form of a differential algebraic equation (DAE). Usually this approach involves a reformulation of the governing DAE in order to lower its index. See [16, 35] for further details.
2. To add a strong penalty potential, which forces the system to stay on the constraint manifold. The introduction of a penalty potential makes the problem highly stiff, which implies that implicit methods are necessary for stability if large time steps are to be used.

Remark 4.1.1. In the multibody software package BEAST constraints are typically modelled as stiff spring–dampers, i.e., the second approach.

For the multibody application we have in mind, the interaction dynamics between body i and body j take the form

$$X_{ij} = X_{ij}^C + X_{ij}^F, \tag{4.3}$$

where:

- X_{ij}^C is due to penalty constraint forces. Thus, it is of a stiff character, meaning that the aimed step size lengths are not small enough to fully resolve the dynamics it gives rise to.

- X_{ij}^F describes the dynamics due to impact and contact forces between body i and j. Such forces are highly complex, and computing them typically requires a search for intersecting surfaces between the bodies, which is computationally expensive. Indeed, in an application such as BEAST these forces are significantly more expensive to evaluate than other types of forces.

The stiff character of the system, due to penalty constraint forces, implies that implicit methods must be used. From an efficiency point of view a standard implicit method is, per time step, more computationally expensive than an explicit ditto, because at each time step a non-linear equation needs to be solved iteratively. In particular, this implies that the right hand side vector field is evaluated several times each step.

In Paper V of the thesis, mechanical multibody systems with governing equations on the form

$$\frac{\mathrm{d}\boldsymbol{z}}{\mathrm{d}t} = X_A(\boldsymbol{z}) + X_B(\boldsymbol{z}),$$

are considered. X_A is expensive to evaluate, but non-stiff. X_B is inexpensive to evaluate, but stiff. A class of integration methods for such problems is suggested. These integrators are "explicit in X_A and implicit in X_B" in the sense that X_A is only evaluated once per step (or two depending on the order), and its Jacobian matrix is not needed. Thus, if X_A is dominating the computational cost, then the proposed integrators are as efficient per time step as standard explicit integrators, but still allow large step sizes to be used, due to the implicit handling of the stiff part X_B. Consistency and linear stability analysis of the proposed methods are also investigated in the paper.

4.2 Library implemented in BEAST

Based on variational integrators, and on the research in Paper I–V, a software library for numerical integration of multibody problems has been implemented in `C++`. With an object oriented class design, the library is built to be as modular as possible. The principle base classes are:

`Body`

An object from this class represents a body in the system with a phase space on the form (4.1). Member variables include state representation of the body (i.e. a coordinate representation of an element in $\mathscr{P}_i$) as well as other body specific parameters such as mass and moments of inertia.

`BodyForce`

Base class for an object that represents an external force acting on one body, e.g. gravity. A reference to the body object is held. There is also a method for computing the

force acting on the body when it is in its current state.

`ConnectionForce`

Base class for a force acting between two bodies, e.g. a contact force. References to both bodies are held, and a method for computing the force.

`SystemIntegrator`

An object from this class represents a full multibody system and a one step integration method used to solve the system. Member variables include a list of `Body` objects, a list of `BodyForce` objects, and a list of `ConnectionForce` objects. There is a step method, that advances the system from its current to its next state.

The advantage with this library design, over general purpose ODE–solver libraries, is that it allows the integration algorithms (`SystemIntegrator` subclasses) to be "aware" of the structure of the multibody system. For example, each force object (`BodyForce` or `ConnectionForce`) has a flag that specifies if it is expensive or not to evaluate (in accordance with the previous section), and a flag for whether or not it is conservative. Yet, its design is not specific to a particular multibody software code. This allows for simple and generic implementation of integration methods, where system specific structures can be utilised to increase efficiency.

A `SystemIntegrator` subclass with the following properties has been implemented:

- The basic integration scheme is based on the method suggested in Paper V, thus separates between expensive and inexpensive force evaluations.
- For constant steps, the integrator is reversible/symmetric and symplectic if all the forces in the system are conservative.
- An adaptive step size technique based on the Sundman transformation is implemented. If used, a scaling function must be specified. For multibody problems with contacts, a suitable scaling function is derived in Paper II.

The implemented software library has been added to the BEAST software. Results for various cases are given in Paper V and in the study below. The efficiency gain of the new solver algorithm increase for larger systems with more degrees of freedom (e.g. models with flexible bodies). Indeed, for such problems the dominating task in the computation is evaluation of Jacobians of contact forces (i.e. the derivatives of X_{ij}^F, see Section 4.1.1), which are not needed in the new algorithm. This has been verified e.g. in the study below. On the other hand, for small problems where the solution is quasi-static (or almost quasi-static), SUNDIALS may do a better job, as the step lengths there are not bounded by the stiffness of X_{ij}^F.

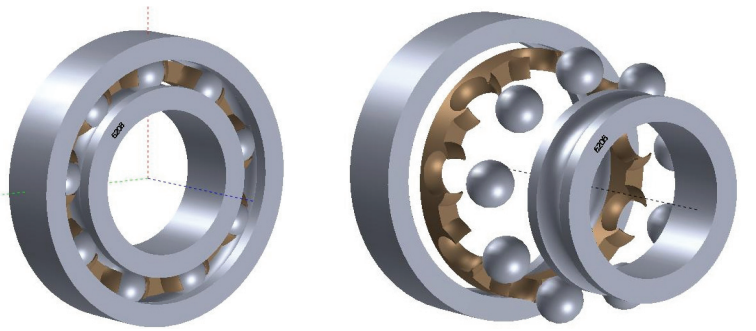

Figure 4.1: A common ball bearing. To the right in exploded view. The bodies in the model are: (1) an outer ring; (2) a cage; (3) nine balls; (4) an inner ring. All elements are steel, except the cage which is plastic.

4.3 Study: Industrial BEAST simulation

In this study a comparison of simulations with the generic ODE–solver CVODE, distributed with the SUNDIALS–package, is compared with the newly implemented semi-explicit solver library. Several cases are studied, representing typical BEAST simulations:

Case 1a: Deep groove ball bearing (rigid) This is a standard deep groove ball bearing of the type shown in Figure 4.1. All the components are simulated as rigid bodies. It is loaded radially and rotated.

Case 1b: Deep groove ball bearing (flexible) Same as above but the inner ring and cage are simulated as elastic bodies.

Case 2: Spherical roller bearing (rigid) A spherical roller bearing with rigid components and with radial load. It is loaded radially and rotated.

Case 3a: Deep groove ball bearing, oval inner ring (1×flexible) A small deep groove ball bearing (50mm outer ring diameter) where the inner-ring has a very small eccentricity. (The original objective of the simulation was to study how the eccentricity affects the internal dynamics of the bearing.) Both the outer ring and the cage are elastic bodies.

Case 3b: Deep groove ball bearing, oval inner ring (2×flexible) Higher resolution in the spatial discretization for the elasticity (twice as many elastic state variables).

Case 3c: Deep groove ball bearing, oval inner ring (3×flexible) Even higher resolution in the spatial discretization for the elasticity (three times as many elastic state variables).

The tolerance settings for the two solvers are tuned to give approximately the same accuracy, by checking optically that the graph of a sensitive state variable (velocity of the cage) are the same. Computational times are shown in in Figure 4.2. Notice that the efficiency gain of the new solver algorithm increases with the complexity of the problem.

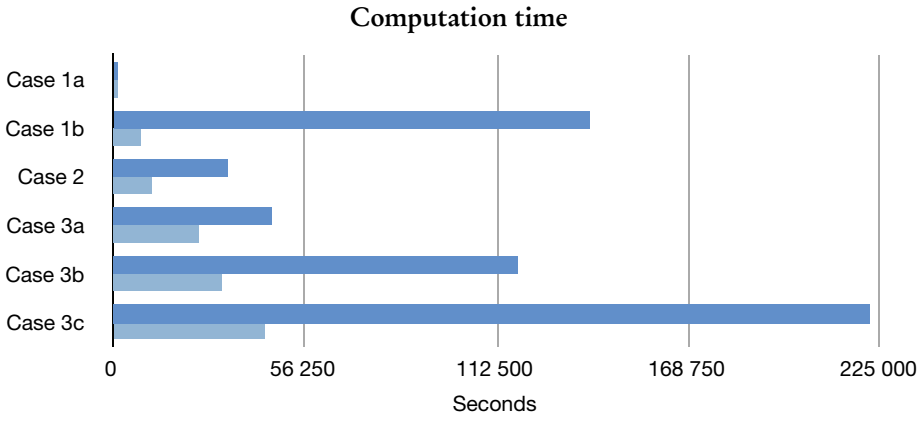

Figure 4.2: Computational time in seconds using BEAST for simulation with approximately the same level of accuracy. For each case, the upper bar is with CVODE and the lower bar is with the new solver package.

Chapter 5

Conclusions

> Not every end is the goal. The end of a melody is not its goal, and yet if a melody has not reached its end, it has not reached its goal. A parable.
>
> *(Friedrich Nietzsche)*

The work in this thesis is concerned with the construction and analysis of efficient numerical integration methods for mechanical problems. In particular, for mechanical multibody problems with complex force laws describing impact and contact between bodies, with application to rolling bearing simulation. The objective of the research is to develop methods that are more efficient and/or more accurate than generic integration algorithms designed for first order ODEs. Motivation for this research comes directly from an industrial need at SKF.

Structure preserving integration algorithms are known to be superior in several fields of application because of their "physically more correct" behaviour in the numerical solution. For example, correct (or "almost correct") energy behaviour. Classically, these types of integrators have been used in celestial mechanics, molecular dynamics, and theoretical physics. A particular hypothesis in our work is that geometric integration algorithms also are favourable for engineering problems such as rotor dynamics and rolling bearing simulations, where they not yet have been used much. This is verified by several simple test examples and by industrial simulations using the BEAST software environment.

Mainly two different routes towards more efficient geometric integrators for the problem class under study have been followed:

1. To use adaptive time stepping. That is, to use so called adaptive geometric integrators. The construction of such integrators is non-trivial, because standard adaptive techniques cannot be used. Indeed, adaptive geometric integration is today a very active research area, with many open questions. Our contributions to the field are in Paper II, Paper III and Paper IV.

2. To exploit the special structure of the multibody systems of interest in order to pin-point expensive and inexpensive computations. In Paper V such an analysis

is carried out, and an efficient method gaining from the specific structure is suggested.

We continue with specific conclusions for each of the three papers.

Paper I An analysis of the geometric structure of non-autonomous mechanical problems is carried out, and geometric numerical methods based on this analysis are tested on classical rotor dynamical problems. The geometric integrators are superior to standard integrators. The paper motivates the use of geometric integrators for engineering problems.

Paper II We show how to construct adaptive integrators within the framework of variational integrators. Further, a time scaling function specifically designed for multibody problems with contacts is suggested.

Numerical examples show that, in comparison with an adaptive BDF method, the proposed integrator is more accurate at equal computational cost. Also, since the proposed integrator is based on variational principles, its energy behaviour is correct, contrary to the energy behaviour of the BDF method.

Paper III Based on a vector field splitting technique in conjunction with Sundman transformation, a new approach for constructing explicit, adaptive, symplectic integrators for separable Hamiltonian systems is presented.

Comparison with explicit, adaptive, reversible integration is carried out for several examples. The examples show that symplecticity and reversibility is preferable over mere reversibility for many types of problems. In particular, for non-reversible problem.

Paper IV A new approach for adaptive geometric integration is obtained by studying time transformation of Nambu–Poisson systems. The approach is based on extension of the phase space, where the additional variable controls the time-stretching rate. The application in mind is adaptive numerical integration by splitting of Nambu–Poisson Hamiltonians. As an example, a novel integration method for the rigid body problem is presented and analysed.

Paper V A new numerical integrator specifically designed for the problem class under study (multibody problems with contact forces between bodies) is suggested. Contrary to standard methods for such problems, the proposed integrator requires only one evaluation of the contact forces per time step, and no contact Jacobians.

Consistency and stability analysis of the proposed integrator is carried out.

Numerical examples show that the proposed integrator is more efficient (in terms of number of contact force evaluations) in comparison with standard implicit integrators.

In addition, a numerical solver library for multibody problems has been implemented in C++. The object oriented design of the library makes it easy to implement adaptive numerical integration algorithms that exploits the special structure of multibody systems. In particular, an adaptive geometric integrator has been implemented in this library. Numerical results for an industrial problems in BEAST show that the new algorithm is more efficient (at the same accuracy level) than a commonly used state-of-the-art generic ODE–solver.

Bibliography

[1] R. Abraham and J. E. Marsden. *Foundations of mechanics*. Benjamin/Cummings Publishing Co. Inc. Advanced Book Program, Reading, Mass., 1978. Second edition, revised and enlarged, With the assistance of Tudor Raţiu and Richard Cushman.

[2] R. Abraham, J. E. Marsden, and T. Ratiu. *Manifolds, tensor analysis, and applications*, volume 75 of *Applied Mathematical Sciences*. Springer-Verlag, New York, second edition, 1988.

[3] D. Alekseevsky and P. Guha. On decomposability of Nambu-Poisson tensor. *Acta Math. Univ. Comenian. (N.S.)*, 65(1):1–9, 1996.

[4] V. I. Arnold. Sur la géométrie différentielle des groupes de Lie de dimension infinie et ses applications à l'hydrodynamique des fluides parfaits. *Ann. Inst. Fourier (Grenoble)*, 16(fasc. 1):319–361, 1966.

[5] V. I. Arnold. *Mathematical methods of classical mechanics*, volume 60 of *Graduate Texts in Mathematics*. Springer-Verlag, New York, second edition, 1989. Translated from the Russian by K. Vogtmann and A. Weinstein.

[6] V. I. Arnold. *Ordinary differential equations*. Universitext. Springer-Verlag, Berlin, 2006. Translated from the Russian by Roger Cooke, Second printing of the 1992 edition.

[7] G. Benettin and A. Giorgilli. On the Hamiltonian interpolation of near-to-the-identity symplectic mappings with application to symplectic integration algorithms. *J. Statist. Phys.*, 74(5-6):1117–1143, 1994.

[8] S. Blanes and C. J. Budd. Adaptive geometric integrators for Hamiltonian problems with approximate scale invariance. *SIAM J. Sci. Comput.*, 26(4):1089–1113 (electronic), 2005.

[9] S. D. Bond and B. J. Leimkuhler. Time-transformations for reversible variable stepsize integration. *Numer. Algorithms*, 19(1-4):55–71, 1998. Differential algebraic equations (Grenoble, 1997).

[10] M. P. Calvo and J. M. Sanz-Serna. Variable steps for symplectic integrators. In *Numerical analysis 1991 (Dundee, 1991)*, volume 260 of *Pitman Res. Notes Math. Ser.*, pages 34–48. Longman Sci. Tech., Harlow, 1992.

[11] R. Chatterjee and L. Takhtajan. Aspects of classical and quantum Nambu mechanics. *Lett. Math. Phys.*, 37(4):475–482, 1996.

[12] S. Cirilli, E. Hairer, and B. Leimkuhler. Asymptotic error analysis of the adaptive Verlet method. *BIT*, 39(1):25–33, 1999.

[13] G. Dahlquist. *Stability and error bounds in the numerical integration of ordinary differential equations*. Inaugural dissertation, University of Stockholm, Almqvist & Wiksells Boktryckeri AB, Uppsala, 1958.

[14] G. G. Dahlquist. A special stability problem for linear multistep methods. *Nordisk Tidskr. Informations-Behandling*, 3:27–43, 1963.

[15] E. Eich. Convergence results for a coordinate projection method applied to mechanical systems with algebraic constraints. *SIAM J. Numer. Anal.*, 30(5):1467–1482, 1993.

[16] E. Eich-Soellner and C. Führer. *Numerical methods in multibody dynamics*. European Consortium for Mathematics in Industry. B. G. Teubner, Stuttgart, 1998.

[17] P. Gautheron. Some remarks concerning Nambu mechanics. *Lett. Math. Phys.*, 37(1):103–116, 1996.

[18] B. Gladman, M. Duncan, and J. Candy. Symplectic integrators for long-term integrations in celestial mechanics. *Celestial Mech. Dynam. Astronom.*, 52(3):221–240, 1991.

[19] I. GmbH. *SIMPACK Multibody Simulation Software*. `www.simpack.com`.

[20] E. Hairer. Backward analysis of numerical integrators and symplectic methods. *Ann. Numer. Math.*, 1(1-4):107–132, 1994. Scientific computation and differential equations (Auckland, 1993).

[21] E. Hairer. Variable time step integration with symplectic methods. *Appl. Numer. Math.*, 25(2-3):219–227, 1997. Special issue on time integration (Amsterdam, 1996).

[22] E. Hairer and C. Lubich. The life-span of backward error analysis for numerical integrators. *Numer. Math.*, 76(4):441–462, 1997.

[23] E. Hairer, C. Lubich, and G. Wanner. Geometric numerical integration illustrated by the störmer/verlet method. *Acta Numer.*, pages 1–51, 2003.

[24] E. Hairer, C. Lubich, and G. Wanner. *Geometric numerical integration*, volume 31 of *Springer Series in Computational Mathematics*. Springer-Verlag, Berlin, second edition, 2006. Structure-preserving algorithms for ordinary differential equations.

[25] E. Hairer, S. P. Nørsett, and G. Wanner. *Solving ordinary differential equations. I*, volume 8 of *Springer Series in Computational Mathematics*. Springer-Verlag, Berlin, 1987. Nonstiff problems.

[26] E. Hairer and G. Söderlind. Explicit, time reversible, adaptive step size control. *SIAM J. Sci. Comput.*, 26(6):1838–1851 (electronic), 2005.

[27] A. C. Hindmarsh, P. N. Brown, K. E. Grant, S. L. Lee, R. Serban, D. E. Shumaker, and C. S. Woodward. SUNDIALS: suite of nonlinear and differential/algebraic equation solvers. *ACM Trans. Math. Software*, 31(3):363–396, 2005.

[28] T. Holder, B. Leimkuhler, and S. Reich. Explicit variable step-size and time-reversible integration. *Appl. Numer. Math.*, 39(3-4):367–377, 2001. Special issue: Themes in geometric integration.

[29] W. Huang and B. Leimkuhler. The adaptive Verlet method. *SIAM J. Sci. Comput.*, 18(1):239–256, 1997. Dedicated to C. William Gear on the occasion of his 60th birthday.

[30] L. Hörmander. Riemannian geometry. Lecture notes, sold at Department of Mathematics, Lund, `www.maths.lth.se/publications/Pure-Lecture-Notes.html`, 1990.

[31] R. Ibáñez, M. de León, J. C. Marrero, and D. Martin de Diego. Dynamics of generalized Poisson and Nambu-Poisson brackets. *J. Math. Phys.*, 38(5):2332–2344, 1997.

[32] A. Iserles, H. Z. Munthe-Kaas, S. P. Nørsett, and A. Zanna. Lie-group methods. In *Acta numerica, 2000*, volume 9 of *Acta Numer.*, pages 215–365. Cambridge Univ. Press, Cambridge, 2000.

[33] C. Kane, J. E. Marsden, M. Ortiz, and M. West. Variational integrators and the Newmark algorithm for conservative and dissipative mechanical systems. *Internat. J. Numer. Methods Engrg.*, 49(10):1295–1325, 2000.

[34] B. Khesin. Topological fluid dynamics. *Notices Amer. Math. Soc.*, 52(1):9–19, 2005.

[35] S. Leyendecker. *Mechanical integrators for constrained dynamical systems in flexible multibody dynamics*. phdthesis, University of Kaiserslautern, 2006. PhD thesis.

[36] G. Marmo, G. Vilasi, and A. M. Vinogradov. The local structure of n-Poisson and n-Jacobi manifolds. *J. Geom. Phys.*, 25(1-2):141–182, 1998.

[37] J. E. Marsden. *Lectures on mechanics*, volume 174 of *London Mathematical Society Lecture Note Series*. Cambridge University Press, Cambridge, 1992.

[38] J. E. Marsden and T. S. Ratiu. *Introduction to mechanics and symmetry*, volume 17 of *Texts in Applied Mathematics*. Springer-Verlag, New York, second edition, 1999. A basic exposition of classical mechanical systems.

[39] J. E. Marsden and M. West. Discrete mechanics and variational integrators. *Acta Numer.*, 10:357–514, 2001.

[40] R. I. McLachlan and G. R. W. Quispel. What kinds of dynamics are there? Lie pseudogroups, dynamical systems and geometric integration. *Nonlinearity*, 14(6):1689–1705, 2001.

[41] R. I. McLachlan and G. R. W. Quispel. Splitting methods. *Acta Numer.*, 11:341–434, 2002.

[42] S. Mikkola and P. Wiegert. Regularizing time transformations in symplectic and composite integration. *Celestial Mech. Dynam. Astronom.*, 82(4):375–390, 2002.

[43] N. Nakanishi. On Nambu-Poisson manifolds. *Rev. Math. Phys.*, 10(4):499–510, 1998.

[44] M. Preto and S. Tremaine. A class of symplectic integrators with adaptive timestep for separable hamiltonian systems. *Astron. J.*, 118(5):2532–2541, 1999.

[45] S. Reich. Backward error analysis for numerical integrators. *SIAM J. Numer. Anal.*, 36(5):1549–1570 (electronic), 1999.

[46] R. Schmid. Infinite dimensional Lie groups with applications to mathematical physics. *J. Geom. Symmetry Phys.*, 1:54–120, 2004.

[47] M. Software. *ADAMS Multibody Simulation Software*. `www.mscsoftware.com`.

[48] L.-E. Stacke and D. Fritzson. Dynamical behaviour of rolling bearings: simulations and experiments. *Proc. Instn. Mech. Engrs.*, 215:499–508, 2001.

[49] D. Stoffer. Variable steps for reversible integration methods. *Computing*, 55(1):1–22, 1995.

[50] J. Struckmeier. Hamiltonian dynamics on the symplectic extended phase space for autonomous and non-autonomous systems. *J. Phys. A*, 38(6):1257–1278, 2005.

[51] L. Takhtajan. On foundation of the generalized Nambu mechanics. *Comm. Math. Phys.*, 160(2):295–315, 1994.

[52] K. Zare and V. Szebehely. Time transformations in the extended phase-space. *Celestial Mech.*, 11:469–482, 1975.

[53] G. Zhong and J. E. Marsden. Lie-Poisson Hamilton-Jacobi theory and Lie-Poisson integrators. *Phys. Lett. A*, 133(3):134–139, 1988.

Paper I

Klas Modin.
Not yet submitted, 2009.

Geometric Integration of Non-autonomous Systems with Application to Rotor Dynamics

Klas MODIN [a,b]

[a] *SKF Engineering & Research Centre*
MDC, RKs–2, SE–415 50 Göteborg, Sweden

[b] *Centre for Mathematical Sciences, Lund University*
Box 118, SE–221 00 Lund, Sweden
E–mail: kmodin@maths.lth.se

March 25, 2009

Abstract

Geometric integration of non-autonomous classical engineering problems, such as rotor dynamics, is investigated. It is shown, both numerically and by backward error analysis, that geometric (structure preserving) integration algorithms are superior to conventional Runge–Kutta methods.

Key-words: Geometric numerical integration, splitting methods, rotor dynamics

1 Introduction

In this paper we study geometric numerical integration algorithms for non-autonomous systems. By classifying the appropriate Lie sub-algebra of vector fields, the standard framework for backward error analysis can be used to explain the superior qualitative behaviour of geometric methods based on the splitting approach.

The current section continues with a brief review of the general framework for geometric methods, mainly following the approach by Reich [2]. In Section 2 we study geometric integration of linear systems with non-constant periodic coefficients. A numerical example from classical rotor dynamics is given. Conclusions are given in Section 3.

We adopt the following notation. $\mathscr{P}$ denotes a phase space manifold of dimension n, with local coordinates $\boldsymbol{x} = (x_1, \ldots, x_n)$. In the case when $\mathscr{P}$ is a linear space we also use P. Further, $\mathfrak{X}(\mathscr{P})$ denotes the linear space of vector fields on $\mathscr{P}$. The flow of $X \in \mathfrak{X}(\mathscr{P})$ is denoted φ_X^t, where t is the time parameter. The Lie derivative along X is denoted $\mathcal{L}_X$. If $X, Y \in \mathfrak{X}(\mathscr{P})$ then the vector field commutator $[X,Y]_{\mathfrak{X}} = \mathcal{L}_X Y$ supplies $\mathfrak{X}(\mathscr{P})$ with an infinite dimensional Lie algebra structure. Its corresponding Lie group is the set $\mathrm{Diff}(\mathscr{P})$ of diffeomorphisms on $\mathscr{P}$, with composition as group operation. (See McLachlan and Quispel [1] and Schmid [3] for issues concerning infinite dimensional Lie groups.)

As usual, the general linear group of $n \times n$–matrices is denoted $\mathrm{GL}(n)$ and its corresponding Lie algebra $\mathfrak{gl}(n)$. We use $[A,B]_{\mathfrak{gl}}$ for the matrix commutator $AB - BA$.

If V is a metric linear space, then the linear space of smooth periodic functions $\mathbb{R} \to \mathsf{V}$ with period $2\pi/\Omega$ is denoted $\mathcal{C}_\Omega(\mathsf{V})$. Notice that this space is closed under differentiation, i.e., if $f \in \mathcal{C}_\Omega(\mathsf{V})$ then it also holds that $f' \in \mathcal{C}_\Omega(\mathsf{V})$.

1.1 Geometric Integration and Backward Error Analysis

Let $\mathfrak{X}_S(\mathscr{P})$ be a sub-algebra of $\mathfrak{X}(\mathscr{P})$, i.e., a linear sub-space which is closed under the commutator. Its corresponding sub-group of $\mathrm{Diff}(\mathscr{P})$ is denoted $\mathrm{Diff}_S(\mathscr{P})$. Let $X \in \mathfrak{X}_S(\mathscr{P})$ be a vector field which is to be integrated numerically. Assume that X can be splitted as a sum of explicitly integrable vector field also belonging to $\mathfrak{X}_S(\mathscr{P})$. That is, $X = Y + Z$ where $Y, Z \in \mathfrak{X}_S(\mathscr{P})$ and φ_Y^t, φ_Z^t can be computed explicitly. By various compositions, various numerical integration schemes for φ_X^t are obtained. The most classical example is $\Phi_h = \varphi_Y^{h/2} \circ \varphi_Z^h \circ \varphi_Y^{h/2}$, which yields a second order symmetric method (h is the step-size parameter of the method). Since $\varphi_Y^t, \varphi_Z^t \in \mathrm{Diff}_S(\mathscr{P})$, and since $\mathrm{Diff}_S(\mathscr{P})$ is closed under composition (since it is the group operation), it holds that $\Phi_h \in \mathrm{Diff}_S(\mathscr{P})$. Thus, the splitting approach yields structure preserving methods, which is a key property.

Backward error analysis for structure preserving integrators deals with the question of finding a modified vector field $\tilde{X} \in \mathfrak{X}_S(\mathscr{P})$ such that $\Phi_h = \varphi_{\tilde{X}}^h$. In conjunction with perturbation theory, such an analysis can be used to study the dynamical properties of Φ_h. For splitting methods, backward error analysis is particularly simple as the modified vector field, at least formally, is obtained from the Baker–Campbell–Hausdorff (BCH) formula. For details on this framework we refer to Reich [2].

2 Linear Systems

In this section we study non-autonomous systems on a linear phase space P with global coordinates $\boldsymbol{x} = (x_1, \ldots, x_n)$. More precisely, let G be a Lie sub-group of $\mathrm{GL}(n)$ and $\mathfrak{g}$ its corresponding Lie sub-algebra. We consider systems of the form

$$\dot{\boldsymbol{x}} = A(t)\boldsymbol{x} + f(t) \tag{1}$$

where $A \in \mathcal{C}_\Omega(\mathfrak{g})$ and $f \in \mathcal{C}_\Omega(\mathsf{P})$ is a smooth vector valued periodic function with period $T = 2\pi/\Omega$. Our objective is to construct geometric integrators for (1). Of course, since the system is linear, there is a closed form formula for its solution. However, in engineering applications, e.g. finite element analysis, the system is typically very large so computing the exponential matrix, which is necessary for the exact solution, is not computationally efficient. Also, it might not be possible to analytically integrate f and A over t, which is necessary for the exact solution.

In order to study dynamical systems of the form (1) in the framework of geometric integration, we need, first of all, to extend the phase space to $\overline{\mathsf{P}} = \mathsf{P} \times \mathbb{R}$ to include the time variable in the dynamics. Coordinates on $\overline{\mathsf{P}}$ are now given by $(\boldsymbol{x}, t)$ and the new independent variable is denoted τ (in practice we always have $t(\tau) = \tau$). Further, we need to find a Lie sub-algebra of $\mathfrak{X}(\overline{\mathsf{P}})$ which captures the form (1). For this purpose, consider the set of vector field on $\overline{\mathsf{P}}$ given by

$$\mathfrak{L}_\Omega(\mathsf{P}, \mathfrak{g}) = \left\{ X \in \mathfrak{X}(\overline{\mathsf{P}}) \,\middle|\, X(\boldsymbol{x}, t) = (A(t)x + f(t), \alpha),\, A \in \mathcal{C}_\Omega(\mathfrak{g}),\, f \in \mathcal{C}_\Omega(\mathsf{P}),\, \alpha \in \mathbb{R} \right\}. \tag{2}$$

We now continue with some results concerning properties of $\mathfrak{L}_\Omega(\mathsf{P}, \mathfrak{g})$. The first result states that it actually *is* a Lie sub-algebra.

Proposition 2.1. *The set of vector fields $\mathfrak{L}_\Omega(\mathsf{P}, \mathfrak{g})$ is a Lie sub-algebra of $\mathfrak{X}(\overline{\mathsf{P}})$.*

Proof. We need to check that $\mathfrak{L}_\Omega(\mathsf{P}, \mathfrak{g})$ is closed under vector operations and under the Lie bracket. That is, $X, Y \in \mathfrak{L}_\Omega(\mathsf{P}, \mathfrak{g})$ should imply $aX + bY \in \mathfrak{L}_\Omega(\mathsf{P}, \mathfrak{g})$ for $a, b \in \mathbb{R}$ and $[X, Y]_{\mathfrak{X}} \in \mathfrak{L}_\Omega(\mathsf{P}, \mathfrak{g})$.

With $X(\boldsymbol{x}, t) = (A(t)\boldsymbol{x} + f(t), \alpha)$ and $Y(\boldsymbol{x}, t) = (B(t)\boldsymbol{x} + g(t), \beta)$ we get $(aX + bY)(\boldsymbol{x}, t) =$

$((aA+bB)(t)\boldsymbol{x}+(af+bg)(t), a\alpha+b\beta)$ which is of the desired form. Further,

$$
\begin{aligned}
[X,Y]_{\mathfrak{X}} &= \begin{pmatrix} A(t) & A'(t)\boldsymbol{x}+f'(t) \\ 0 & 0 \end{pmatrix}\begin{pmatrix} B(t)\boldsymbol{x}+g(t) \\ \beta \end{pmatrix} - \begin{pmatrix} B(t) & B'(t)\boldsymbol{x}+g'(t) \\ 0 & 0 \end{pmatrix}\begin{pmatrix} A\boldsymbol{x}+f(t) \\ \alpha \end{pmatrix} \\
&= \begin{pmatrix} (A(t)B(t)-B(t)A(t)+\beta A'(t)-\alpha B'(t))\boldsymbol{x}+A(t)g(t)-B(t)f(t)+\beta f'(t)-\alpha g'(t) \\ 0 \end{pmatrix}
\end{aligned}
$$

which is of the desired form since $AB-BA+\beta A'-\alpha B' = [A,B]_{\mathrm{GL}}+\beta A'+\alpha B' \in \mathcal{C}_\Omega(\mathfrak{g})$ and $(Ag - Bf+\beta f'-\alpha g') \in \mathcal{C}_\Omega(\mathsf{P})$. □

From the proof above we immediately obtain the following corollary.

Corollary 2.1. *The set* $\mathfrak{l}_\Omega = \mathcal{C}_\Omega(\mathfrak{g}) \times \mathcal{C}_\Omega(\mathsf{P}) \times \mathbb{R}$ *equipped with the induced vector operation*

$$a(A,f,\alpha)+b(B,g,\beta) = (aA+bB, af+bg, a\alpha+b\beta), \quad a,b\in\mathbb{R}$$

and with the bracket operation

$$[(A,f,\alpha),(B,g,\beta)]_{\mathfrak{L}} = ([A,B]_{\mathrm{GL}}+\beta A'+\alpha B', Ag-Bf+\beta f'-\alpha g', 0)$$

is a Lie algebra which is isomorphic to $\mathfrak{L}_\Omega(\mathsf{P},\mathfrak{g})$ *with isomorphism* $\mathfrak{l}_\Omega \ni (A,f,\alpha) \mapsto (A\boldsymbol{x}+f,\alpha) \in \mathfrak{L}_\Omega(\mathsf{P},\mathfrak{g})$.

Since $\mathcal{C}_\Omega(\mathsf{P})$ and $\mathcal{C}_\Omega(\mathfrak{g})$ are infinite dimensional it follows that $\mathfrak{l}_\Omega$, and therefore also $\mathfrak{L}_\Omega(\mathsf{P},\mathfrak{g})$, is infinite dimensional. However, a finite dimensional sub-space of $\mathcal{C}_\Omega(\mathsf{P})$ is given by

$$\mathcal{C}_{\Omega,k}(\mathsf{P}) = \Big\{ f\in\mathcal{C}_\Omega(\mathsf{P}) \,\Big|\, f(t) = \boldsymbol{a}_0 + \sum_{i=1}^{k} \boldsymbol{a}_i\cos(i\Omega t)+\boldsymbol{b}_i\sin(i\Omega t),\ \boldsymbol{a}_i,\boldsymbol{b}_i\in\mathsf{P}\Big\} \tag{3}$$

which is the sub-space of $\mathcal{C}_\Omega(\mathsf{P})$ with angular frequencies bounded by $k\Omega$. Notice that the dimension of $\mathcal{C}_{\Omega,k}(\mathsf{P})$ is $(2k+1)n$ and that $\mathcal{C}_{\Omega,\infty}(\mathsf{P}) = \mathcal{C}_\Omega(\mathsf{P})$ and $\mathcal{C}_{\Omega,0}(\mathsf{P}) = \mathsf{P}$. Further, $\mathcal{C}_{\Omega,k}(\mathsf{P})$ is closed under differentiation. Clearly, these results also holds for the corresponding sub-space $\mathcal{C}_{\Omega,l}(\mathfrak{g})$ of $\mathcal{C}_\Omega(\mathfrak{g})$, except that the dimension is given by $(2l+1)\dim\mathfrak{g}$ instead.

By replacing $\mathcal{C}_\Omega(\mathsf{P})$ with $\mathcal{C}_{\Omega,k}(\mathsf{P})$ and $\mathcal{C}_\Omega(\mathfrak{g})$ with $\mathcal{C}_{\Omega,l}(\mathfrak{g})$ we get the sub-spaces $\mathfrak{l}_{\Omega,k,l} = \mathcal{C}_{\Omega,l}(\mathfrak{g}) \times \mathcal{C}_{\Omega,m}(\mathsf{P}) \times \mathbb{R}$ of $\mathfrak{l}_\Omega$. In general $\mathfrak{l}_{\Omega,k,l}$ is *not* a sub-algebra, due to the fact that $A,B\in\mathcal{C}_{\Omega,l}(\mathfrak{g})$ does not in general imply $AB\in\mathcal{C}_{\Omega,l}(\mathfrak{g})$. However, in some special cases the implication holds true.

Proposition 2.2. *The sub-spaces* $\mathfrak{l}_{\Omega,k,0} = \mathfrak{g}\times\mathcal{C}_{\Omega,k}(\mathsf{P})\times\mathbb{R}$ *and* $\mathfrak{l}_{\Omega,k,\infty} = \mathcal{C}_\Omega(\mathfrak{g})\times\mathcal{C}_{\Omega,k}(\mathsf{P})\times\mathbb{R}$ *are Lie sub-algebras of* $\mathfrak{l}_\Omega$. *Further,* $\mathfrak{l}_{\Omega,k,0}$ *is finite dimensional with dimension* $\dim\mathfrak{g}+(2k+1)n+1$.

Clearly, $\mathfrak{l}_{\Omega,k,0}$ and $\mathfrak{l}_{\Omega,k,\infty}$ induces corresponding Lie sub-algebras $\mathfrak{L}_{\Omega,k,0}(\mathsf{P},\mathfrak{g})$ and $\mathfrak{L}_{\Omega,k,\infty}(\mathsf{P},\mathfrak{g})$ of $\mathfrak{L}_\Omega(\mathsf{P},\mathfrak{g})$.

2.1 Geometric Integration

In this section we describe an approach for geometric integration of of systems of the form (1). The approach is based on splitting. To this extent we write (1) as an extended system

$$\frac{\mathrm{d}}{\mathrm{d}\tau}\begin{pmatrix}\boldsymbol{x}\\ t\end{pmatrix} = \begin{pmatrix} A(t)\boldsymbol{x}+f(t)\\ 1\end{pmatrix} \equiv X(\boldsymbol{x},t)\,. \tag{4}$$

It is clear that $X\in\mathfrak{L}_\Omega(\mathsf{P},\mathfrak{g})$. Since $\mathfrak{L}_\Omega(\mathsf{P},\mathfrak{g})$ is a Lie sub-algebra of $\mathfrak{X}(\overline{\mathsf{P}})$ it corresponds to a Lie sub-group Diff_Ω of $\mathrm{Diff}(\overline{\mathsf{P}})$. Geometric integration of (4) now means to find a one-step integration algorithm $\Phi_h\in\mathrm{Diff}_\Omega$. There are of several ways to obtain such integrators. One of the simplest, but yet most powerful ways, is to use a splitting approach. That is, to split the vector field X as a sum of two vector fields each of them of the form (4).

	Value	Unit
m	1	kg
k	1	N/m
Ω	1.02	rad/s
ε	0.1	m · kg
x_0	(0,0,0,0)	(m,m,m/s,m/s)

Table 1: Data used in the simulations of the rotor dynamical problem.

2.2 Example: Linear Rotor Dynamics

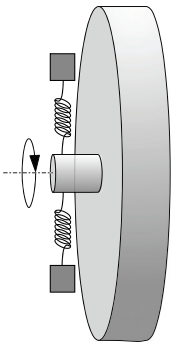

This example is the simplest possible rotor dynamical problem. It consists of a disc attached to a shaft which is rotating with constant angular velocity Ω. The shaft is held by a bearing, which is modelled as a linear spring with stiffness k. (See figure.) The disc is slightly unbalanced, i.e., its centre of mass does not align with rotational axis. This implies a time-dependent periodic centrifugal force acting on the rotor.

The phase space for this system is given by $\mathsf{P} = \mathbb{R}^4$, with coordinates $\boldsymbol{x} = (q_1, q_2, p_1, p_2)$, which is the horizontal and vertical position of the shaft in a plane perpendicular to the axis of rotation, and their corresponding momenta. The equations of motion are of the form (4) with

$$A = \begin{pmatrix} 0 & 0 & m^{-1} & 0 \\ 0 & 0 & 0 & m^{-1} \\ -k & 0 & 0 & 0 \\ 0 & -k & 0 & 0 \end{pmatrix} \qquad \text{and} \qquad f(t) = \varepsilon\Omega^2 \begin{pmatrix} 0 \\ 0 \\ -\cos(\Omega t) \\ \sin(\Omega t) \end{pmatrix}$$

where m is the total mass and ε is the magnitude of the unbalance.

It holds that $A^T J + JA = 0$, so A is an element in the canonical symplectic Lie sub-algebra of $\mathfrak{gl}(4)$, i.e., we have $\mathfrak{g} = \mathfrak{sp}(4)$. Further, since A is independent of t, and f only contains a single frequency, the appropriate Lie sub-algebra of $\mathfrak{X}(\mathbb{R}^4)$ is $\mathfrak{L}_{\Omega,1,0}(\mathbb{R}^4, \mathfrak{sp}(4))$, which is finite dimensional.

The eigenvalues of A are $\pm i\sqrt{k/m}$. Thus if Ω is close to a multiple of the eigen frequency $\omega = \sqrt{k/m}$ of the system starts to resonate. In this example we investigate how well various numerical integrators capture that behaviour, both qualitatively and quantitatively.

For the data given in Table 2.2 the problem is numerically integrated with four different methods, two which are geometric and two which are not.

Method	Geometric?
Implicit midpoint	Yes
Splitting method	Yes
Heun's method	No
Implicit extrapolation method	No

The results of the x_1–variable are shown in Figure 1. Notice that the geometric integrators captures the resonance phenomena in a qualitatively correct way, whereas the non-geometric methods does not show the correct behaviour.

3 Conclusions

A structural analysis of non-autonomous systems has been carried out using the framework of Lie sub-algebras of the Lie algebra of vector fields. As a direct application, backward error analysis results

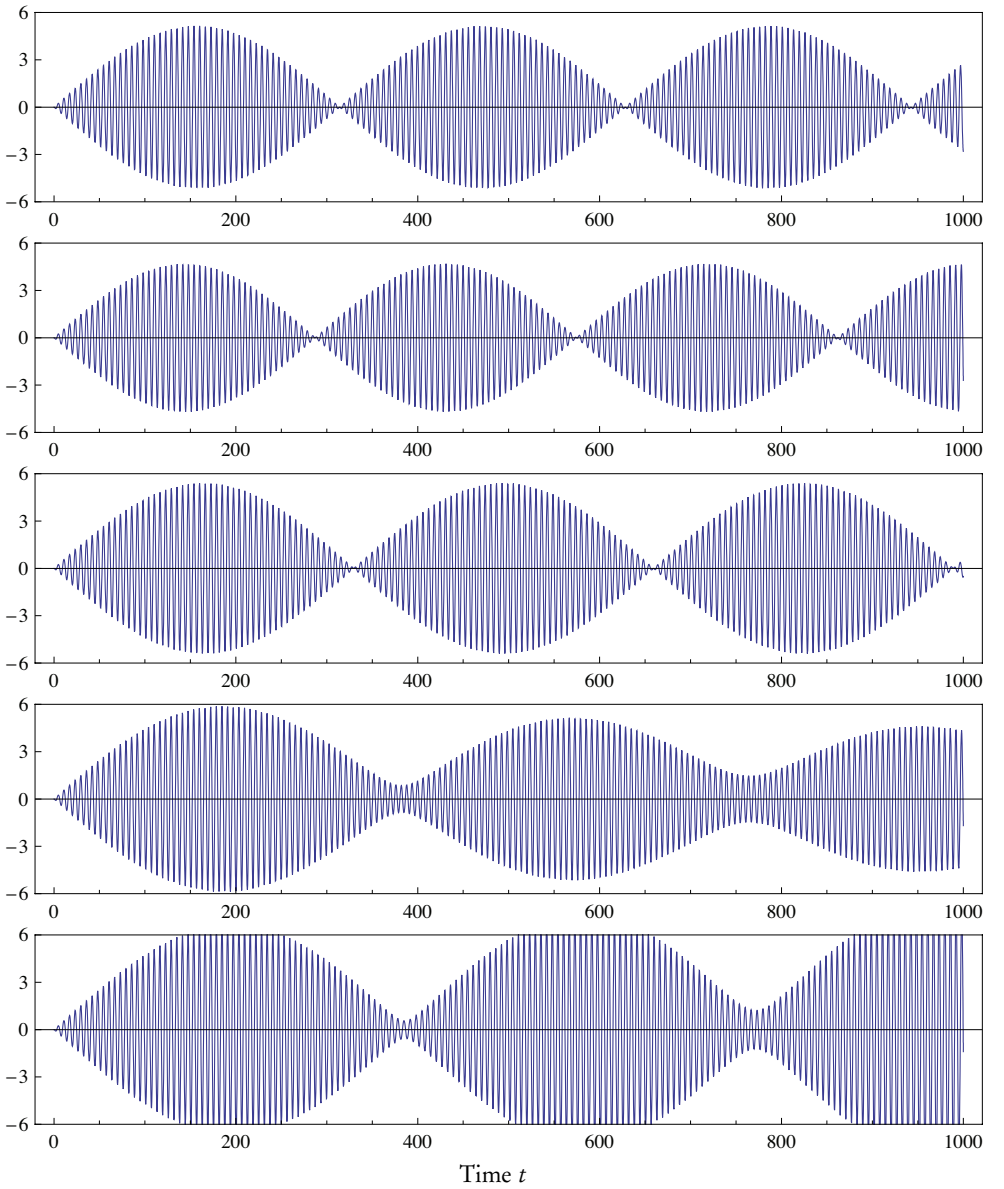

Figure 1: Results for q_1 variable for the simple linear rotor example. *From top:* (1) exact solution, (2) implicit midpoint, geometric, (3) Störmer–Verlet, geometric, (4) implicit Runge–Kutta, non-geometric, (5) explicit Runge-Kutta, non-geometric. All methods are second order accurate. Notice the superior qualitative and quantitative behaviour of the geometric methods.

are obtained for this class of problems. Numerical examples of a classical rotor dynamical problem show that the geometric methods preserving the structure of the problem indeed are favourable over non-geometric dito.

Acknowledgement The author is grateful to Dag Fritzson, Claus Führer and Gustaf Söderlind for helpful discussions. The author would also like to thank SKF for the support given.

References

[1] R. I. McLachlan and G. R. W. Quispel. What kinds of dynamics are there? Lie pseudogroups, dynamical systems and geometric integration. *Nonlinearity*, 14(6):1689–1705, 2001.

[2] S. Reich. Backward error analysis for numerical integrators. *SIAM J. Numer. Anal.*, 36(5):1549–1570 (electronic), 1999.

[3] R. Schmid. Infinite dimensional Lie groups with applications to mathematical physics. *J. Geom. Symmetry Phys.*, 1:54–120, 2004.

Paper II

Klas Modin and Claus Führer.
ZAMM Z. Angew. Math. Mech., 86(10):785–794, 2006.

ZAMM · Z. Angew. Math. Mech. **86**, No. 10, 785 – 794 (2006) / **DOI** 10.1002/zamm.200610286

Time-step adaptivity in variational integrators with application to contact problems

Klas Modin[1,*] **and Claus Führer**[2,**]

[1] SKF Engineering Research Centre, MDC RKs–2, 415 50 Göteborg, Sweden
[2] Centre for Mathematical Sciences, Lund University, Box 118, 221 00 Lund, Sweden

Received 15 February 2006, accepted 8 June 2006
Published online 9 October 2006

Key words variational integrators, variable step-size methods, Poincaré transformations, time scaling, contact problems
MSC (2000) 37M15

Variable time-step methods, with general step-size control objectives, are developed within the framework of variational integrators. This is accomplished by introducing discrete transformations similar to Poincarés time transformation. While gaining from adaptive time-steps, the resulting integrators preserve the structural advantages of variational integrators, i. e., they are symplectic and momentum preserving. As an application, the methods are utilized for dynamic multibody systems governed by contact force laws. A suitable scaling function defining the step-size control objective is derived.

1 Introduction

1.1 Motivation and overview

The philosophy behind variable time-step integrators is to increase efficiency by adapting the time-step "on the fly", during the integration process. For systems with heavily alternating dynamics, the gain in efficiency due to variable time-steps can be substantial. For example, consider a dynamic system that describes the motion of a rolling bearing under some loading conditions. Typically, the components frequently bounce, roll and slide against each other, see [13]. Thus, depending on the current state of the system, the governing equations vary from a non-stiff character (typical when the components are either not in contact at all, or when there is slow motion in the active contacts) to a stiff character (typical during heavy impacts at high relative velocities). In these situations a variable time-step integrator is favourable as it, ideally, regularizes the problem by adapting the time-step to the local character of the governing equations.

Variational integrators form a class of methods specifically designed for dynamic mechanical systems. In contrast to standard methods designed for general ordinary differential equations, variational integrators "replicate" much of the qualitative structure of analytical mechanics. Indeed, they are symplectic and preserve momentum maps.

The theory of variational integrators is developed for autonomous systems and for constant time-steps. An extension to non-autonomous systems is given in [12]. An extension to variable time-steps is given in [8], where it is shown that by taking an extended velocity phase space approach one naturally leads to variational integrators in which the time-step varies so that energy is exactly conserved. However, this step-size control objective is generally not preferable when it comes to efficiency.

Our objective in the paper is to develop time-step adaptivity, for more general step-size control objectives, within the framework of variational integrators, and to give applications to multibody systems governed by contact force laws of penalty type. The resulting methods benefit both from structural advantages, i. e., they are symplectic and momentum preserving, and from adaptivity, i. e., the time-step can be adapted to the local character of the governing equations to increase efficiency. Throughout the paper we restrict ourselves to autonomous systems in order to fit the standard framework of variational integrators.

Next to the organization of the paper. The remainder of this section outlines some known results, which are essential to the subsequent sections. First we give a brief review of variational integrators, followed by an equally brief review of dynamic time transformations for Hamiltonian systems. Sect. 2 contains the main result: variable time-step variational integrators are developed. Some properties of the resulting integrators, and relation to integrators for Hamiltonian systems, are also derived. In Sect. 3 applications to dynamic systems governed by contact force laws are given. The first example is a simple, but numerically intricate, "contact test problem". The second example is a billiard, i. e., a multiple of balls bouncing against each other and surrounding walls.

* Corresponding author, e-mail: klas.modin@na.lu.se, Phone: +46 31 337 3276
** e-mail: claus@maths.lth.se

1.2 Review of variational integrators

For background reading on analytical mechanics, see e. g. [1,11].

Let Q be the configuration manifold of some autonomous mechanical system with local coordinates denoted q. Let $(q, \dot{q})$ denote the corresponding induced local coordinates on the tangent bundle TQ (the velocity phase space). Further, let $L : TQ \to \mathbb{R}$ be a Lagrangian function for the system. Hamilton's principle states that if $\gamma : [0, a] \to Q$ is a motion of the system, then it extremizes the action functional

$$S(\gamma) = \int_0^a L\left(\gamma(t), \gamma'(t)\right) \,\mathrm{d}t\,, \tag{1}$$

i. e., its variation is zero for solution curves: $\delta S = 0$. From this principle a second order differential equation is derived by differentiation and partial integration. The result is the Euler–Lagrange equation

$$\frac{d}{dt}\left(\frac{\partial L}{\partial \dot{q}}\right) - \frac{\partial L}{\partial q} = 0\,. \tag{2}$$

We assume that the Euler–Lagrange equation (2), together with some initial conditions $(q_{\text{init}}, \dot{q}_{\text{init}}) \in TQ$, define a unique solution curve $[0, a] \to Q$.

The standard numerical approach is to discretize eq. (2) in time by some scheme, e. g. a Runge–Kutta scheme, which yields a numerical integrator. Generally, such a scheme is designed to be zero stable and to give a good local approximation of the exact solution. However, due to Hamilton's principle, the exact solution possesses certain qualitative properties, e. g. symplecticity and momentum preservation, which are typically lost in a standard discretization.

The key point in variational integrators is to directly discretize Hamilton's principle. This approach leads to the formulation of discrete mechanical systems. For an extensive treatment of the theory, and for an account of its origin, see [12] and references therein. In short, discretization of the action functional (1) leads to the concept of an action sum

$$S_d(\gamma_d) = \sum_{k=1}^{n-1} L_d(q_{k-1}, q_k)\,, \qquad \gamma_d = (q_0, \ldots, q_{n-1}) \in Q^n\,, \tag{3}$$

where $L_d : Q \times Q \to \mathbb{R}$ is an approximation of L called the discrete Lagrangian. Hence, in the discrete setting the correspondence to the velocity phase space TQ is $Q \times Q$. An intuitive motivation for this is that two points close to each other correspond approximately to the same information as one point and a velocity vector. The discrete Hamilton's principle states that if γ_d is a motion of the discrete mechanical system then it extremizes the action sum, i. e., $\delta S_d = 0$. By differentiation and rearranging of the terms (rearranging corresponds to partial integration in the continuous case), the discrete Euler-Lagrange (DEL) equation is obtained:

$$D_2 L_d(q_{k-1}, q_k) + D_1 L_d(q_k, q_{k+1}) = 0\,, \tag{4}$$

where D_1, D_2 denote differentiation with respect to the first and second slot respectively. The DEL equation defines a discrete flow $F_d : (q_{k-1}, q_k) \mapsto (q_k, q_{k+1})$ called a variational integrator. Due to the variational approach, F_d possesses qualitative properties similar to those in continuous mechanics. Indeed, F_d can, through the discrete Legendre transform, be given as a symplectic map on T^*Q. Furthermore, if G is a Lie group with Lie algebra $\mathfrak{g}$, and L_d is invariant under an action $\Phi : G \times Q \to Q$, then there is a discrete version of Noether's theorem which states that F_d conserves a corresponding momentum map $J_{L_d} : Q \times Q \to \mathfrak{g}^*$. (See [12, Part 1] for details.)

The construction of L_d from L depends on a discretization step-size parameter ε. We write $L_d(q_0, q_1; \varepsilon)$ when the dependence needs to be expressed. L_d is said to be of order r relative to L if

$$L_d\left(\gamma(0), \gamma(\varepsilon); \varepsilon\right) - \int_0^\varepsilon L\left(\gamma(u), \gamma'(u)\right) \,\mathrm{d}u = \mathcal{O}(\varepsilon^{r+1}) \tag{5}$$

for solution curves γ of eq. (2). It is shown in [12, Part 2] that if L_d is of order r relative to L then the order of accuracy of the corresponding variational integrator is r.

If Q is a linear space, a class of low order discretizations is given by

$$L_d^\alpha(q_0, q_1; \varepsilon) = \varepsilon L\left((1-\alpha)q_0 + \alpha q_1, \frac{q_1 - q_0}{\varepsilon}\right)\,, \quad 0 \le \alpha \le 1\,, \tag{6}$$

and by the symmetrized version

$$L_d^{\text{sym},\alpha} = \tfrac{1}{2}\left(L_d^\alpha + L_d^{1-\alpha}\right)\,. \tag{7}$$

Often L is in the standard form

$$L(q,\dot{q}) = \tfrac{1}{2}\dot{q}^T M\dot{q} - V(q)\,, \qquad q \in Q = \mathbb{R}^m\,, \tag{8}$$

where M is a mass matrix and V a potential function. In this case, the variational integrator given by eq. (6) with $\alpha = 1/2$ turns out to be the classical implicit midpoint rule. Further, the choice $\alpha = 0$ gives the symplectic Euler method. The discretization (7) with $\alpha = 0$ or $\alpha = 1$ gives the Störmer–Verlet method, which is explicit and of second order. See [12, Part 2] for other well known integrators that can be interpreted as variational integrators.

A graphical comparison between the variational and the standard approach to numerical integrators is given in Fig. 1.

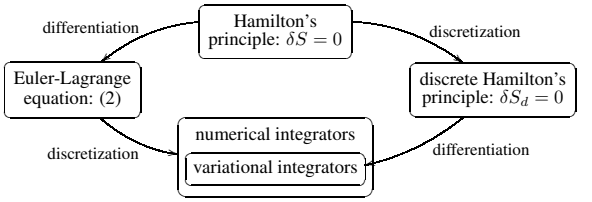

Fig. 1 *Left branch:* the classical approach leading to standard integrators. *Right branch:* the discrete mechanical approach leading to variational integrators, which is a subclass of standard integrators.

Recall that solution curves of an autonomous Lagrangian mechanical system preserve energy, i. e., they have a first integral given by

$$E(q,\dot{q}) = \frac{\partial L(q,\dot{q})}{\partial \dot{q}}\,\dot{q} - L(q,\dot{q})\,. \tag{9}$$

Thus, the energy of a solution curve is determined by its initial conditions: $E_0 = E(q_{\text{init}}, \dot{q}_{\text{init}})$. According to [9], energy for a discrete mechanical system is defined as $E_d(q_0, q_1) = -\partial/\partial\varepsilon L_d(q_0, q_1; \varepsilon)$. Variational integrators do not exactly preserve E_d. However, it has been observed numerically, e. g. in [8], that the long-time energy behaviour for variational integrators is "nice", in the sense that the discrete energy $E_d(q_k, q_{k+1})$ oscillates with a small amplitude about the correct value E_0. Partially, this behaviour can be explained by backward error analysis combined with perturbation theory, as developed in [6].

1.3 Review of time transformations in Hamiltonian mechanics

For background reading on time transformations in Hamiltonian mechanics, see [15] and references therein. For background on numerical integration of Hamiltonian systems, see [6, 10].

Let T^*Q be the phase space of a mechanical system with Hamiltonian function $H : T^*Q \to \mathbb{R}$. Let (q, p) be canonical coordinates on T^*Q. The canonical equations of motion corresponding to H are

$$\frac{dp}{dt} = -\frac{\partial H(q,p)}{\partial q}\,, \quad \frac{dq}{dt} = \frac{\partial H(q,p)}{\partial p}\,. \tag{10}$$

A Sundman transformation is a dynamic time transformation $s \leftrightarrow t$ defined by $dt/ds = g(q,p)$, where g is a strictly positive function on T^*Q called a time scaling function. In the new independent parameter s, eqs. (10) transform to

$$\frac{dp}{ds} = -g(q,p)\frac{\partial H(q,p)}{\partial q}\,, \quad \frac{dq}{ds} = g(q,p)\frac{\partial H(q,p)}{\partial p}\,. \tag{11}$$

If g fulfills the reversibility condition $g(q,p) = g(q,-p)$, then symmetric equidistant discretization schemes may be used on eq. (11) to yield variable time-step methods with good long-time behavior, e. g. near energy preservation. See [3, 4, 7].

A drawback of Sundman transformations is that the eqs. (11) generally fail to be canonical. Indeed, as is pointed out in [14], they can only be canonical if g is a first integral of eq. (10). By using another class of time transformations, so called Poincaré transformations, it is possible to overcome this obstacle. The key is to introduce a new Hamiltonian function

$$\bar{H}(q,p) = g(q,p)(H(q,p) - H_0)\,, \tag{12}$$

where $H_0 = H(p_{\text{init}}, q_{\text{init}})$ and $(q_{\text{init}}, p_{\text{init}})$ are the initial conditions. The canonical equations for $\bar{H}$ are

$$\begin{aligned}
\frac{dp}{ds} &= -\frac{\partial \bar{H}(q,p)}{\partial q} = -g(q,p)\frac{\partial H(q,p)}{\partial q} - \frac{\partial g(q,p)}{\partial q}(H(q,p) - H_0)\,,\\
\frac{dq}{ds} &= \frac{\partial \bar{H}(q,p)}{\partial p} = g(q,p)\frac{\partial H(q,p)}{\partial p} + \frac{\partial g(q,p)}{\partial p}(H(q,p) - H_0)\,.
\end{aligned} \tag{13}$$

It is a straightforward result that the solution curves ζ of eq. (10) and $\bar{\zeta}$ of eq. (13), with matching initial conditions $(q_{\text{init}}, p_{\text{init}})$, are related to each other by a reparametrization:

$$\bar{\zeta}(s) = \zeta(\sigma(s))\,, \quad \sigma(s) = \int_0^s g(\bar{\zeta}(u))\,\mathrm{d}u\,. \tag{14}$$

Variable time-step symplectic methods are obtained by applying equidistant symplectic discretizations to (13). See [2,5].

Remark 1.1 The Hamiltonian $\bar{H}$ is generally not separable, even though H is. An immediate consequence is that the construction of explicit methods becomes troublesome. Indeed, discretizations that yield explicit symplectic methods for separable Hamiltonians, generally fail to be explicit for non-separable Hamiltonians. However, by imposing additional conditions on g, e. g. that it only depends on position coordinates, it is still possible to attain explicit methods, see [5, Sect. 4].

2 Variable time-step variational integrators

2.1 Time transformations in Lagrangian mechanics

In this section we derive some results on time transformations in Lagrangian mechanics. The results are later used in the construction of adaptive variational integrators.

In order to introduce a dynamic time transformation, with a strictly positive scaling function l on TQ, we consider a transformed Lagrangian $\bar{L}$ defined by

$$\bar{L}(q,\dot{q}) = l(q,\dot{q})\left(L\left(q, \frac{\dot{q}}{l(q,\dot{q})}\right) + E_0\right)\,. \tag{15}$$

The following result asserts that $\bar{L}$ is properly defined.

Proposition 2.1 *Let γ be the solution curve of a system with Lagrangian function L and initial conditions $(q_{init}, \dot{q}_{init})$. Let $\bar{\gamma}$ be the solution curve of the system with Lagrangian function $\bar{L}$ defined by eq.* (15) *and initial conditions $(\bar{q}_{init}, \dot{\bar{q}}_{init})$, where $\bar{q}_{init} = q_{init}$ and $\dot{\bar{q}}_{init} = l(\bar{q}_{init}, \dot{\bar{q}}_{init})\dot{q}_{init}$. Then γ and $\bar{\gamma}$ are related by a reparametrization $t = \sigma(s)$:*

$$\gamma(\sigma(s)) = \bar{\gamma}(s)\,, \quad \sigma(s) = \int_0^s l\left(\bar{\gamma}(u), \bar{\gamma}'(u)\right)\,\mathrm{d}u\,. \tag{16}$$

Proof. As σ is a strictly monotone C^1–function we have $\gamma'(t) = \frac{1}{\sigma'(s)}\frac{d}{ds}\gamma(\sigma(s))$. Since $\gamma(t)$ fulfills the Euler–Lagrange equation for L, it holds that

$$\frac{d}{ds}\frac{\partial L}{\partial \dot{q}}\left(\gamma(\sigma(s)), \frac{1}{\sigma'(s)}\frac{d}{ds}\gamma(\sigma(s))\right) - \sigma'(s)\frac{\partial L}{\partial q}\left(\gamma(\sigma(s)), \frac{1}{\sigma'(s)}\frac{d}{ds}\gamma(\sigma(s))\right) = 0\,. \tag{17}$$

Due to energy conservation $E\left(\gamma(\sigma(s)), \frac{1}{\sigma'(s)}\frac{d}{ds}\gamma(\sigma(s))\right) - E_0 = 0$ we may add

$$\begin{aligned}&\frac{d}{ds}\left(\frac{\partial l}{\partial \dot{q}}\left(\gamma(\sigma(s)), \frac{d}{ds}\gamma(\sigma(s))\right)\left(E\left(\gamma(\sigma(s)), \frac{1}{\sigma'(s)}\frac{d}{ds}\gamma(\sigma(s))\right) - E_0\right)\right)\\ &-\frac{\partial l}{\partial q}\left(\gamma(\sigma(s)), \frac{d}{ds}\gamma(\sigma(s))\right)\left(E\left(\gamma(\sigma(s)), \frac{1}{\sigma'(s)}\frac{d}{ds}\gamma(\sigma(s))\right) - E_0\right)\end{aligned}$$

to the right hand side of eq. (17) without affecting it. With the substitution eq. (16) this is precisly $\bar{\gamma}$ inserted in the Euler–Lagrange equation for $\bar{L}$. From the chain rule it is clear that $(\bar{\gamma}(0), \bar{\gamma}'(0))$ is given by $(\bar{q}_{\text{init}}, \dot{\bar{q}}_{\text{init}})$. □

As l is a function on TQ it might in itself be thought of as a Lagrangian function. From eq. (9) it follows that the energy associated with l is $e(q,\dot{q}) = \frac{\partial l(q,\dot{q})}{\partial \dot{q}}\dot{q} - l(q,\dot{q})$. The energy associated with $\bar{L}$ is given by the product

$$\bar{E}(q,\dot{q}) = -e(q,\dot{q})\left(E\left(q, \frac{\dot{q}}{l(q,\dot{q})}\right) - E_0\right)\,. \tag{18}$$

Due to energy conservation we have $\bar{E}(\bar{\gamma}(s), \bar{\gamma}'(s)) = 0$. In fact, it follows from Proposition 2.1 that

$$E\left(\bar{\gamma}(s), \frac{\bar{\gamma}'(s)}{l(\bar{\gamma}(s), \bar{\gamma}'(s))}\right) = E_0\,. \tag{19}$$

Remark 2.2 A solution to a Hamiltonian system is a path $t \mapsto \zeta(t)$ in the phase space T^*Q. Likewise, it is common to think of a solution to a Lagrangian system as a path $t \mapsto (\gamma(t), \gamma'(t))$ in the velocity phase space TQ. A fundamental difference between the time transformations described in this section and Poincaré time transformations is that the latter preserves the phase space path whereas the former does not. A pratical consequence is that, in our approach, the scaling function is given in scaled coordinates.

2.2 Discrete time-scaling transformations

The framework of discrete mechanics is developed by "discrete imitation" of principles in Lagrangian mechanics. Following this guideline it is natural to consider discrete counterparts to the principles in Sect. 2.1. First, we introduce a discrete scaling function l_d, which is a positive function on $Q \times Q$ depending on the discretization parameter ε. We say that l_d is an order r approximation of l if

$$l_d\left(\bar{\gamma}(0), \bar{\gamma}(\varepsilon); \varepsilon\right) - \int_0^{\varepsilon} l\left(\bar{\gamma}(u), \bar{\gamma}'(u)\right)\, \mathrm{d}u = \mathcal{O}(\varepsilon^{r+1})\,. \tag{20}$$

Next, we introduce a transformed discrete Lagrangian

$$\bar{L}_d(q_0, q_1; \varepsilon) = L_d\left(q_0, q_1\,;\, l_d(q_0, q_1; \varepsilon)\right) + l_d(q_0, q_1; \varepsilon) E_0\,. \tag{21}$$

The idea is that if L_d approximates L, then $\bar{L}_d$ should approximate $\bar{L}$ in eq. (15). We now give a result which validates this idea.

Proposition 2.3 *Let l_d be an order r approximation of l and let L_d be of order r relative to L. Then $\bar{L}_d$, given by eq.* (21)*, is of order r relative to $\bar{L}$ in eq.* (15)*.*

Proof. Due to Proposition 2.1 we have (with the same symbols)

$$\bar{L}_d(\bar{\gamma}(0), \bar{\gamma}(\varepsilon); \varepsilon) - \int_0^{\varepsilon} \bar{L}\left(\bar{\gamma}(u), \bar{\gamma}'(u)\right)\, \mathrm{d}u = \bar{L}_d\left(\bar{\gamma}(0), \bar{\gamma}(\varepsilon); \varepsilon\right) - \int_0^{\sigma(\varepsilon)} \left(L\left(\gamma(u), \gamma'(u)\right) + E_0\right)\, \mathrm{d}u\,. \tag{22}$$

From the assumption on l_d and the definition of $\bar{L}_d$ it follows that

$$\bar{L}_d\left(\bar{\gamma}(0), \bar{\gamma}(\varepsilon); \varepsilon\right) - L_d\left(\gamma(0), \gamma(\sigma(\varepsilon)); \sigma(\varepsilon)\right) - \sigma(\varepsilon) E_0 = \mathcal{O}(\varepsilon^{r+1})\,. \tag{23}$$

Substituting eq. (23) in eq. (22) yields

$$\begin{aligned} &\bar{L}_d(\bar{\gamma}(0), \bar{\gamma}(\varepsilon); \varepsilon) - \int_0^{\varepsilon} \bar{L}\left(\bar{\gamma}(u), \bar{\gamma}'(u)\right)\, \mathrm{d}u \\ &= L_d\left(\gamma(0), \gamma(\sigma(\varepsilon)); \sigma(\varepsilon)\right) - \int_0^{\sigma(\varepsilon)} L\left(\gamma(u), \gamma'(u)\right)\, \mathrm{d}u + \mathcal{O}(\varepsilon^{r+1}) = \mathcal{O}(\sigma(\varepsilon)^{r+1}) + \mathcal{O}(\varepsilon^{r+1})\,, \end{aligned} \tag{24}$$

where the last equality follows from the assumption on L_d. The result now follows since $\sigma(\varepsilon)/\varepsilon$ is bounded near $\varepsilon = 0$. □

In particular, for systems on the standard form eq. (8), we consider discrete scaling functions on the form $l_d^{\beta}(q_0, q_1; \varepsilon) = \varepsilon l\left((1-\beta)q_0 + \beta q_1, \frac{q_0 - q_1}{\varepsilon}\right)$. Together with the discrete Lagrangians L_d^{α} in eq. (6) these scaling functions yield a class of time-scaling transformed discrete Lagrangians $\bar{L}_d^{\alpha,\beta}$ and a corresponding symmetric class

$$\bar{L}_d^{\mathrm{sym},\alpha,\beta} = \tfrac{1}{2}\left(\bar{L}_d^{\alpha,\beta} + \bar{L}_d^{1-\alpha,1-\beta}\right)\,. \tag{25}$$

The DEL equations for $\bar{L}_d^{\alpha,\beta}$ and for $\bar{L}_d^{\mathrm{sym},\alpha,\beta}$ define variable time-step integrators $\bar{F}_d^{\alpha,\beta}$ and $\bar{F}_d^{\mathrm{sym},\alpha,\beta}$. $\bar{F}_d^{\alpha,\beta}$ is of order two if and only if $\alpha = 1/2$, otherwise it is of order one. $\bar{F}_d^{\mathrm{sym},\alpha,\beta}$ is of order two.

Generally these methods are implicit. However, if $\alpha = \beta = 0$ and l only depends on q, the method $\bar{F}_d^{\alpha,\beta}$ can be made explicit by solving a second degree polynomial equation. Indeed, the DEL equation in this case is on the form

$$q_2 - q_1 = (c + \|q_2 - q_1\|_M^2) v\,, \qquad \|q\|_M = q^T M q\,, \tag{26}$$

where $c \in \mathbb{R}$ and $v \in Q$ depend on q_0 and q_1, but not on q_2. By taking the squared energy norm on both sides, a scalar second degree polynomial equation in $\|q_2 - q_1\|_M^2$ is obtained. As this equation can be solved analytically, an explicit expression for q_2 is retrieved from eq. (26).

3 Application to contact problems

3.1 Problem formulation

Consider a mechanical system of $b = b_{\text{dyn}} + b_{\text{fixed}}$ bodies. Let $q = (q^1, \dots, q^{b_{\text{dyn}}})$ be position coordinates for body 1 to b_{dyn}. The remaining bodies are fixed. Let d_{ij} for $1 \le i < j \le b$ be the shortest distance between body i and j, negative when the bodies intersect. If each body has a smooth boundary, then $d_{ij} = d_{ij}(q)$ is a smooth function of q.

Let $\Delta(d) = \max(0, -d)$. To each pair of bodies there is a non-negative function $V_{ij} : \mathbb{R} \to \mathbb{R}_+$, such that $V_{ij}(\Delta(d_{ij}))$ as a potential function describes interaction between body i and j due to contact. That is, V_{ij} defines the contact model used. It is required that $V_{ij}(0) = V'_{ij}(0) = 0$, so that $V_{ij}(\Delta(d_{ij}))$ is a continuously differentiable function of q, which is necessary in order for the Euler–Lagrange equation to be well posed. For simplicity we assume that the only forces in the system are contact forces. The potential function for the entire system is given by

$$V = \sum_{i<j} V_{ij}\left(\Delta(d_{ij})\right) , \tag{27}$$

and the Lagrangian function by eq. (8), with a block diagonal non-singular mass matrix M.

3.2 Choice of scaling function

In this section a suitable scaling function l is derived. We restrict ourselves to the case where l only depends on position coordinates.

Consider a test problem in the standard form eq. (8), with $Q = \mathbb{R}$, $M = 1$ and potential function $V(q) = \omega^2 q^2/2$. With initial conditions $(0, \dot{q}_{\text{init}})$ the solution is $\gamma(t) = \dot{q}_{\text{init}} \sin(\omega t)/\omega$. In order to "normalize" the stiffness in the equation, we seek a scaling function which scales approximatelly as $1/\omega$. Thus, a natural choice is $l(q) = (|V''(q)| + c_{\text{lim}})^{-1/2}$, where $c_{\text{lim}} > 0$ is a "limiter factor" to limit the scaling when V'' vanishes. Another motivation for this choice is that, on velocity level, the principle local error term for a first order constant time-step integrator is proportional to V''.

For a system with potential function in the form (27) we have

$$V''(q) = \sum_{i<j} V''_{ij}\left(\Delta(d_{ij})\right) \Delta'(d_{ij})^2 A_{ij} A_{ij}^T + V'_{ij}\left(\Delta(d_{ij})\right) B_{ij} , \quad A_{ij} = \frac{\partial}{\partial q} d_{ij} , \quad B_{ij} = \frac{\partial^2}{\partial q^2} \Delta(d_{ij}) . \tag{28}$$

There is a problem with this expression: A_{ij} and B_{ij} are discontinuous, since Δ is not continuously differentiable. Our solution is to introduce a smooth penalty parameter defined by

$$\tilde{\Delta}(d) = \int_0^{-d} \left(\frac{\arctan(-x/c_{\text{smooth}})}{\pi} + \tfrac{1}{2} \right) \mathrm{d}x , \quad c_{\text{smooth}} > 0 \tag{29}$$

and replace Δ in eq. (27) by $\tilde{\Delta}$. The function then obtained is denoted $\tilde{V}$. Now, a natural choice of scaling function is $l(q) = (\|\tilde{V}''(q)\| + c_{\text{lim}})^{-1/2}$. With this construction, the scaling function fulfills the required regularity, i. e., it is continuously differentiable. However, its derivative $\partial l/\partial q$, which is needed in the DEL equation, is a rather complicated function. Indeed, it requires the derivatives $\partial^3 d_{ij}/\partial q^3$, so for complex models it is expensive to evaluate. A simplification is to assume that $\partial d_{ij}/\partial q^i = \partial d_{ij}/\partial q^j \approx \mathrm{Id}$ (the identity matrix) and that off diagonal elements of $A_{ij} A_{ij}^T$ are zero. This simplification is used in Example 3.3 below.

Remark 3.1 We stress that the introduced smoothness is *not* used to modify the contact model defined by (27). It is only used in order to construct a suitable scaling function. That is, we use V, not $\tilde{V}$, as potential function for the problem.

3.3 Numerical examples

Example 3.2 The aim of this example is to investigate how the methods derived in Sect. 2 adapt to instant stiffness switches in the Euler–Lagrange equation.

In view of Sect. 3.1, we consider the system defined by: $b_{\text{dyn}} = 1$, $b_{\text{fixed}} = 2$, $d_{12}(q) = -q$, $d_{13}(q) = q$, $V_{12}(\Delta) = K_1 \Delta^2/2$, $V_{13}(\Delta) = K_2 \Delta^2/2$. It describes a particle bouncing between a soft and a stiff wall. The potential function is

$$V(q) = K_1 \max(0, q)^2/2 + K_2 \min(0, q)^2/2 , \quad q \in Q = \mathbb{R} . \tag{30}$$

The stiffness parameters are $K_1 = 1$ and $K_2 = 10^4$, and the initial conditions are $q_{\text{init}} = 1$, $\dot{q}_{\text{init}} = 0$. Notice that the solution is periodic and that it can be calculated analytically.

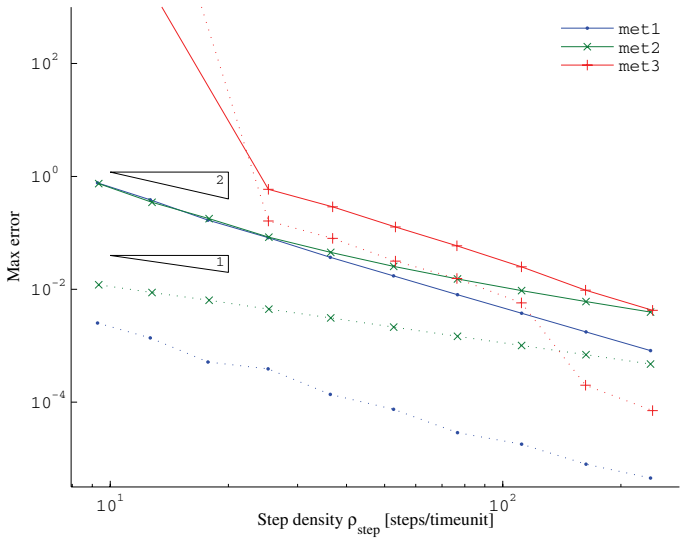

Fig. 2 (online colour at: www.zamm-journal.org) Results from Example 3.2. The maximal error in position (full drawn lines) and energy (dotted lines) versus the step density ρ_{step}. The triangles show order 1 and order 2 slopes.

Table 1 Settings for `met1`, `met2` and `met3` in Example 3.2.

	ε	c_{lim}	c_{smooth}
`met1`	$[0.01, 0.3]$	0	0.033ε
`met2`	$[0.01, 0.3]$	0	0.04ε

	Abs. tol.	Rel. tol.
`met3`	[2.2e–7, 1.5e–3]	Abs. tol.

The problem was integrated from $t_{\text{start}} = 0$ to $t_{\text{end}} = 200$ (which is about 63 periods) with the following methods:

`met1` Defined by $\bar{L}_d^{\alpha,\beta}$ with $\alpha = \beta = 1/2$ and scaling function as in Sect. 3.2 (non-simplified).

`met2` Defined by $\bar{L}_d^{\alpha,\beta}$ with $\alpha = \beta = 0$ and scaling function as in Sect. 3.2 (non-simplified).

`met3` MATLAB's `ode15s` BDF–method with maximal order 2.

For each method 10 different simulations, with decreasing tolerance, were computed. See Table 1 for the exact settings used. The mean step density ρ_{step} for a simulation is defined as

$$\rho_{\text{step}} = \frac{\text{number of steps}}{t_{\text{end}} - t_{\text{start}}} .$$

For each simulation the maximum global errors in position and in energy versus the step density ρ_{step} are plotted in Fig. 2. The results show that `met1` and `met2` are competitive in comparison with `met3`, especially at low accuracy levels (small step densities). The error in energy is plotted in Fig. 3. Notice that `met1` and `met2` show the good long time energy behaviour which is typical for variational integrators. The behaviour of the time-step sequence for the methods is plotted in Fig. 4.

Example 3.3 This example constitutes a simple billiard: $b_{\text{dyn}} = 4$ balls bouncing agains each other and surrounding walls. The walls are given by the square

$$\left\{(q^x, q^y) \in \mathbb{R}^2 ;\ 0 \le q^x \le 1,\ 0 \le q^y \le 1\right\}$$

and the radius of the balls is 0.1. In terms of Sect. 3.1, the potential function is defined by $V_{ij}(\Delta) = K\Delta^2/2$, with $K = 10^4$, i. e., a linear penalty contact model with stiffness K is used for all the contacts.

As initial positions, the balls are placed such that if the first ball has initial velocity $(\dot{q}^x, \dot{q}^y) = (1, 1)$ and the other balls have zero initial velocity, then the exact solution is periodic. See Fig. 5. Due to momentum and energy conservation

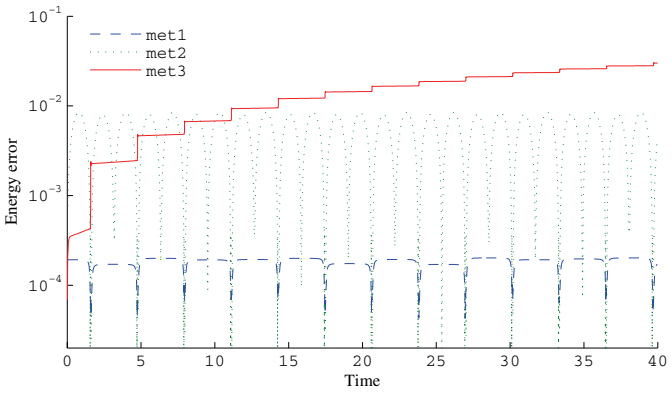

Fig. 3 (online colour at: www.zamm-journal.org) Results from Example 3.2. The error in energy versus time for the first 40 time units for each of the tested methods (taken from the 5:th tolerance level). Notice the good long time behaviour of `met1` and `met2`. This property is typical for variational integrators.

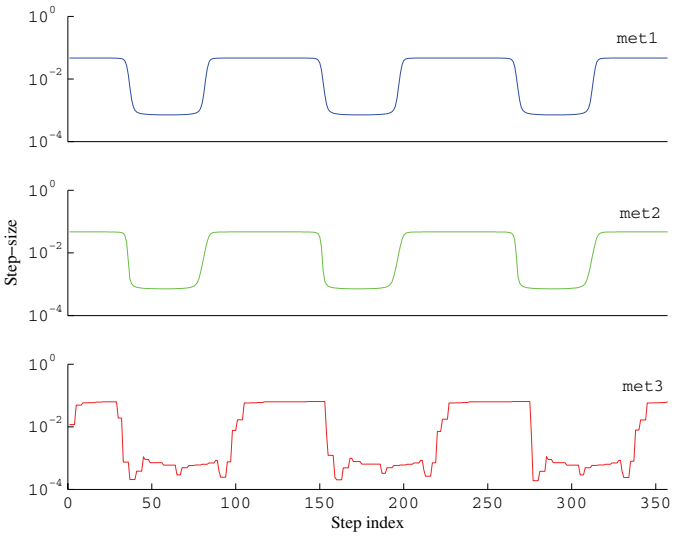

Fig. 4 (online colour at: www.zamm-journal.org) Results from Example 3.2. Comparison between the time-step sequence of the tested methods, for simulations with about the same step density ρ_{step} (taken from the 5th tolerance level). Notice the smoother step-size behaviour of `met1` and `met2` compared with `met3`.

Ball 1 should make a full stop after impact with Ball 2 which should continue with the same velocity as Ball 1 had before the impact.

The problem was integrated from $t_{\text{start}} = 0$ to $t_{\text{end}} = 2.0$ with `met1`, `met2` and `met3` using the simplified scaling function derived in Sect. 3.2. Each method was used with 10 different tolerance levels. At t_{end} the speed of Ball 1–3 in the exact solution is zero. Hence, the sum of the speeds of Ball 1–3 can be used as an error measure. See Fig. 6 for a plot of this measure versus the step density and Fig. 7 for a plot of the step-size behaviour for the first 1000 steps. As in the previous example, `met1` and `met2` perform well compared with `met3`.

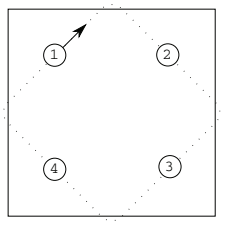

Fig. 5 Setup in Example 3.3. The initial velocity of Ball 1 is such that the dotted path is followed in the exact solution.

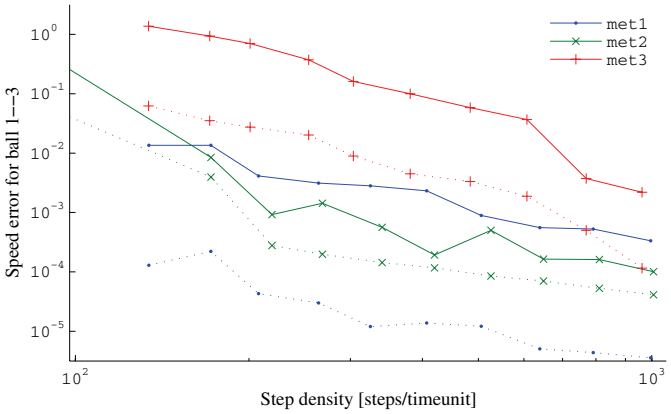

Fig. 6 (online colour at: www.zamm-journal.org) Error in speed at t_{end} for Ball 1–3 (full drawn lines) and error in energy (dotted lines) versus step density ρ_{step} for each tested method.

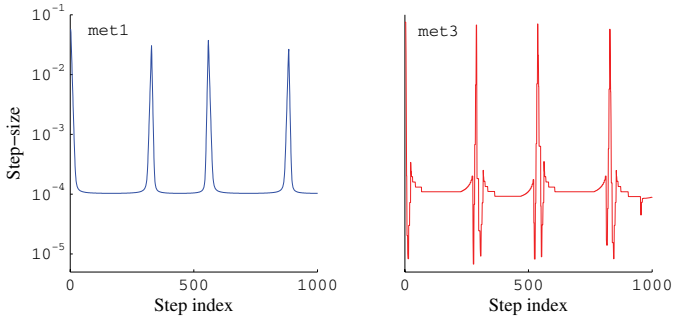

Fig. 7 (online colour at: www.zamm-journal.org) Step-size sequence for the first 1000 steps with `met1` and `met3` (taken from the 10th tolerance level). Notice again that `met1` yields a smoother step-size sequence than `met3`. Also, the "drops" in `met3` down to about 10^{-5}, which are likely due to failed steps, do not occur in `met1`.

4 Conclusions

Variable time-step methods have been developed within the framework of variational integrators. Hence, adaptive integrators with structural properties suitable for mechanical problems have been obtained. A time scaling function suitable for dynamic multibody problems governed by contact force laws of penalty type have been developed. Numerical examples with methods from the class given by $\bar{L}_d^{\alpha,\beta}$ have been tested with the derived scaling function. The results show that the methods adapt the time-step length to contact conditions in a more stable and more efficient way than a standard adaptive BDF method.

Acknowledgements The authors are grateful to Dag Fritzson and Gustaf Söderlind for helpful discussions and comments on the work.

References

[1] V. I. Arnold, Mathematical methods of classical mechanics (Springer-Verlag, New York, 1989).
[2] S. Blanes and C. J. Budd, Explicit, adaptive, symplectic (easy) integrators using scale invariant regularisations and canonical transformations, Celest. Mech. Dyn. Astron. (Netherlands) **89**, 383–405 (2004).

[3] S. Blanes and C.J. Budd, Adaptive geometric integrators for hamiltonian problems with approximate scale invariance, SIAM J. Sci. Comput. **26**, 1089–1113 (2005).
[4] S.D. Bond and B.J. Leimkuhler, Time-transformations for reversible variable stepsize integration, Numer. Algorithms (Netherlands) **19**(1–4), 55–71 (1998).
[5] E. Hairer, Variable time step integration with symplectic methods, Appl. Numer. Math. **25**, 219–227 (1997).
[6] E. Hairer, C. Lubich, and G. Wanner, Geometric Numerical Integration (Springer-Verlag, Berlin, 2002).
[7] E. Hairer and G. Söderlind, Explicit, time-reversible, adaptive step size control, accepted for publication in SIAM J. Sci. Comput. (2005).
[8] C. Kane, J. Marsden, M. Ortiz, and M. West, Variational integrators and the newmark algorithm for conservative and dissipative mechanical systems, Int. J. Numer. Math. Eng. **49**, 1295–1325 (2000).
[9] C. Kane, J.E. Marsden, and M. Ortiz, Symplectic-energy-momentum preserving variational integrators, J. Math. Phys. **40**(7), 3353–3371 (1999).
[10] B. Leimkuhler and S. Reich, Simulating Hamiltonian Dynamics (Cambridge University Press, Cambridge, 2004).
[11] J.E. Marsden and T.S. Ratiu, Introduction to Mechanics and Symmetry, second ed. (Springer-Verlag, New York, 1999).
[12] J.E. Marsden and M. West, Discrete mechanics and variational integrators, Acta Numer. **10**, 357–514 (2001).
[13] L. Stacke and D. Fritzson, Dynamical behaviour of rolling bearings: simulations and experiments, Proc. Inst. Mech. Eng. **215**, 499–508 (2001).
[14] D. Stoffer, Variable steps for reversible integration methods, Computing **55**(1), 1–22 (1995).
[15] J. Struckmeier, Hamiltonian dynamics on the symplectic extended phase space for autonomous and non-autonomous systems, J. Phys. A: Math. Gen. **38**, 1257–1278 (2005).

Book Review

Russel C. Hibbeler, Technische Mechanik, Pearson Education München et al., *Band 2 Festigkeitslehre*, 5., überarb. u. erw. Auflage 2005, 1000 S., gebunden, EUR 49.95, CHF 83.50, ISBN 3-8273-7134-1 und *Band 3 Dynamik*, 10., überarb. u. erw. Auflage 2006, 900 S., gebunden, EUR 49.95, CHF 83.50, ISBN 3-8273-7135-X

Mit den beiden Bücher schließt der dreibändige Grundkurs Technische Mechanik (wie er an deutschen Universitäten und Fachhochschulen üblicherweise gelehrt wird) ab. Dieser Kurs ist hauptsächlich auf Studiengänge des Maschinenbaus orientiert, wobei diese Einschränkung hauptsächlich auf die Beispiele hinweist. Die Lehrinhalte zur Theorie sind für alle Studienrichtungen weitgehend identisch.

Die Bücher stellen eine Alternative zu den zahlreichen auf dem Büchermarkt befindlichen Grundkursen dar. Das Besondere ist der „typische amerikanische Stil“, der insbesondere auf zahlreichen Beispielen (durchgerechnet mit vollständiger Lösung) beruht. Damit erhält der Studierende einen anschaulichen Einblick in das von vielen als schwer empfundene Lehrgebiet. Gleichzeitig eignet es sich sehr gut als Buch zum Selbststudium, wobei auch hier unterstützende Aufgaben (nur mit Lösungen) helfen. Ein weiterer Vorteil ist die Unterstützung des Textes durch Bilder.

Der Band 2 gliedert sich in 14 Kapitel: Spannung, Verzerrung, mechanische Materialeigenschaften, Zug/Druck, Torsion, Biegung, Biegung-Verformung, Querkraftschub, ebener und räumlicher Spannungszustand, ebener und räumlicher Verzerrungszustand, komplizierte Bauteile und Belastungen, Dimensionierung von Balken und Wellen, Knicken von Druckstäben, Energiemethoden. Mit den Anhängen (Geometrische Eigenschaften einer Fläche, Geometrische Eigenschaften von Profilträgern, Neigungswinkel und Durchbiegung von Balken) werden wichtige Informationen für die Lösung praktischer Probleme bereitgestellt. Im Band 3 sind in 12 Kapiteln die Elemente der Dynamik behandelt: Kinetik eines Massenpunktes: Bewegungsgleichung, Kinetik eines Massenpunktes: Arbeit und Energie, Kinetik eines Massenpunktes: Impuls und Drehimpuls, Ebene Kinematik eines starren Körpers: Bewegungsgleichungen, Ebene Kinematik eines starren Körpers: Arbeit und Energie, Ebene Kinematik eines starren Körpers: Impuls und Drehimpuls, Räumliche Kinematik eines starren Körpers, Räumliche Kinetik eines starren Körpers, Analytische Prinzipien, Schwingungen. Dazu gibt es die Anhänge (Mathematische Ausdrücke, Numerische und Computergestützte Rechnung, Vektorrechnung) sowie Wiederholungskapitel. Letztere bieten eine weitere Möglichkeit zum Selbststudium.

Halle (Saale) **Barbara Renner**

Paper III

Klas Modin.
J. Mult. Body Dyn., 222(4):289–300, special issue on Newtonian mechanics, 2008

On explicit adaptive symplectic integration of separable Hamiltonian systems

K Modin[1,2]
[1]SKF Engineering and Research Centre, MDC, Göteborg, Sweden
[2]Centre for Mathematical Sciences, Lund University, Box 118, SE-221 00 Lund, Sweden. email: kmodin@maths.lth.se

The manuscript was received on 20 June 2008 and was accepted after revision for publication on 20 august 2008.

DOI: 10.1243/14644193JMBD171

Abstract: Based on a known observation that symplecticity is preserved under certain Sundman time transformations, adaptive symplectic integrators of an arbitrary order are constructed for separable Hamiltonian systems, for two classes of scaling functions. Due to symplecticity, these adaptive integrators have excellent long-time energy behaviour, which is theoretically explained using standard results on the existence of a modified Hamiltonian function.

In Contrast to reversible adaptive integration, the constructed methods have good long-time behaviour also for non-reversible systems. Numerical examples of this are given.

Keywords: symplectic integration, adaptivity, variable step-size

1 INTRODUCTION

In 1687, Newton published *Philosophiae Naturalis Principia Mathematica* [**1**] in which his second axiom of mechanics first appeared.

Newton's second axiom. *The rate of change of momentum of a body is proportional to the resultant force acting on the body and is in the same direction.*

Later, in his work *Decouverte d'un nouveau principe de Mecanique* [**2**] published 1752, Euler stated it on the differential form, which is the most familiar one known today

$$m\dot{\boldsymbol{v}} = \boldsymbol{F} \tag{1}$$

where m is the mass of a particle, $\boldsymbol{v} = (v^1, v^2, v^3)$ is its velocity vector and $\boldsymbol{F}$ is the net force acting on it.

See reference [**3**, Part II] for further reading on the history of Newtonian mechanics.

During the early evolution of mechanics, the concept of 'force' was not altogether clear, despite Newton's work. In particular, the relation between force and energy was diffuse. Indeed, there was a dispute on conservation laws in mechanics, and their connection to Newton's second axiom. Followers of Newton and Descartes considered conservation of momentum $\sum_i m_i \boldsymbol{v}_i$ as the guiding principle, whereas the German scholars, headed by Leibniz, considered conservation of what was called *vis viva* (living force) $\sum_i m_i |\boldsymbol{v}_i|^2$ to be more fundamental. The dispute was eventually solved when Lagrange in 1788 published *Méchanique analytique* [**4**]. Heavily influenced by Euler's work, Lagrange suggested that the governing equations for any mechanical system have the form

$$\frac{\mathrm{d}}{\mathrm{d}t}\frac{\partial L}{\partial \dot{\boldsymbol{q}}} = \frac{\partial L}{\partial \boldsymbol{q}} \tag{2}$$

where $L = T - V$ (the quantity today called the *Lagrangian*) is the difference between kinetic energy $T = \sum_i m_i |\boldsymbol{v}_i|^2/2$ and potential energy V. Lagrange also showed that the form of these equations, today called the Euler–Lagrange equations, remain the same regardless of which coordinates $\boldsymbol{q} = (q^1, \ldots, q^d)$ are used.

See reference [**5**, Part II] for a thorough account of Lagrangian mechanics and reference [**3**, Part III] for details on its history.

A further reformulation of mechanics is the so-called Hamilton–Jacobi theory. Hamilton, who had been working in optics, applied his ideas on ray theory to the field of dynamics in two ground-breaking publications [**6**, **7**]. In doing so, he found that the path integral between two points on a solution to the Euler–Lagrange equations fulfills a partial differential

equation. He then deduced that the full solution to the Euler–Lagrange equations could be obtained by solving this partial differential equation. Further, he showed that the Euler–Lagrange equations, when expressed using canonical coordinates $\boldsymbol{q}$ and $\boldsymbol{p} = \partial L/\partial \dot{\boldsymbol{q}}$, constitute a particularly symmetric set of first-order differential equations

$$\dot{\boldsymbol{q}} = \frac{\partial H}{\partial \boldsymbol{p}}, \quad \dot{\boldsymbol{p}} = -\frac{\partial H}{\partial \boldsymbol{q}} \tag{3}$$

where $H = T + V$ is the total energy of the system (today called the Hamiltonian). From a theoretic viewpoint, the framework of Hamiltonian mechanics is often easier to work with than Lagrangian mechanics due to its rich geometric structure. In particular, a solution to the Hamilton equations (3) preserves the canonical symplectic form.

Comprehensive references on Hamiltonian mechanics are [**5**, Part III], [**8**], and [**9**]. They also serve as preliminaries for the continuation of the current paper. See reference [**3**, Part IV] for details on the history of Hamiltonian mechanics.

This paper is concerned with the numerical integration of a mechanical system expressed on the Hamiltonian form (3). More precisely, with the construction of explicit adaptive numerical integration algorithms for separable Hamiltonian systems. That is, for systems on a symplectic vector space $\mathcal{P}$ (called phase space) of dimension 2d, with canonical coordinates $\boldsymbol{z} = (\boldsymbol{q}, \boldsymbol{p})$, and with a Hamiltonian function of the form

$$H(\boldsymbol{q}, \boldsymbol{p}) = T(\boldsymbol{p}) + V(\boldsymbol{q})$$

By 'adaptive', it is meant that the time step is varied in correspondence to the local character of the dynamics.

The vector field on $\mathcal{P}$ obtained from H by the Hamilton equations (3) is denoted X_H. Thus, the governing equations are

$$\dot{\boldsymbol{z}} = X_H(\boldsymbol{z}) = X_T(\boldsymbol{z}) + X_V(\boldsymbol{z}) \tag{4}$$

The corresponding flow map is denoted φ_H^t.

A general question of interest in the numerical integration of equation (4) is the near conservation of first integrals over long time intervals. It is well known that a symplectic integrator of order r applied to equation (4) corresponds (at least formally) to the exact flow of a modified Hamiltonian system with a Hamiltonian function $\tilde{H}(\boldsymbol{z}) = H(\boldsymbol{z}) + \mathcal{O}(h^r)$, where h is the step size [**10**, section IX.3]. In particular, the existence of a (formal) modified Hamiltonian implies that H is nearly conserved for exponentially long times, if the numerical solution stays on a compact subset of $\mathcal{P}$, [**10**, section IX.8]. For Hamiltonian problems that are integrable or near-integrable (in the classical Arnold–Liouville sense), symplectic integrators will give a linear global error growth, and all the action variables (first integrals) will be nearly conserved for exponentially long times [**10**, chapter X]. For reversible integrators, it is known that if equations (4) is integrable reversible (see [**10**, section XI.1]), i.e. the problem is reversible and there is a reversible diffeomorphism into action–angle variables, then all action variables are nearly conserved (in particular the Hamiltonian). However, in general, a reversible integrator does not yield the near conservation of H, not even if equation (4) is reversible, as is demonstrated in references [**11**] and [**12**].

Since the Hamiltonian vector fields X_T and X_V are explicitly integrable, i.e. the flows φ_T^t and φ_V^t can be explicitly computed (in this case simply by applying forward Euler), it is possible to construct explicit symplectic integrators for equation (4). Indeed, by various compositions of φ_T^t with φ_V^t symplectic integrators of low or high orders may be constructed. These are so-called Hamiltonian splitting methods [**13**–**15**]. As an example, the Störmer–Verlet method, which is symmetric and of the second order, is given by the symmetric composition $\varphi_T^{t/2} \circ \varphi_V^t \circ \varphi_T^{t/2}$.

Implementation of adaptive step-size control for geometric methods is non-trivial. Indeed, for symplectic and/or reversible methods, conventional step-size strategies destroy the structure-preserving properties that give their excellent long time behaviour, noticed in references [**16**] and [**17**]. As a remedy, the common approach is to introduce a dynamic time transformation of the original system, and then to utilize a structure-preserving discretization of the transformed system. This technique allows the construction of adaptive geometric methods, i.e. methods that uphold good long-time behaviour and at the same time gain from adaptivity in terms of improved local accuracy.

This article investigates techniques for fully explicit adaptive symplectic integrators for problems of the form (4). Different techniques, allowing for different types of scaling functions, are considered.

This section continues with a review of different time transformation techniques used in conjunction with geometric integration. The main results are in section 2, where two classes of explicit, adaptive, symplectic methods are suggested. Comparison with the adaptive reversible method based on step density transformation is given in section 3 for several problems. Conclusions are given in section 4.

In the matter of notation, $|\boldsymbol{v}|$ is used for the Euclidean norm of coordinate vectors, and $\boldsymbol{u} \cdot \boldsymbol{v}$ for the Euclidean inner product. The canonical Poisson bracket between two smooth real-valued functions on $\mathcal{P}$ is denoted $\{G, H\}$. The canonical symplectic matrix is denoted J.

1.1 Time transformation techniques

In principle, three types of time-transformed reformulations of equation (4) have been considered. Below, each of them is reviewed.

1.1.1 *Sundman transformation*

The idea is to introduce a new independent variable τ such that $\mathrm{d}t/\mathrm{d}\tau = G(\boldsymbol{z})$, where G is a positive function on $\mathcal{P}$ called the scaling function. Substituting $t \leftrightarrow \tau$ in equation (4) gives a new time-transformed system

$$\frac{\mathrm{d}\boldsymbol{z}}{\mathrm{d}\tau} = G(\boldsymbol{z})X_H(\boldsymbol{z}) \quad \text{or shorter} \quad \frac{\mathrm{d}\boldsymbol{z}}{\mathrm{d}\tau} = X_{G,H}(\boldsymbol{z}) \tag{5}$$

Indeed, the relation between the flow φ_H of equation (4) and $\varphi_{G,H}$ of equation (5) is given by a reparametrization of time

$$\begin{aligned} &\varphi^{\tau}_{G,H}(\boldsymbol{z}) = \varphi_H^{\sigma(\tau,\boldsymbol{z})}(\boldsymbol{z}) \quad \text{where} \\ &\sigma(\tau,\boldsymbol{z}) = \int_0^{\tau} G(\varphi^{x}_{G,H}(\boldsymbol{z}))\mathrm{d}x \end{aligned} \tag{6}$$

During the integration, physical time is reconstructed by the equation $\mathrm{d}t/\mathrm{d}\tau = G(\boldsymbol{z})$. Since equation (4) is autonomous, reconstruction of time does not alter the dynamics of the system.

If the system (5) is reversible, i.e. $X_{G,H}(\boldsymbol{q},\boldsymbol{p}) = -X_{G,H}(\boldsymbol{q},-\boldsymbol{p})$, then a reversible discretization of equation (5) yields a reversible adaptive method. In particular, it is possible to construct explicit, adaptive, reversible methods with this approach [**18**].

It was noticed in reference [**19**] that the vector field $X_{G,H}$ in equation (5) is symplectic if and only if $X_H \| X_G$, i.e. if the vector fields X_H and X_G are parallel. In turn, this implies that G must be of the form $G(\boldsymbol{z}) = g(H(\boldsymbol{z}))$. Since this essentially leads to constant steps (up to the numerical error in the conservation of the Hamiltonian) the Sundman transformation has not been used for constructing symplectic integrators. (The necessity of $X_H \| X_G$ is referred to as a 'disappointing fact' in reference [**10**, section VIII.2.1].) However, in conjunction with splitting, Sundman transformations still allow the construction of explicit adaptive symplectic integrators for a family of scaling functions, as is described in section 2 of this article.

1.1.2 *Poincaré transformation*

Here, a transformed Hamiltonian is introduced by

$$K(\boldsymbol{z}) = G(\boldsymbol{z})(H(\boldsymbol{z}) - H_0) \tag{7}$$

where H_0 is the value of H at the initial conditions $\boldsymbol{z}_0 \in \mathcal{P}$. Then, on the level set

$$\mathcal{P}^{H_0} = \{\boldsymbol{z} \in \mathcal{P};\ H(\boldsymbol{z}) = H_0\}$$

the flow φ_K^{τ} is a time transformation of φ_H^t, with a scaling function $G(\boldsymbol{z})$. Thus, by utilizing a symplectic integrator for the Hamiltonian system given by K, adaptive symplectic integration of equation (4) is obtained [**20–22**].

Notice that K is not separable although H is, which makes it cumbersome to construct explicit adaptive methods based on this approach. However, if G only depends on $\boldsymbol{q}$, then the symplectic Euler method turns out to be semi-explicit, in the sense that only a second-order scalar polynomial equation needs to be solved [**20**]. Furthermore, it is sometimes possible to introduce a symplectic change of coordinates so that K becomes separable. This approach is taken in references [**23**] and [**24**] to construct 'Explicit, Adaptive, SYmplectic (EASY)' integrators. However, the construction of arbitrary-order explicit methods based on the Poincaré transformation (7), for general scaling objectives, is still an open problem.

In reference [**25**], a time transformation similar to the Poincaré transformation, but formulated in the framework of Lagrangian mechanics, is used to achieve adaptivity for variational integrators (see reference [**26**]).

Step density transformation. This approach was suggested in reference [**27**]. An augmented phase space $\mathcal{P} \times \mathbb{R}$, with coordinates $(\boldsymbol{z}, \varrho)$, is introduced. Let Q be a strictly positive function on $\mathcal{P}$. The augmented set of governing equations is given by

$$\begin{aligned} \frac{\mathrm{d}\boldsymbol{z}}{\mathrm{d}\tau} &= X_H(\boldsymbol{z})/\varrho \\ \frac{\mathrm{d}\varrho}{\mathrm{d}\tau} &= \{Q,H\}(\boldsymbol{z})/Q(\boldsymbol{z}) \end{aligned} \tag{8}$$

Physical time is reconstructed with the equation $\mathrm{d}t/\mathrm{d}\tau = 1/\varrho$. Notice that the scaling function is $1/\varrho$, and that Q/ϱ is a first integral of equation (8). Thus, the step-size density ϱ is determined by the step density objective function Q. If equation (4) is reversible, and Q fulfils $Q(\boldsymbol{q},\boldsymbol{p}) = Q(\boldsymbol{q},-\boldsymbol{p})$, then equation (8) is reversible with respect to $(\boldsymbol{q},\boldsymbol{p},\varrho) \mapsto (\boldsymbol{q},-\boldsymbol{p},\varrho)$.

By splitting equation (8) into explicitly integrable parts, and then conducting a symmetric composition, an adaptive reversible integrator is obtained. A main result in reference [**27**] is that if equation (4) is integrable reversible, then this integrator will nearly conserve all action variables, including the additional first integral $\varrho/Q(\boldsymbol{z})$, for exponentially long times.

2 EXPLICIT, ADAPTIVE, SYMPLECTIC INTEGRATION OF EQUATION (4)

In this section, two different techniques for the construction of explicit, adaptive, symplectic integration

of equation (4) are discussed. The first approach is feasible for a family of scaling functions based on kinetic and potential energy. The second approach is feasible for integrable systems and scaling functions that are independent of $\boldsymbol{p}$.

2.1 Scaling based on kinetic and potential energy

Denote with $\mathcal{F}_T$ the vector space

$$\mathcal{F}_T = \{S \in \mathcal{C}^\infty(\mathcal{P}, \mathbb{R});\ X_T \parallel X_S\}$$

Let $S \in \mathcal{F}_T$. Then, the Sundman transformed system

$$\frac{\mathrm{d}\boldsymbol{z}}{\mathrm{d}\tau} = S(\boldsymbol{z})X_T(\boldsymbol{z}) \quad \text{or shorter} \quad \frac{\mathrm{d}\boldsymbol{z}}{\mathrm{d}\tau} = X_{S,T}(\boldsymbol{z}) \tag{9}$$

is symplectic, and corresponds to a time transformation of X_T. One obtains the following result.

Lemma 1

The system (9) has the following properties.

1. It is Hamiltonian with a globally defined Hamiltonian function, i.e. there exists a function E on $\mathcal{P}$ such that $X_E = X_{S,T}$. Furthermore, E is independent of $\boldsymbol{q}$.
2. The flow $\varphi_{S,T} = \varphi_E$ is explicitly integrable.

Proof
The vector field in equation (9) is symplectic on all of $\mathcal{P}$. Thus, the map $JX'_{S,T}(\boldsymbol{z})$ is symmetric for all $\boldsymbol{z} \in \mathcal{P}$. From the integrability lemma [**10**, Lemma 2.7, Ch. VI] it follows that there exists a globally defined Hamiltonian E on $\mathcal{P}$ such that $X_{S,T} = X_E$. Since $X_E \| X_T$ and T is independent of $\boldsymbol{q}$, it holds that $\partial E/\partial \boldsymbol{q} = 0$, i.e. E is independent of $\boldsymbol{q}$. For this reason, it also follows that X_E is explicitly integrable by the explicit Euler method.

In symmetry, if $U \in \mathcal{F}_V$, then $\varphi_{U,V} = \varphi_F$ is a symplectic flow of a Hamiltonian system for some Hamiltonian function F on $\mathcal{P}$.

The notion here is to find $S \in \mathcal{F}_T$ and $U \in \mathcal{F}_V$ such that they are equal on the exact solution trajectory, i.e. such that

$$S(\varphi_H^t(\boldsymbol{z}_0)) = U(\varphi_H^t(\boldsymbol{z}_0)) \quad \text{for all } t \tag{10}$$

By composing $\varphi_{S,T}$ with $\varphi_{U,V}$, and asserting theoretically that $S(\boldsymbol{z}) \approx U(\boldsymbol{z})$ throughout the simulation, it is then possible to achieve explicit, adaptive, symplectic integration schemes.

The Hamiltonian $H = T + V$ is conserved by the exact flow. Hence, knowing the energy level H_0 on a trajectory of φ_H, it is possible to compute the value of V from the value of T, and the other way around. The idea is to use a scaling objective that is a function of the kinetic energy T and the potential energy V, i.e. of the form $\boldsymbol{z} \mapsto g(T(\boldsymbol{p}), V(\boldsymbol{q}))$. On the level set $\mathcal{P}^{H_0}$, one then obtains

$$\begin{aligned} g(T(\boldsymbol{p}), V(\boldsymbol{q})) &= \underbrace{g(T(\boldsymbol{p}), H_0 - T(\boldsymbol{p}))}_{S(\boldsymbol{p})} \\ &= \underbrace{g(H_0 - V(\boldsymbol{q}), V(\boldsymbol{q}))}_{U(\boldsymbol{q})} \end{aligned} \tag{11}$$

Theorem 2

With S and U as in equation (11), the vector field

$$\begin{aligned} X_{S,T|U,V}(\boldsymbol{z}) &= X_{S,T}(\boldsymbol{z}) + X_{U,V}(\boldsymbol{z}) \\ &= S(\boldsymbol{p})X_T(\boldsymbol{z}) + U(\boldsymbol{q})X_V(\boldsymbol{z}) \end{aligned}$$

has the following properties.

1. It is Hamiltonian with a globally defined separable Hamiltonian function $C(\boldsymbol{q}, \boldsymbol{p}) = E(\boldsymbol{p}) + F(\boldsymbol{q})$.
2. On the level set $\mathcal{P}^{H_0}$, its flow $\varphi_{S,T|U,V} = \varphi_C$ is a time transformation of φ_H with a scaling function g.

Proof
It holds that $S \in \mathcal{F}_T$ and $U \in \mathcal{F}_V$. Thus, from Lemma 1 it follows that

$$X_{S,T|U,V} = X_E + X_F = X_{E+F}$$

where E is independent of $\boldsymbol{q}$ and F is independent of $\boldsymbol{p}$. Thus, $X_{S,T|U,V}$ is a Hamiltonian vector field corresponding to the separable Hamiltonian $C = E + F$.

The set $\mathcal{P}^{H_0}$ is a sub-manifold of $\mathcal{P}$. X_H restricted to $\mathcal{P}^{H_0}$ is a vector field on $\mathcal{P}^{H_0}$, i.e. it is tangent to $\mathcal{P}^{H_0}$ (since H is conserved by its flow). Thus, the Sundman transformed vector field gX_H, restricted to $\mathcal{P}^{H_0}$, is also a vector field on $\mathcal{P}^{H_0}$. Since $U = S$ on $\mathcal{P}^{H_0}$ it follows that $X_C = gX_H$ on $\mathcal{P}^{H_0}$. Thus, φ_C, restricted to $\mathcal{P}^{H_0}$, is a time transformation of φ_H with a scaling function g.

From the time scaling property in Theorem 2, it follows that adaptive methods for equation (4) are obtained by numerical integration of $\dot{\boldsymbol{z}} = X_C(\boldsymbol{z})$. Since the Hamiltonian C is separable, Hamiltonian splitting methods can be used to construct symplectic methods. Indeed, any order r composition of the form

$$\Phi_\epsilon = \varphi_{U,V}^{\epsilon\alpha_1} \circ \varphi_{S,T}^{\epsilon\beta_1} \circ \cdots \circ \varphi_{U,V}^{\epsilon\alpha_k} \circ \varphi_{S,T}^{\epsilon\beta_k} \tag{12}$$

leads to an explicit, adaptive, symplectic integrator of order r. For order conditions on the composition coefficients α_i and β_i [**13–15**].

Remark

The class of methods (12), restricted to the case $g(T, V) = g(V)$, coincide with the family of methods

suggested in reference [**28**]. Interestingly, the derivation there is completely different: it is based on a special type of Poincaré transformation that preserves separability of the Hamiltonian.

Remark

The approach presented in this section may be extended to other types of splittings $H = H_1 + H_2$, as long as H_1 and H_2 are explicitly integrable.

2.1.1 *Long-time behaviour*

For the proposed class of integrators (12) to be successful, it is essential that the discrete trajectory generated by Φ_ϵ stays $\mathcal{O}(\epsilon^r)$ close to the level set $\mathcal{P}^{H_0}$. In turn, that implies that the energy H is nearly conserved and the 'scaling consistency condition' $S(\boldsymbol{z}) = U(\boldsymbol{z})$ is nearly upheld. The standard tool at hand is backward error analysis. In the spirit of reference [**20**, Theorem 4], one obtains the following result.

Theorem 3

There exists a modified Hamiltonian depending on ϵ

$$\widetilde{H}_\epsilon(\boldsymbol{z}) = H(\boldsymbol{z}) + \epsilon^r H_r(\boldsymbol{z}) + \epsilon^{r+1} H_{r+1}(\boldsymbol{z}) + \cdots$$

and a modified time transformation depending on ϵ

$$\widetilde{\sigma}_\epsilon(\tau, \boldsymbol{z}) = \sigma(\tau, \boldsymbol{z}) + \epsilon^r \sigma_r(\tau, \boldsymbol{z}) + \epsilon^{r+1} \sigma_{r+1}(\tau, \boldsymbol{z}) \cdots$$

such that (formally)

$$(\Phi_\epsilon)^n(\boldsymbol{z}_0) = \varphi^{\widetilde{\sigma}_\epsilon(n\epsilon, \boldsymbol{z}_0)}_{\widetilde{H}_\epsilon}(\boldsymbol{z}_0)$$

Proof

It follows from equation (11) that E is of the form $E(\boldsymbol{p}) = e(T(\boldsymbol{p})) = \int_0^{T(\boldsymbol{p})} g(x, H_0 - x)\mathrm{d}x + \text{const}$. Since the scaling function g is strictly positive, e is bijective. Likewise, $F(\boldsymbol{q}) = f(V(\boldsymbol{q}))$, where f is bijective.

Since Φ_ϵ is a Hamiltonian splitting method, in particular symplectic, it corresponds to the flow $\varphi^\epsilon_{\widetilde{C}_\epsilon}$ of a modified Hamiltonian

$$\widetilde{C}_\epsilon(\boldsymbol{z}) = C(\boldsymbol{z}) + \epsilon^r C_r(\boldsymbol{z}) + \epsilon^{r+1} C_{r+1}(\boldsymbol{z}) + \cdots$$

Next, $\widetilde{E}_\epsilon = \widetilde{C}_\epsilon - F$ and $\widetilde{F}_\epsilon = \widetilde{C}_\epsilon - \widetilde{E}_\epsilon$, and further $\widetilde{T}_\epsilon = e^{-1}(\widetilde{E}_\epsilon)$, $\widetilde{V}_\epsilon = f^{-1}(\widetilde{F}_\epsilon)$, and $\widetilde{H}_\epsilon = \widetilde{T}_\epsilon + \widetilde{V}_\epsilon$ are defined. Notice that $\widetilde{A}_\epsilon = A + \mathcal{O}(\epsilon^r)$ for $A = E, F, T, V, H$, respectively.

$\widetilde{T}_\epsilon$ and $\widetilde{V}_\epsilon$ may be chosen so that $\widetilde{H}_\epsilon(\boldsymbol{z}_0) = H_0$. Let $\widetilde{S}_\epsilon(\boldsymbol{z}) = g(\widetilde{T}_\epsilon(\boldsymbol{z}), H_0 - \widetilde{T}_\epsilon(\boldsymbol{z}))$ and $\widetilde{U}_\epsilon(\boldsymbol{z}) = g(H_0 - \widetilde{V}_\epsilon(\boldsymbol{z}), \widetilde{V}_\epsilon(\boldsymbol{z}))$. It holds that $\widetilde{S}_\epsilon \in \mathcal{F}_{\widetilde{T}_\epsilon}$ and $\widetilde{U}_\epsilon \in \mathcal{F}_{\widetilde{V}_\epsilon}$. Thus, it follows from the same reasoning as in Theorem 2 that on the level set $\widetilde{\mathcal{P}}^{H_0} = \{\boldsymbol{z} \in \mathcal{P}; \widetilde{H}_\epsilon(\boldsymbol{z}) = H_0\}$, the flow $\varphi_{\widetilde{C}_\epsilon}$ is a time transformation of $\varphi_{\widetilde{H}_\epsilon}$ with a scaling function $\widetilde{g}_\epsilon(\boldsymbol{z}) = g(\widetilde{T}_\epsilon(\boldsymbol{z}), \widetilde{V}_\epsilon(\boldsymbol{z}))$. Set $\widetilde{\sigma}_\epsilon(\tau, \boldsymbol{z}) = \int_0^\tau \widetilde{g}_\epsilon(\varphi^x_{\widetilde{C}_\epsilon}(\boldsymbol{z}))\mathrm{d}x$ to the corresponding reparametrisation of time. Since $\boldsymbol{z}_0 \in \widetilde{\mathcal{P}}^{H_0}$, the Theorem follows by expansion in ϵ.

The existence of a formal modified Hamiltonian $\widetilde{H}$, asserted by Theorem 3, implies that the discrete trajectory generated by Φ_ϵ will stay $\mathcal{O}(\epsilon^r)$ close to $\mathcal{P}^{H_0}$ for exponentially long integration times [**10**, section IX.8].

2.1.2 *Possible scaling objectives*

Below, is a list of well-known scaling objectives that are of the form (11).

1. The kinetic energy is frequently of the standard form $T(\boldsymbol{p}) = |\boldsymbol{p}|^2/2$. For such problems, the scaling function
$$S(\boldsymbol{p}) = \sqrt{T(\boldsymbol{p})} \tag{13}$$
yields equidistance in $\boldsymbol{q}$-space, i.e. the scaling is such that $|\boldsymbol{q}_k - \boldsymbol{q}_{k+1}|$ is constant throughout the discrete trajectory. This choice was suggested in reference [**10**, VIII.2.1].
2. The inverse of Lagrangian action $L(\boldsymbol{q}, \boldsymbol{p}) = T(\boldsymbol{p}) - V(\boldsymbol{q})$ may be used. This choice was suggested in reference [**29**].
3. Many N-body problems have a potential function of the form
$$V(\boldsymbol{q}) = -\sum_i V_i(|\mathsf{D}_i \boldsymbol{q}|) \tag{14}$$
where D_i are difference matrices and V_i are strictly positive functions $\mathbb{R} \to \mathbb{R}$ that grow to infinity at zero. The singularities correspond to collisions between particles. Since it is essential to decrease the time step during 'close encounters', the scaling function
$$U(\boldsymbol{q}) = \frac{1}{(-V(\boldsymbol{q}))^\alpha} \tag{15}$$
is suitable. The choice of optimal α depend on the order of the singularities of the functions V_i. For gravitational potentials of the Newton type, the choice $\alpha = 3/2$ is frequently used.

2.2 Scaling independent of $\boldsymbol{p}$

Consider a Poincaré transformed system with a scaling function independent of $\boldsymbol{p}$. That is, a system with a Hamiltonian of the form

$$K(\boldsymbol{z}) = G(\boldsymbol{q})(H(\boldsymbol{z}) - H_0) = G(\boldsymbol{q})(T(\boldsymbol{p}) + V(\boldsymbol{q}) - H_0) \tag{16}$$

As mentioned in the introduction, K cannot, in general, be split into integrable parts.

The notion here is to duplicate the phase space to $\mathcal{P}^2 = \mathcal{P} \times \mathcal{P}$, with coordinates $(\boldsymbol{z}^0, \boldsymbol{z}^1)$. Notice that $\mathcal{P}^2$ inherits the canonical symplectic form on $\mathcal{P}$, with conjugate coordinates $(\boldsymbol{q}^0, \boldsymbol{q}^1)$ and $(\boldsymbol{p}^0, \boldsymbol{p}^1)$. The canonical Poisson bracket on $\mathcal{P}^2$ is given by

$$\{A, B\}^2 = \frac{\partial A}{\partial \boldsymbol{q}^0}\frac{\partial B}{\partial \boldsymbol{p}^0} - \frac{\partial B}{\partial \boldsymbol{q}^0}\frac{\partial A}{\partial \boldsymbol{p}^0} + \frac{\partial A}{\partial \boldsymbol{q}^1}\frac{\partial B}{\partial \boldsymbol{p}^1} - \frac{\partial B}{\partial \boldsymbol{q}^1}\frac{\partial A}{\partial \boldsymbol{p}^1} \tag{17}$$

Given a Hamiltonian of the form (16), it is extended to $\mathcal{P}^2$ by

$$K^2(\boldsymbol{z}^0, \boldsymbol{z}^1) = 2K(\boldsymbol{z}^{1/2}) = 2G(\boldsymbol{q}^{1/2})(T(\boldsymbol{p}^{1/2}) + V(\boldsymbol{q}^{1/2}) - H_0)$$

where $\boldsymbol{z}^{1/2} = \Pi(\boldsymbol{z}^0, \boldsymbol{z}^1)$ and $\Pi : \mathcal{P}^2 \to \mathcal{P}$ is the projection given by $(\boldsymbol{z}^0, \boldsymbol{z}^1) \mapsto (\boldsymbol{z}^0 + \boldsymbol{z}^1)/2$. One obtains the following result.

Lemma 4

For the relation between the system on $\mathcal{P}$ with Hamiltonian K and the system on $\mathcal{P}^2$ with Hamiltonian K^2 it holds that

$$\varphi^\tau_{K^2}(\boldsymbol{z}^0, \boldsymbol{z}^1) = (\varphi^\tau_K(\boldsymbol{z}^{1/2}) + \boldsymbol{z}^0 - \boldsymbol{z}^{1/2}, \varphi^\tau_K(\boldsymbol{z}^{1/2}) + \boldsymbol{z}^1 - \boldsymbol{z}^{1/2})$$

and

$$\Pi(\varphi^\tau_{K^2}(\boldsymbol{z}^0, \boldsymbol{z}^1)) = \varphi^\tau_K(\Pi(\boldsymbol{z}^0, \boldsymbol{z}^1))$$

Proof
Since $\partial K^2/\partial \boldsymbol{z}^0$ always equals $\partial K^2/\partial \boldsymbol{z}^1$, it follows that the governing equations for the $\boldsymbol{z}^0$–part and the $\boldsymbol{z}^1$–part are the same. Thus, $\boldsymbol{z}^0(t) - \boldsymbol{z}^1(t) = \text{const}$. Now, the first assertion follows from the identity $\varphi^0_{K^2}(\boldsymbol{z}^0, \boldsymbol{z}^1) = (\boldsymbol{z}^0, \boldsymbol{z}^1)$. The last assertion is an obvious consequence of the first.

From a Taylor expansion of K^2, it follows that

$$K^2(\boldsymbol{z}^0, \boldsymbol{z}^1) = \underbrace{G(\boldsymbol{q}^0)(H(\boldsymbol{z}^1) - H_0)}_{K^{01}(\boldsymbol{z}^0, \boldsymbol{z}^1)} + \underbrace{G(\boldsymbol{q}^1)(H(\boldsymbol{z}^0) - H_0)}_{K^{10}(\boldsymbol{z}^0, \boldsymbol{z}^1)} + \mathcal{O}(|\boldsymbol{z}_1 - \boldsymbol{z}_0|^2) \tag{18}$$

The flow of $X_{K^{01}+K^{10}}$ coincides with the flow of X_{K^2} on the level-set $\mathcal{P}^2|_{\boldsymbol{z}^0=\boldsymbol{z}^1} = \{(\boldsymbol{z}^0, \boldsymbol{z}^1) \in \mathcal{P}^2; \boldsymbol{z}^0 = \boldsymbol{z}^1\}$. The idea with this construction is that K^{01} and K^{10} can be further split into explicitly integrable Hamiltonian systems, since H is separable. Indeed, it holds that

$$K^{01}(\boldsymbol{z}^0, \boldsymbol{z}^1) = \underbrace{G(\boldsymbol{q}^0)T(\boldsymbol{p}^1)}_{E^{01}(\boldsymbol{z}^0, \boldsymbol{z}^1)} + \underbrace{G(\boldsymbol{q}^0)V(\boldsymbol{q}^1)}_{F^{01}(\boldsymbol{z}^0, \boldsymbol{z}^1)}$$

$$K^{10}(\boldsymbol{z}^0, \boldsymbol{z}^1) = \underbrace{G(\boldsymbol{q}^1)T(\boldsymbol{p}^0)}_{E^{10}(\boldsymbol{z}^1, \boldsymbol{z}^0)} + \underbrace{G(\boldsymbol{q}^1)V(\boldsymbol{q}^0)}_{F^{10}(\boldsymbol{z}^1, \boldsymbol{z}^0)}$$

and it is straightforward to check that $E^{01}, F^{01}, E^{10}, F^{10}$ are explicitly integrable by the explicit Euler method. By (multiple) compositions of $\varphi_{E^{01}}, \varphi_{F^{01}}, \varphi_{E^{10}}$, and $\varphi_{F^{10}}$ a family of symplectic maps that approximates the flow of $\varphi_{K^{01}+K^{10}}$ is obtained. If initial conditions are chosen on $\mathcal{P}^2|_{\boldsymbol{z}^0=\boldsymbol{z}^1}$, this family of methods also approximates the flow φ_{K^2}, which in turn reproduces the flow φ_K, by Lemma 4. Thus, explicit, adaptive, symplectic methods can be constructed for separable systems, for scaling functions independent of $\boldsymbol{p}$.

2.3 Long-time behaviour

Since a method constructed in the manner described is symplectic, it corresponds (formally) to the flow of a modified Hamiltonian $\widetilde{K}^2_\epsilon$. For the method to be useful, it is essential that the first integrals $\boldsymbol{z}^0 - \boldsymbol{z}^1$ of K^2 are nearly conserved. If K^2 constitutes a non-integrable system, then a perturbation of it does not, in general, give a system where $\boldsymbol{z}^0 - \boldsymbol{z}^1 = \text{const}$ is nearly upheld. However, if K^2 is integrable, or near integrable, then in a neighbourhood of $\mathcal{P}^2|_{\boldsymbol{z}^0=\boldsymbol{z}^1}$ the modified Hamiltonian $\widetilde{K}^2_\epsilon$ can be seen as a perturbation of K^2, and the Hamiltonian perturbation theory can be used to assert the near conservation of the first integrals $\boldsymbol{z}^0 - \boldsymbol{z}^1$.

The following result is obtained, which asserts that (near) integrability of K is preserved by K^2.

Lemma 5

If K constitutes a (perturbed) integrable system on $\mathcal{P}$, then K^2 constitutes a (perturbed) integrable system on $\mathcal{P}^2$.

Proof
Assume first that K gives an integrable system. Let $I_1, \ldots, I_d$ denote its first integrals, which are in involution (i.e. $\{I_j, I_i\} = 0$). From Lemma 4, it then follows that $I^2_i(\boldsymbol{z}^0, \boldsymbol{z}^1) = I_i(\boldsymbol{z}^{1/2})$ for $i = 1, \ldots, d$ are first integrals in involution of the duplicated system with a Hamiltonian K^2. One needs to find d additional first integrals in involution. It has already been seen that the functions $Q^2_i(\boldsymbol{z}^0, \boldsymbol{z}^1) = q^0_i - q^1_i$ are first integrals. Thus, it remains to be shown that they are in involution, i.e. that $\{Q^2_i, Q^2_j\}^2 = 0$ and $\{I^2_i, Q^2_j\}^2 = 0$. From (17), it follows directly that $\{Q^2_i, Q^2_j\}^2 = 0$ for all i, j. For the

other, one obtains

$$\{I_i^2, Q_j^2\}^2 = \frac{\partial I_i^2}{\partial p_j^0}\frac{\partial Q_j^2}{\partial q_j^0} + \frac{\partial I_i^2}{\partial p_j^1}\frac{\partial Q_j^2}{\partial q_j^1} = \frac{\partial I_i^2}{\partial p_j^0} - \frac{\partial I_i^2}{\partial p_j^1} = 0$$

If K constitutes a perturbed integrable system, it is of the form $K = L + M$, where L is integrable and M is a small perturbation. It then follows from the definition of K^2 and the first part of the Lemma that $K^2 = L^2 + M^2$, where L^2 is integrable and M^2 is a small perturbation.

Since $\widetilde{K}_\epsilon^2$ is a perturbation of $K^{01} + K^{10}$, which in turn is a perturbation of K^2 (in a neighbourhood of $\mathcal{P}^2|_{z^0=z^1}$), it follows from reference [**10**, Theorem 4.3, section X.4.3] that, with initial conditions in $\mathcal{P}^2|_{z^0=z^1}$ and ϵ small enough, the flow $\varphi^\tau_{\widetilde{K}_\epsilon^2}$ nearly preserves the first integrals of $\varphi^\tau_{K^2}$ up to $\mathcal{O}(\epsilon^r)$ for exponentially long times. By Hairer *et al.* [**10**, Remark 4.8, section X.4.3], the result can be extended to the case when K^2 is near integrable, in which case $\varphi^\tau_{\widetilde{K}_\epsilon^2}$ nearly preserves the near first integrals of $\varphi^\tau_{K^2}$. Using Lemma 5, it is now concluded that the constructed methods are useful in the case when K is integrable or near integrable.

3 NUMERICAL EXAMPLES

In this section, some numerical examples of the adaptive, explicit, symplectic schemes derived in section 2 are given, and the result is compared with the algorithm based on the step density transformation, described in section 1. In particular, the following methods are used.

`SYMM` The adaptive version of the Störmer–Verlet method, suggested in reference [**27**]. It is symmetric and second-order accurate, but not symplectic.

`SYMP(T,V)` Integrator suggested in section 2.1 given by $\varphi^{\epsilon/2}_{U,V} \circ \varphi^{\epsilon}_{S,T} \circ \varphi^{\epsilon/2}_{U,V}$. It is symmetric, symplectic, and second-order accurate.

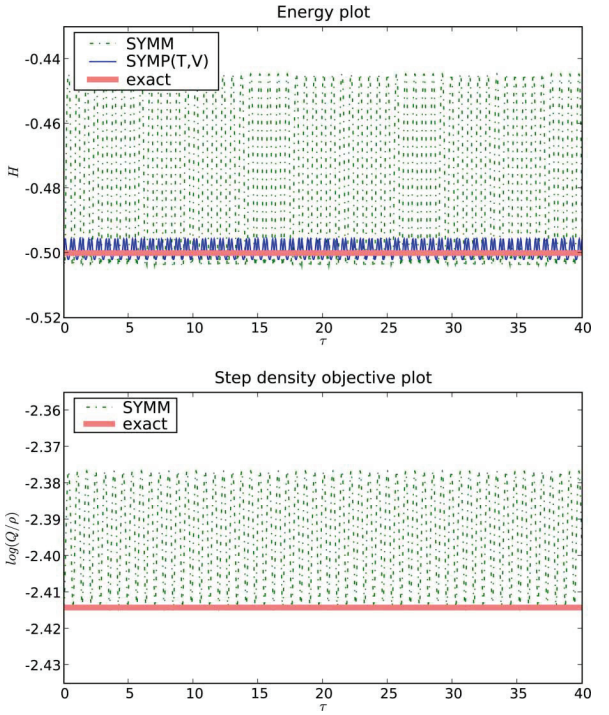

Fig. 1 Results from example 1 (upper). Comparison of energy behaviour for the methods `SYMM` and `SYMP(T,V)` (lower). Additional first integral $\log(Q(\boldsymbol{z})/\varrho$ corresponding to step-size density objective for the `SYMM` method

`SYMP(q)` Integrator suggested in section 2.2 given by

$$\Phi_\epsilon = \varphi_{E^{01}}^{\epsilon/2} \circ \varphi_{F^{01}}^{\epsilon} \circ \varphi_{E^{01}}^{\epsilon/2} \circ \varphi_{E^{10}}^{\epsilon/2} \circ \varphi_{F^{10}}^{\epsilon} \circ \varphi_{E^{10}}^{\epsilon/2}$$

The discrete trajectory is defined by $z_n = \Pi(\Phi_\epsilon^n(z_0, z_0))$. It is symplectic (on $\mathcal{P}^2$) and second-order accurate.

3.1 Example 1: Kepler problem

The Kepler problem has become a standard test problem for the validation of adaptive geometric integrators. The phase space is given by $\mathcal{P} = \mathbb{R}^4$ and the Hamiltonian by

$$H(\boldsymbol{q}, \boldsymbol{p}) = T(\boldsymbol{p}) + V(\boldsymbol{q}) = \frac{|\boldsymbol{p}|^2}{2} - \frac{1}{|\boldsymbol{q}|}$$

The initial conditions are chosen as

$$q_1(0) = 1 - e, \quad q_2(0) = 0, \quad p_1(0) = 0,$$

$$p_2(0) = \sqrt{\frac{1+e}{1-e}}$$

with eccentricity $e = 0.8$.

The scaling function $U(\boldsymbol{q}) = 1/(-V(\boldsymbol{q}))^\alpha$, with $\alpha = 3/2$ is chosen. This choice was previously used in reference [**20**], [**23**], and [**27**]. The corresponding density objective is $Q = 1/U$.

It is well known that the Kepler problem is integrable in the Arnold–Liouville sense, i.e. there exists two first integrals which are in involution. The problem is also reversible integrable, i.e. the diffeomorphism into action–angle variables is a reversible transformation.

The problem was integrated with `SYMM` and `SYMP(T,V)`, with a step-size parameter $\epsilon = 0.02$. The energy error is plotted in Fig. 1 (upper). The error in the step-size density objective $Q(\boldsymbol{q})/\varrho$ is plotted in Fig. 1 (lower). Notice that both the methods show no tendency to an energy drift, which is in accordance with the theory. However, the error constant

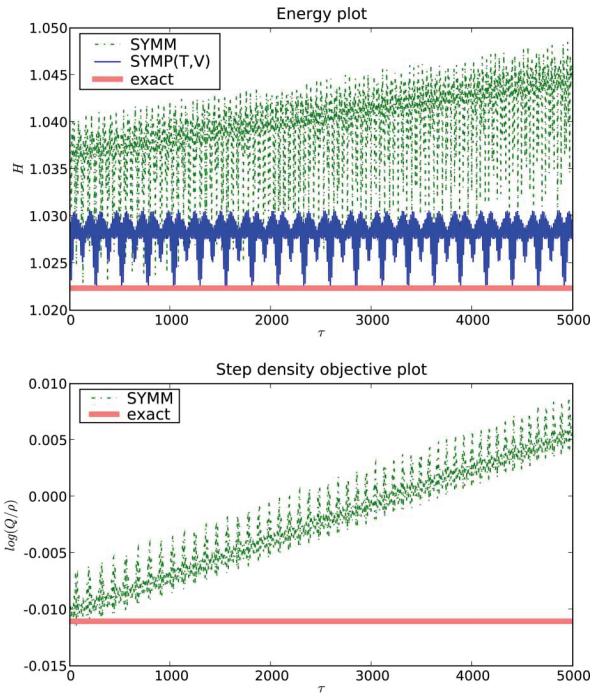

Fig. 2 Results from example 2 (upper). Comparison of energy behaviour for the methods `SYMM` and `SYMP(T,V)` (lower). Additional first integral $\log(Q(z)/\varrho$ corresponding to step-size density objective for the `SYMM` method

for the SYMP(T,V) method is smaller than that for SYMM.

3.2 Example 2: non-reversible oscillator (a)

This example is a particle moving on the real line, bouncing between two potential walls. A small perturbation is introduced, such that the problem is not reversible in p, nor in q. The Hamiltonian is given by

$$H(q,p) = T(p) + V(q) = \frac{p^2}{2} - \varepsilon\frac{p^3}{3} + \frac{1}{q^2} + \frac{1}{(q-10)^2} + \varepsilon q$$

The initial conditions are chosen as

$$q(0) = 1, \quad p(0) = 0$$

The perturbation parameter is set to $\varepsilon = 0.01$.

Close to the singular points $q = 0$ and $q = 10$, the step size needs to be small to capture the dynamics. Up to the small perturbation parameter, the potential function in this problem has the form (14). Thus, a fairly suitable scaling function is $U(q) = 1/V(q)^{\alpha}$; $\alpha = 1/2$ is chosen.

Simulations with SYMM and SYMP(T,V) were carried out with a step-size parameter $\epsilon = 0.2$.

Since the problem is not reversible, the theoretic results developed in reference [**27**] on long-time energy conservation of SYMM does not apply. Being symplectic, the SYMP(T,V) method, however, does retain good long-time energy conservation, regardless of reversability. The simulations confirm this. Indeed, in Fig. 2, it is seen that the SYMM show substantial linear drift in energy, whereas SYMP(T,V) does not. Furthermore, the step-size density objective $\log(Q(q)/\rho)$ of SYMP(T,V) also drifts, which means that relatively soon in the simulation the step-size selection is incorrect.

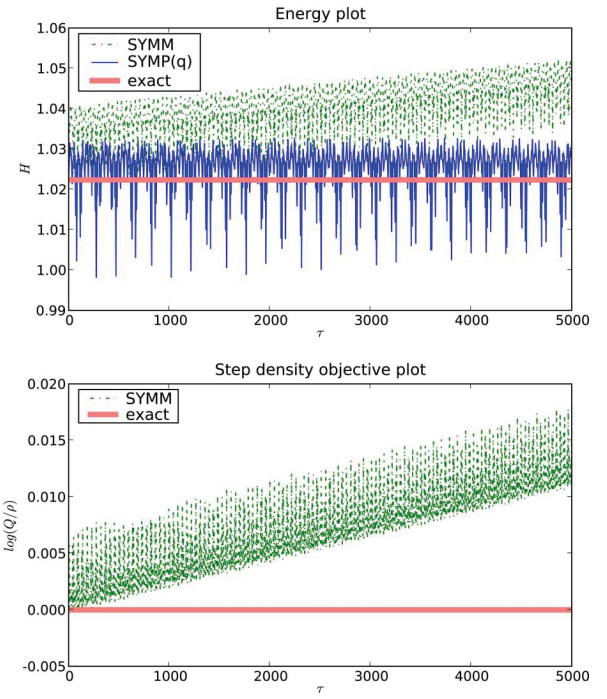

Fig. 3 Results from example 3 (upper). Comparison of energy behaviour for the methods SYMM and SYMP(p) (lower). Additional first integral $\log(Q(z)/\varrho$ corresponding to step-size density objective for the SYMM method

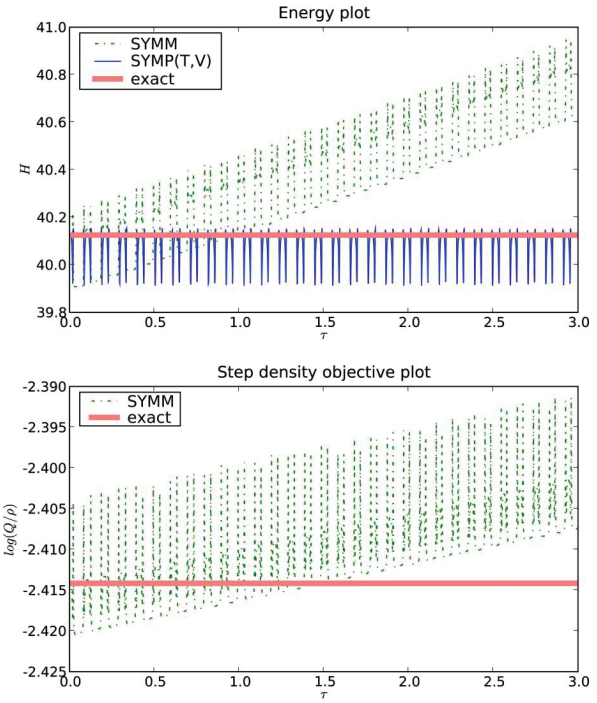

Fig. 4 Results from example 4 (upper). Comparison of energy behaviour for the methods `SYMM` and `SYMP(T,V)` additional first integral $\log(Q(z)/\varrho$ corresponding to step-size density objective for the `SYMM` method

3.3 Example 3: non-reversible oscillator (b)

In this example, the non-reversible oscillator is considered again. However, a somewhat different scaling objective is considered, given by

$$G(q) = \frac{1}{q^2} + \frac{1}{(q-10)^2}$$

i.e. the perturbation term is not included. Due to this fact, `SYMP(T,V)` cannot be used. However, as the scaling is independent of p, the method `SYMP(q)` can be used.

Simulations with `SYMM` and `SYMP(q)` were carried out with the same setup as in example 2 (except for the slightly different scaling objective).

As in the previous example, drift-off still occurs for the `SYMM` method, as is shown in Fig. 3. One can also see that the drift-off does not occur for the `SYMP(q)` method, due to its symplecticity. However, it should be noted that if $\epsilon = 0.3$ is used instead of $\epsilon = 0.2$, then `SYMP(q)` behaves in a chaotic manner. This is due to the fact that the perturbation away from K^2 (section 2.2) then becomes so large that the system is no longer near integrable.

3.4 Example 4: magnetically perturbed pendulum

This example consists of a planar pendulum of length and mass 1, which is affected by gravity g, and by a magnetically repelling point source of strength μ, which is placed at a distance a δ from the circle traced out by the pendulum. The Hamiltonian is given by

$$H(q,p) = T(p) + V(q) = \frac{p^2}{2} - g\cos(q) + \frac{\mu}{\cos(q)^2 + (1+\delta-\sin(q))^2}$$

The initial conditions

$$q(0) = \pi/2, \quad p(0) = 1/2$$

are chosen such that the kinetic energy is large enough for the pendulum to keep rotating in the same direction. Gravity is set to $g = 1$, and the magnetic source at distance $\delta = 0.05$ with strength $\mu = 0.1$.

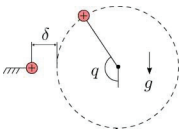

Again, the scaling function is chosen as $U(q) = 1/V(q)^{\alpha}$, with $\alpha = 1/2$, which corresponds to small steps near the magnetic point source, disregarding the $g\cos(q)$ term. Simulations with `SYMM` and `SYMP(T,V)` were carried out with step-size parameter $\epsilon = 0.001$.

Notice that the problem is reversible, i.e. $T(p) = T(-p)$. However, as the pendulum is rotating in the same direction all the time, one always obtains $p > 0$, which means that reversibility is 'not seen'. So, even though the problem is reversible, the reversible method `SYMM` has drift both in energy and in the step-size density objective, as is shown in Fig. 4. The symplectic method `SYMP(T,V)` behaves according to theory, i.e. there is no energy drift.

4 CONCLUSIONS

Based on splitting, two approaches for explicit, adaptive, and symplectic integration of separable Hamiltonian problems have been developed for two families of scaling functions. Second-order versions of the integrators have been compared with the state-of-the-art explicit, adaptive, reversible integrator suggested in reference [**27**], for four example problems. For non-reversible problems, or reversible problems where reversability is 'not shown', the proposed integrators have superior long-time energy behaviour.

ACKNOWLEDGEMENTS

The author is grateful to Dag Fritzson, Claus Führer, and Gustaf Söderlind for helpful and inspiring discussions. The author would also like to thank SKF for the support given.

REFERENCES

1 **Newton, I.** *Philosophiae naturalis principia mathematica*, Londini anno MDCLXXXVII, 1687.
2 **Euler, L.** Decouverte d'un nouveau principe de mecanique. *Mémoires de l'académie des sciences de Berlin*, 1752, **6**, 185–217.
3 **Dugas, R.** *A history of mechanics*, 1988 (Dover Publications Inc., New York). (With a foreword by Louis de Broglie, Translated from the French by J. R. Maddox, Reprint of the 1957 translation).
4 **Lagrange, J. L.** *Mécanique analytique*, 1788 (Paris).
5 **Arnold, V. I.** *Mathematical methods of classical mechanics*, *Graduate texts in mathematics*, 2nd edition, vol. 60, 1989 (Springer-Verlag, New York). (Translated from the Russian by K. Vogtmann and A. Weinstein).
6 **Hamilton, S. W. R.** *First essay on a general method in dynamics*, 1834 (Royal Society of London Philosophical Transactions, London).
7 **Hamilton, S. W. R.** *Second essay on a general method in dynamics*, 1835 (Royal Society of London Philosophical Transactions, London).
8 **Marsden J. E.** and **Ratiu, T. S.** *Introduction to mechanics and symmetry, vol. 17 of texts in applied mathematics*, 2nd edition, 1999 (Springer-Verlag, New York).
9 **Holm, D. D.** *Geometric mechanics. Part I*, 2008 (Imperial College Press, London).
10 **Hairer, E., Lubich, C.,** and **Wanner, G.** *Geometric numerical integration*, vol. 31 of Springer Series in Computational Mathematics, 2nd edition, 2006 (Springer-Verlag, Berlin).
11 **Faou, E., Hairer, E.,** and **Pham, T.-L.** Energy conservation with non-symplectic methods: examples and counter-examples. *BIT*, 2004, **44**(4), 699–709.
12 **McLachlan, R. I.** and **Perlmutter, M.** Energy drift in reversible time integration. *J. Phys. A*, 2004, **37**(45), L593–L598.
13 **Yoshida, H.** Construction of higher order symplectic integrators. *Phys. Lett. A*, 1990, **150**(5–7), 262–268.
14 **Murua, A.** and **Sanz-Serna, J. M.** Order conditions for numerical integrators obtained by composing simpler integrators. *R. Soc. Lond. Philos. Trans. Ser. A Math. Phys. Eng. Sci.*, 1999, **357**(1754), 1079–1100.
15 **McLachlan, R. I.** and **Quispel, G. R. W.** Splitting methods. *Acta Numer.*, 2002, **11**, 341–434.
16 **Gladman, B., Duncan, M.,** and **Candy, J.** Symplectic integrators for long-term integrations in celestial mechanics. *Celestial Mech. Dynam. Astronom.*, 1991, **52**(3), 221–240.
17 **Calvo, M. P.** and **Sanz-Serna, J. M.** Variable steps for symplectic integrators. In *Numerical analysis 1991* (*Dundee, 1991*), *Pitman Research in Notes Mathematical Series*, vol. 260, 1992, pp. 34–48 (Longman Scientific & Technical, Harlow).
18 **Huang, W.** and **Leimkuhler, B.** The adaptive Verlet method. *SIAM J. Sci. Comput.*, 1997, **18**(1), 239–256.
19 **Stoffer, D.** Variable steps for reversible integration methods. *Computing*, 1995, **55**(1), 1–22.
20 **Hairer, E.** Variable time step integration with symplectic methods. *Appl. Numer. Math.*, 1997, **25**(2–3), 219–227.
21 **Reich, S.** Backward error analysis for numerical integrators. *SIAM J. Numer. Anal.*, 1999, **36**(5), 1549–1570.
22 **Mikkola, S.** and **Wiegert, P.** Regularizing time transformations in symplectic and composite integration. *Celestial Mech. Dynam. Astronom.*, 2002, **82**(4), 375–390.
23 **Blanes, S.** and **Budd, C. J.** Explicit adaptive symplectic (easy) integrators: a scaling invariant generalisation of the Levi-Civita and KS regularisations. *Celestial Mech. Dynam. Astronom.*, 2004, **89**(4), 383–405.

24 Blanes, S. and **Budd, C. J.** Adaptive geometric integrators for Hamiltonian problems with approximate scale invariance. *SIAM J. Sci. Comput.*, 2005, **26**(4), 1089–1113.

25 Modin, K. and **Führer, C.** Time-step adaptivity in variational integrators with application to contact problems. *ZAMM Z. Angew. Math. Mech.*, 2006, **86**(10), 785–794.

26 Marsden, J. E. and **West, M.** Discrete mechanics and variational integrators. *Acta Numer.*, 2001, **10**, 357–514.

27 Hairer, E. and **Söderlind, G.** Explicit, time reversible, adaptive step size control. *SIAM J. Sci. Comput.*, 2005, **26**(6), 1838–1851.

28 Preto, M. and **Tremaine, S.** A class of symplectic integrators with adaptive timestep for separable hamiltonian systems. *Astron. J.*, 1999, **118** (5), 2532–2541.

29 Zare, K. and **Szebehely, V.** Time transformations in the extended phase-space, *Celestial Mech.*, 1975, **11**, pp. 469–482.

Paper IV

Klas Modin.
J. Gen. Lie Theory Appl., 3(1):39–52, 2009.

Journal of Generalized Lie Theory and Applications Vol. 3 (2009), No. 1, 39–52

Time transformation and reversibility of Nambu–Poisson systems

Klas MODIN [a,b]

[a] *Centre for Mathematical Sciences, Lund University, Box 118, SE–221 00 Lund, Sweden*
E-mail: kmodin@maths.lth.se

[b] *SKF Engineering & Research Centre, MDC, RKs–2, SE–415 50 Göteborg, Sweden*

Abstract

A time transformation technique for Nambu–Poisson systems is developed, and its structural properties are examined. The approach is based on extension of the phase space $\mathscr{P}$ into $\bar{\mathscr{P}} = \mathscr{P} \times \mathbb{R}$, where the additional variable controls the time-stretching rate. It is shown that time transformation of a system on $\mathscr{P}$ can be realised as an extended system on $\bar{\mathscr{P}}$, with an extended Nambu–Poisson structure. In addition, reversible systems are studied in conjunction with the Nambu–Poisson structure. The application in mind is adaptive numerical integration by splitting of Nambu–Poisson Hamiltonians. As an example, a novel integration method for the rigid body problem is presented and analysed.

2000 MSC: 37M99, 22E70, 53Z05, 34A26

1 Introduction

In 1973 Nambu [23] suggested a generalisation of Hamiltonian mechanics, taking the Liouville condition on volume preservation in phase space as a governing principle. Nambu postulated that the governing equations for a dynamical system on $\mathbb{R}^n$ should have the form

$$\frac{\mathrm{d}x_i}{\mathrm{d}t} = \sum_{j_1,\dots,j_{n-1}} \epsilon_{ij_1\dots j_{n-1}} \frac{\partial H_1}{\partial x_{j_1}} \frac{\partial H_2}{\partial x_{j_2}} \cdots \frac{\partial H_{n-1}}{\partial x_{j_{n-1}}} \tag{1.1}$$

where ϵ is the Levi–Civita tensor over n indices, and $H_1, \dots, H_{n-1}$ are smooth real valued functions on $\mathbb{R}^n$ called Hamiltonian functions. Notice that the vector field in equation (1.1) is source free (its divergence is zero), which implies that the corresponding phase flow is volume preserving.

Later Takhtajan [27] formalised Nambu's framework by introducing the concept of Nambu–Poisson brackets on general phase space manifolds. Based on Takhtajan's work the geometry of Nambu–Poisson structures has been explored in several papers [6, 4, 5, 21, 11, 22, 28, 29].

In this paper we study time transformation of Nambu–Poisson systems. Such transformations are important in the construction and analysis of adaptive structure preserving numerical time stepping methods [26, 10, 3, 7, 24, 18, 2, 20, 19]. The idea is to obtain time step adaptivity by equidistant discretisation in the transformed variable, which corresponds to non-equidistant discretisation in the original time variable. Although numerical integration is a main motivation, the focus in the paper is not on numerical issues, but rather on structural properties.

The current section continues with a brief review of Nambu–Poisson mechanics, and of a time transformation method by Hairer and Söderlind [9]. The main results are in Section 2, where time transformation for Nambu–Poisson systems is developed. In Section 3, the Nambu–Poisson

structure is studied in conjunction with reversibility. As an application, we show in Section 4 how to construct fully explicit, adaptive numerical integration methods based on splitting of the Nambu–Poisson Hamiltonians. In particular, a novel method for the free rigid body. Conclusions are given in Section 5.

We adopt the following notation. $\mathscr{P}$ denotes a phase space manifold of dimension n, with local coordinates $\boldsymbol{x} = (x_1, \dots, x_n)$. The algebra of smooth real valued functions on $\mathscr{P}$ is denoted $\mathcal{F}(\mathscr{P})$. Further, $\mathfrak{X}(\mathscr{P})$ denotes the linear space of vector fields on $\mathscr{P}$. The Lie derivative along $X \in \mathfrak{X}(\mathscr{P})$ is denoted $\mathcal{L}_X$. If $X, Y \in \mathfrak{X}(\mathscr{P})$ then the commutator $[X, Y] = \mathcal{L}_X Y$ supplies $\mathfrak{X}(\mathscr{P})$ with an infinite dimensional Lie algebra structure. Its corresponding Lie group is the set $\mathrm{Diff}(\mathscr{P})$ of diffeomorphisms on $\mathscr{P}$, with composition as group operation. (See McLachlan and Quispel [16] and Schmid [25] for issues concerning infinite dimensional Lie groups.) If $\Phi \in \mathrm{Diff}(\mathscr{P})$ then Φ^* denotes the pull-back map and Φ_* the push-forward map imposed by Φ.

1.1 Nambu–Poisson mechanics

In Hamiltonian mechanics, the phase space manifold $\mathscr{P}$ is equipped with a Poisson structure, defined by a bracket operation $\{\cdot_1, \cdot_2\} : \mathcal{F}(\mathscr{P}) \times \mathcal{F}(\mathscr{P}) \to \mathcal{F}(\mathscr{P})$ that is skew-symmetric, fulfils the Leibniz rule and the Jacobi identity. Nambu–Poisson mechanics is a generalisation.

Definition 1.1. A Nambu–Poisson manifold of order k consists of a smooth manifold $\mathscr{P}$ together with a multilinear map

$$\{\cdot_1, \dots, \cdot_k\} : \underbrace{\mathcal{F}(\mathscr{P}) \times \ldots \times \mathcal{F}(\mathscr{P})}_{k \text{ times}} \to \mathcal{F}(\mathscr{P})$$

that fulfils:

- total skew-symmetry

$$\{H_1, \dots, H_k\} = \mathrm{sgn}(\sigma)\{H_{\sigma_1}, \dots, H_{\sigma_k}\} \tag{1.2a}$$

- Leibniz rule

$$\{GH_1, \dots, H_k\} = G\{H_1, \dots, H_m\} + H_1\{G, H_2, \dots, H_k\} \tag{1.2b}$$

- fundamental identity

$$\begin{aligned}\{H_1, \dots, H_{k-1}, \{G_1, \dots, G_k\}\} = {} & \{\{H_1, \dots, H_{k-1}, G_1\}, G_2, \dots, G_k\} \\ & + \{G_1, \{H_1, \dots, H_{k-1}, G_2\}, G_3, \dots, G_k\} + \dots \\ & + \{G_1, \dots, G_{k-1}, \{H_1, \dots, H_{k-1}, G_k\}\}\end{aligned} \tag{1.2c}$$

Remark 1.1. The case $k = 2$ coincides with ordinary Poisson manifolds.

The first two conditions, total skew-symmetry (1.2a) and Leibniz rule (1.2b), are straightforward: they imply that the bracket is of the form

$$\{H_1, \dots, H_k\} = \eta(\mathrm{d}H_1, \dots, \mathrm{d}H_k)$$

for some totally skew-symmetric contravariant k–tensor η [27]. The third condition, the fundamental identity (1.2c), is more intricate. The range of possible Poisson–Nambu brackets is heavily restricted by this condition [27].

A Nambu–Poisson system on a Nambu–Poisson manifold of order k is determined by $k-1$ Hamiltonian function $H_1, \ldots, H_{k-1} \in \mathcal{F}(\mathscr{P})$. The governing equations are

$$\frac{\mathrm{d}F}{\mathrm{d}t} = \{H_1, \ldots, H_{k-1}, F\} \qquad \forall\, F \in \mathcal{F}(\mathscr{P}) \tag{1.3a}$$

which may also be written

$$\frac{\mathrm{d}\boldsymbol{x}}{\mathrm{d}t} = X_{H_1,\ldots,H_{k-1}}(\boldsymbol{x}) \tag{1.3b}$$

where $X_{H_1,\ldots,H_{k-1}} \in \mathfrak{X}(\mathscr{P})$ is defined by $\mathcal{L}_{X_{H_1,\ldots,H_{k-1}}} F = \{H_1, \ldots, H_{k-1}, F\}$. The corresponding flow map is denoted $\varphi^t_{H_1,\ldots,H_{k-1}}$. Notice that due to skew symmetry of the bracket, all the Hamiltonians $H_1, \ldots, H_{k-1}$ are first integrals, which follows from equation (1.3a).

Due to the fundamental identity (1.2c), Nambu–Poisson systems fulfil certain properties which have direct counterparts in Hamiltonian mechanics (the case $k = 2$).

Theorem 1.1 (Takhtajan [27])**.** *The set of first integrals of system* (1.3) *is closed under the Nambu–Poisson bracket. That is, if $G_1, \ldots, G_k$ are first integrals, then $\{G_1, \ldots, G_k\}$ is again a first integral.*

Theorem 1.2 (Takhtajan [27])**.** *The flow of system* (1.3) *preserves the Nambu–Poisson structure. That is,*

$$\{G_1, \ldots, G_k\} \circ \varphi^t_{H_1,\ldots,H_{k-1}} = \{G_1 \circ \varphi^t_{H_1,\ldots,H_{k-1}}, \ldots, G_n \circ \varphi^t_{H_1,\ldots,H_{k-1}}\} \qquad \forall\, G_1, \ldots, G_k \in \mathcal{F}(\mathscr{P})$$

or equivalently

$$\mathcal{L}_{X_{H_1,\ldots,H_{k-1}}} \eta = 0 \tag{1.4}$$

Remark 1.2. The set of vector fields that fulfils equation (1.4) is denoted $\mathfrak{X}_\eta(\mathscr{P})$. Clearly $\mathfrak{X}_\eta(\mathscr{P})$ is closed under linear combinations, so it is a sub-space of $\mathfrak{X}(\mathscr{P})$. Further, since $\mathcal{L}_{[X,Y]}\eta = \mathcal{L}_X(\mathcal{L}_Y\eta) - \mathcal{L}_Y(\mathcal{L}_X\eta)$ it is also closed under the commutator. Thus, $\mathfrak{X}_\eta(\mathscr{P})$ is a Lie sub-algebra of $\mathfrak{X}(\mathscr{P})$. Correspondingly, $\mathrm{Diff}_\eta(\mathscr{P})$ denotes the Lie sub-group of $\mathrm{Diff}(\mathscr{P})$ that preserves the Nambu–Poisson structure. An element $\Phi \in \mathrm{Diff}_\eta(\mathscr{P})$ is called an η–map.

Remark 1.3. It is important to point out that in general not every $X \in \mathfrak{X}_\eta(\mathscr{P})$ corresponds to a Nambu–Poisson system, i.e., a system of the form of equation (1.3). The reason is that the set of vector fields of the form of equation (1.3) is not closed under linear combinations.

There are also fundamental differences between Hamiltonian and Nambu–Poisson mechanics, i.e., between $k = 2$ and $k \geq 3$. In particular there is the following result, conjectured by Chatterjee and Takhtajan [4] and later proved by several authors.

Theorem 1.3 ([6, 1, 22, 11, 13])**.** *A totally skew-symmetric contravariant tensor of order $k \geq 3$ is a Nambu–Poisson tensor if and only if it is locally decomposable about any regular point. That is, about any point $\boldsymbol{x} \in \mathscr{P}$ such that $\eta(\boldsymbol{x}) \neq 0$ there exist local coordinates $(x_1, \ldots, x_k, x_{k+1}, \ldots, x_n)$ such that*

$$\eta = \frac{\partial}{\partial x_1} \wedge \cdots \wedge \frac{\partial}{\partial x_k}$$

Thus, every Nambu–Poisson tensor with $k \geq 3$ is in essence a determinant on a sub-manifold of dimension k. It is not so for Poisson tensors.

1.2 Time transformation of dynamical systems

In this section we review the time transformation technique developed in Hairer and Söderlind [9]. Consider a dynamical system

$$\frac{\mathrm{d}\boldsymbol{x}}{\mathrm{d}t} = X(\boldsymbol{x}), \qquad X \in \mathfrak{X}(\mathscr{P}) \tag{1.5}$$

Its flow map is denoted φ_X^t. Introduce an extended phase space $\bar{\mathscr{P}} = \mathscr{P} \times \mathbb{R}$, with local coordinates $\bar{\boldsymbol{x}} = (\boldsymbol{x}, \xi)$. The projection $\bar{\mathscr{P}} \ni \bar{\boldsymbol{x}} \mapsto \boldsymbol{x} \in \mathscr{P}$ is denoted Π, and $\bar{\mathscr{P}} \ni \bar{\boldsymbol{x}} \mapsto \xi \in \mathbb{R}$ is denoted π. Let $Q \in \{F \in \mathcal{F}(\mathscr{P}); F > 0\}$ and consider the extension of system (1.5) into

$$\begin{cases} \dfrac{\mathrm{d}\boldsymbol{x}}{\mathrm{d}\tau} = X(\boldsymbol{x})/\xi \\ \dfrac{\mathrm{d}\xi}{\mathrm{d}\tau} = (\mathcal{L}_X Q)(\boldsymbol{x})/Q(\boldsymbol{x}) \end{cases} \qquad \text{or shorter} \qquad \frac{\mathrm{d}\bar{\boldsymbol{x}}}{\mathrm{d}\tau} = \bar{X}(\bar{\boldsymbol{x}}) \tag{1.6}$$

The flows of the two systems are related by a reparametrisation $t \leftrightarrow \tau$.

Theorem 1.4 (Hairer and Söderlind [9])**.** *The flow of the extended system* (1.6) *restricted to* $\mathscr{P}$ *is a time transformation of the flow of system* (1.5)*. That is,*

$$\Pi\varphi_{\bar{X}}^{\tau}(\bar{\boldsymbol{x}}) = \varphi_X^{\sigma(\tau,\bar{\boldsymbol{x}})}(\boldsymbol{x}), \quad \forall\, \bar{\boldsymbol{x}} \in \bar{\mathscr{P}}, \tau \in \mathbb{R} \qquad \textit{where} \qquad \sigma(\tau,\bar{\boldsymbol{x}}) \equiv \int_0^\tau \frac{\mathrm{d}s}{\pi\varphi_{\bar{X}}^s(\bar{\boldsymbol{x}})}$$

Further, $Q(\boldsymbol{x})/\xi$ *is a first integral of system* (1.6)*.*

Proof. From equation (1.6) it follows directly that $\Pi_*\bar{X}$ is parallel with X. Thus, $\Pi\varphi_{\bar{X}}^{\tau}$ and φ_X^t define the same phase diagrams. It remains to find the relation between t and τ. Since $\mathrm{d}x/\,\mathrm{d}t = (\,\mathrm{d}t/\,\mathrm{d}\tau)(\,\mathrm{d}x/\,\mathrm{d}\tau)$ it follows from equation (1.6) that $\mathrm{d}t/\,\mathrm{d}\tau = 1/\xi$. Integration of this relation gives $\sigma(\tau,\bar{\boldsymbol{x}})$. Further, straightforward calculations and utilisation of the governing equations (1.6) show that $\mathrm{d}(Q(\boldsymbol{x})/\xi)/\,\mathrm{d}\tau = 0$. □

Remark 1.4. It is clear that the time transformation is determined by Q. Since Q is strictly positive, the map $\sigma(\,\cdot\,,\bar{\boldsymbol{x}}) : \mathbb{R} \to \mathbb{R}$ is bijective, i.e., the reparametrisation $t \leftrightarrow \tau$ is bijective.

In Hairer and Söderlind [9], the motivation for the extended time transformation (1.6) is to construct explicit adaptive numerical integrators for *reversible systems*. The key is that under reversibility of Q, the extended time transformation (1.6) preserves reversibility. First, recall the basic definitions of reversible systems.

Definition 1.2. Let $R \in \mathrm{Diff}(\mathscr{P})$.

- A vector field $X \in \mathfrak{X}(\mathscr{P})$ is called reversible with respect to R if $R_* \circ X = -X \circ R$, or equivalently $\mathrm{d}(R(\boldsymbol{x}))/\,\mathrm{d}t = -(X \circ R)(\boldsymbol{x})$.
- A diffeomorphism $\Phi \in \mathrm{Diff}(\mathscr{P})$ is called reversible with respect to R if $R \circ \Phi = \Phi^{-1} \circ R$.

It is a well known result that the flow of a system is reversible if and only if its corresponding vector field is reversible [12, 8]. Now, concerning time transformation of reversible systems, it is straightforward to check the following result.

Theorem 1.5 (Hairer and Söderlind [9])**.** *If* $X \in \mathfrak{X}(\mathscr{P})$ *is reversible with respect to* R *and* $Q \in \mathcal{F}(\mathscr{P})$ *fulfils* $Q = Q \circ R$*, then the vector field* $\bar{X} \in \mathfrak{X}(\bar{\mathscr{P}})$ *in equation* (1.6) *is reversible with respect to* $\bar{R} : \bar{\boldsymbol{x}} \mapsto (R(\boldsymbol{x}), \xi)$*.*

2 Nambu–Poisson extensions and time transformations

In this section we develop a time transformation technique for Nambu–Poisson systems. Let $\mathscr{P}$ be a Nambu–Poisson manifold of order k and η its Nambu–Poisson tensor. Consider again the extended phase space $\bar{\mathscr{P}} = \mathscr{P} \times \mathbb{R}$. Our first goal is to introduce a Nambu–Poisson structure on $\bar{\mathscr{P}}$. The most natural extension of the Nambu–Poisson tensor η is given by

$$\bar{\eta} = \eta \wedge \frac{\partial}{\partial \xi} \tag{2.1}$$

It is not obvious that the bracket corresponding to $\bar{\eta}$ will fulfil the fundamental identity (1.2c). For example, in the canonical Poisson case, i.e., $k = 2$, it is not so if $n \geq 3$.

Lemma 2.1. *If $k \geq 3$ or $k = n = 2$, then $\bar{\eta}$ given by equation (2.1) defines a Nambu–Poisson structure of order $k+1$ on $\bar{\mathscr{P}}$.*

Proof. If $k \geq 3$ then it follows from Theorem 1.3 that η is decomposable about its regular points, and when $k = n = 2$ it is obviously so. Thus, $\eta \wedge \frac{\partial}{\partial \xi}$ is also decomposable about its regular points, so the assertion follows from Theorem 1.3. □

The bracket associated with $\bar{\eta}$ is denoted $\bar{\{}\cdot, \ldots, \cdot\bar{\}}$.

Let $H_1, \ldots, H_{k-1} \in \mathcal{F}(\mathscr{P})$ be the Hamiltonians for a Nambu–Poisson system on $\mathscr{P}$, i.e., of the form of system (1.3). Further, let $G \in \mathcal{F}(\bar{\mathscr{P}})$ and consider the system on $\bar{\mathscr{P}}$ given by

$$\frac{\mathrm{d}F}{\mathrm{d}\tau} = \bar{\{}H_1, \ldots, H_{k-1}, G, F\bar{\}}, \quad \forall\, F \in \mathcal{F}(\bar{\mathscr{P}}) \tag{2.2}$$

Remark 2.1. A functions $H \in \mathcal{F}(\mathscr{P})$ is considered to belong to $\mathcal{F}(\bar{\mathscr{P}})$ by the natural extension $\bar{\boldsymbol{x}} \mapsto H(\boldsymbol{x})$. Likewise, $\bar{H} \in \mathcal{F}(\bar{\mathscr{P}})$ is considered to be a function in $\mathcal{F}(\mathscr{P})$ depending on the parameter ξ. Thus, $\bar{\{}\cdot, \ldots, \cdot\bar{\}}$ is defined also for elements in $\mathcal{F}(\mathscr{P})$ and vice versa.

We continue with the main result in the paper. It states that time transformation of a Nambu–Poisson system can be realised as an extended Nambu–Poisson system.

Theorem 2.1. *Let $G \in \mathcal{F}(\bar{\mathscr{P}})$ and assume the conditions in Lemma 2.1 are valid. Then:*

1. *The extended system (2.2) is a Nambu–Poisson system.*
2. *Its flow restricted to $\mathscr{P}$ is a time transformation, determined by the additional first integral G, of the flow of system (1.3). That is,*

$$\Pi \varphi^{\tau}_{H_1,\ldots,H_{k-1},G}(\bar{\boldsymbol{x}}) = \varphi^{\sigma(\tau,\bar{\boldsymbol{x}})}_{H_1,\ldots,H_{k-1}}(\boldsymbol{x}), \quad \forall\, \bar{\boldsymbol{x}} \in \bar{\mathscr{P}}, \tau \in \mathbb{R}$$

where

$$\sigma(\tau, \bar{\boldsymbol{x}}) \equiv \int_0^{\tau} \frac{\partial G}{\partial \xi}\big(\varphi^{s}_{H_1,\ldots,H_{k-1},G}(\bar{\boldsymbol{x}})\big)\, \mathrm{d}s$$

Proof. The first assertion follows directly from Lemma 2.1, since $\bar{\eta}$ is a Nambu–Poisson tensor. Since H_i for $i = 1, \ldots, k-1$ are independent of ξ, it follows from the definition (2.1) of $\bar{\eta}$ that

$$\bar{\{}H_1, \ldots, H_{k-1}, G, F\bar{\}} = \frac{\partial G}{\partial \xi}\{H_1, \ldots, H_{k-1}, F\} - \frac{\partial F}{\partial \xi}\{H_1, \ldots, H_{k-1}, G\}$$

Thus, for $F = x_1, \ldots, x_n$, the governing equations (2.2) are parallel with those of system (1.3a), i.e., $\Pi\varphi^{\tau}_{H_1,\ldots,H_{k-1},G}$ and $\varphi^{t}_{H_1,\ldots,H_{k-1}}$ defined the same phase diagram. The relation between τ and t is given by $\mathrm{d}t/\,\mathrm{d}\tau = \partial G/\partial\xi$, which, after integration, gives the desired form of $\sigma(\tau, \bar{\boldsymbol{x}})$. □

It is straightforward to check the following corollary, which shows that the technique used by Hairer and Söderlind [9], reviewed in Section 1.2, is a special case.

Corollary 2.1. *The case* $G(\bar{\boldsymbol{x}}) = \log(\xi/Q(\boldsymbol{x}))$ *coincides with the transformation* (1.6) *applied to system* (1.3).

3 Reversible Nambu–Poisson systems

Recall that the time transformation by Hairer and Söderlind [9] is developed with reversible systems in mind. In the previous section we developed a similar approach, but based on the Nambu–Poisson framework. One may ask under what conditions a Nambu–Poisson system is reversible, and in what sense the time transformation technique developed above preserves reversibility. These questions are studied in this section.

As a first step, we have some results on necessary and sufficient conditions for a Nambu–Poisson system to be reversible.

Proposition 3.1. *Let* $R \in \mathrm{Diff}(\mathscr{P})$. *Then* $X_{H_1,\ldots,H_{k-1}}$ *is reversible with respect to* R *if and only if*

$$\{H_1, \ldots, H_{k-1}, F \circ R\} = -\{H_1, \ldots, H_{k-1}, F\} \circ R, \quad \forall\, F \in \mathcal{F}(\mathscr{P}) \tag{3.1}$$

Proof. Since R is a diffeomorphism it holds that $\mathcal{F}(\mathscr{P}) \circ R = \mathcal{F}(\mathscr{P})$, so the governing equations (1.3a) are equivalent to

$$\frac{\mathrm{d}(F \circ R)}{\mathrm{d}t} = \{H_1, \ldots, H_{k-1}, F \circ R\}, \quad \forall\, F \in \mathcal{F}(\mathscr{P})$$

This is equivalent to

$$\frac{\mathrm{d}(F \circ R)}{\mathrm{d}t} = -\{H_1, \ldots, H_{k-1}, F\} \circ R, \quad \forall\, F \in \mathcal{F}(\mathscr{P})$$

if and only if condition (3.1) holds. The last set of equations is exactly the condition on $X_{H_1,\ldots,H_{k-1}}$ for reversibility with respect to R. □

If R is a Nambu–Poisson map the assertion may be stated in the following way instead.

Corollary 3.1. *Let* R *be a Nambu–Poisson map, i.e.,* $R \in \mathrm{Diff}_{\eta}(\mathscr{P})$. *Then* $X_{H_1,\ldots,H_{k-1}}$ *is reversible with respect to* R *if and only if*

$$\{H_1, \ldots, H_{k-1}, F\} = -\{H_1 \circ R, \ldots, H_{k-1} \circ R, F\}, \quad \forall\, F \in \mathcal{F}(\mathscr{P}) \tag{3.2}$$

Proof. With F set to $F \circ R$, it is clear that the condition (3.2) is equivalent to the condition (3.1) if $R \in \mathrm{Diff}_{\eta}(\mathscr{P})$. □

As a generalisation of Theorem 1.5, we now show in what way reversibility of a Nambu–Poisson system is preserved by the time transformed extended system (2.2).

Theorem 3.1. *Let the system* (1.3) *be reversible with respect to* R*. Then the extended time transformed Nambu–Poisson system* (2.2) *is reversible with respect to* $\bar{R} : \bar{\boldsymbol{x}} \mapsto (R(\boldsymbol{x}), \xi)$ *if* $G \circ \bar{R} = G$*.*

Proof. Since $\partial H_i/\partial \xi = 0$ we have

$$\bar{\{}H_1, \dots, H_{k-1}, G, F \circ \bar{R}\bar{\}} = \frac{\partial G}{\partial \xi}\{H_1, \dots, H_{k-1}, F \circ \bar{R}\} - \frac{\partial (F \circ \bar{R})}{\partial \xi}\{H_1, \dots, H_{k-1}, G\}$$

Since $\bar{R}$ maps ξ to ξ it holds that $\partial(F \circ \bar{R})/\partial\xi = \partial F/\partial\xi \circ \bar{R}$. Further, $G = G \circ \bar{R}$ yields $\partial G/\partial\xi = \partial G/\partial\xi \circ \bar{R}$ and

$$\{H_1, \dots, H_{k-1}, G\} = \{H_1, \dots, H_{k-1}, G \circ \bar{R}\}$$

Altogether we now have

$$\begin{aligned}
\bar{\{}H_1, \dots, H_{k-1}, G, F \circ \bar{R}\bar{\}} &= \frac{\partial G}{\partial \xi} \circ \bar{R}\{H_1, \dots, H_{k-1}, F \circ \bar{R}\} - \frac{\partial F}{\partial \xi} \circ \bar{R}\{H_1, \dots, H_{k-1}, G \circ \bar{R}\} \\
&= -\frac{\partial G}{\partial \xi} \circ \bar{R}\{H_1, \dots, H_{k-1}, F\} \circ \bar{R} + \frac{\partial F}{\partial \xi} \circ \bar{R}\{H_1, \dots, H_{k-1}, G\} \circ \bar{R} \\
&= -\bar{\{}H_1, \dots, H_{k-1}, G, F\bar{\}} \circ \bar{R}
\end{aligned}$$

where the stipulation that system (1.3) is reversible have been used in conjunction with Proposition 3.1. Application of Proposition 3.1 again completes the assertion. □

4 Application: numerical integration by splitting

The main motivation for extended time transformations is to construct adaptive numerical integration algorithms. By a *numerical integrator* for a dynamical system $X \in \mathfrak{X}(\mathscr{P})$, we mean a family of near identity maps $\Phi_h \in \mathrm{Diff}(\mathscr{P})$, such that Φ_h is an approximation of the exact flow φ_X^h. Numerical solution "paths" are obtained by the discrete dynamical system $\boldsymbol{x}_{k+1} = \Phi_h(\boldsymbol{x}_k)$. The integrator Φ_h is *consistent of order* p if $\Phi_h - \varphi^h = \mathcal{O}(h^p)$, which in particular implies $\Phi_0 = \mathrm{Id}$. It is *explicit* if $\Phi_h(\boldsymbol{x})$ can be computed by a finite algorithm. Notice that Φ_h is not a one parameter group, i.e., $\Phi_h \circ \Phi_s \neq \Phi_{h+s}$.

When constructing numerical integrators, one typically tries to preserve as much as possible of the underlying qualitative structure of the exact flow. In our case, we like Φ_h to preserve the Nambu–Poisson structure, and in presence also reversibility. In addition, time step adaptivity is crucial in order for the integration method to be computationally efficient. Indeed, we would like to vary the step size h during the integration process according to the present local character of the dynamics, without destroying the structural properties of the method. The standard approach, motivating our work, is to utilise a time transformation $t \leftrightarrow \tau$ that preserves the structure of the original system, and then construct a τ–equidistant numerical integrator for transformed system. An equivalent view point is to say that the time transformation should regularise the problem, so that it becomes easier to integrate numerically.

Splitting is a compelling technique for the construction of structure preserving integrators [17]. The basic idea is as follows. Let $\mathfrak{X}_A(\mathscr{P})$ be a Lie sub-algebra of $\mathfrak{X}(\mathscr{P})$, and let $\mathrm{Diff}_A(\mathscr{P})$ be the corresponding Lie sub-group of $\mathrm{Diff}(\mathscr{P})$. Assume that $X \in \mathfrak{X}_A(\mathscr{P})$ can be splitted into explicitly

integrable sub-system, each of which is a system in $\mathfrak{X}_A(\mathscr{P})$. That is, $X = X_1 + \ldots + X_k$, where $X_i \in \mathfrak{X}_A(\mathscr{P})$ and $\varphi^t_{X_i}(\boldsymbol{x})$ can be computed explicitly. A numerical integrator for X is obtained by $\Phi_h = \varphi^h_{X_1} \circ \cdots \circ \varphi^h_{X_k}$. It is clear that Φ_h is an approximation of φ^h_X, and that $\Phi_h \in \mathrm{Diff}_A(\mathscr{P})$. Further, by the Baker–Campbell–Hausdorff (BCH) formula, it follows that Φ_h is the exact flow of a modified vector field $\tilde{X}_h \in \mathfrak{X}_A(\mathscr{P})$, i.e., $\Phi_h = \varphi^h_{\tilde{X}_h}$. This information is crucial for the analysis of Φ_h. For example, if $\mathfrak{X}_A(\mathscr{P})$ is the Lie-algebra corresponding to a Poisson structure on $\mathscr{P}$, then Φ_h will exactly conserve a modified Hamiltonian, which is $\mathcal{O}(h^p)$–close to the Hamiltonian for the original problem [8].

Remark 4.1. Due to convergence issues, the BCH formula needs to be truncated, which implies that assertions on Φ_h, coming from $\tilde{X}$, are valid only for exponentially long times, i.e., up to time scales of order $\mathcal{O}(\exp(\mathcal{O}(1/h^p)))$. See Hairer et. al. [8] for details.

Our notion for the construction of integrators is to utilise the results in Section 2–3, and consider splitting of the individual Nambu–Poisson Hamiltonians.

Let η be a Nambu–Poisson tensor. The set of Nambu–Poisson maps which are reversible with respect to R is denoted $\mathrm{Diff}_{\eta,R}(\mathscr{P})$. If $\Phi, \Psi \in \mathrm{Diff}_{\eta,R}(\mathscr{P})$, then in general we have

$$R \circ \Phi \circ \Psi = \Phi^{-1} \circ R \circ \Psi = \Phi^{-1} \circ \Psi^{-1} \circ R \neq (\Phi \circ \Psi)^{-1} \circ R$$

Thus, $\mathrm{Diff}_{\eta,R}(\mathscr{P})$ is not closed under composition, so it is not a sub-group of $\mathrm{Diff}(\mathscr{P})$. However, $\mathrm{Diff}_{\eta,R}(\mathscr{P})$ is closed under the symmetric group operation $(\Phi, \Psi) \mapsto \sqrt{\Phi} \circ \Psi \circ \sqrt{\Phi}$, which we write as $\Phi \circledcirc \Psi$. Further, from the symmetric BCH formula (cf. [15]) it follows that if $X, Y \in \mathfrak{X}_{\eta,R}(\mathscr{P})$, then the vector field Z such that $\varphi^t_Z = \varphi^t_X \circledcirc \varphi^t_Y$ belongs to $\mathfrak{X}_{\eta,R}(\mathscr{P})$.

Remark 4.2. For near identity maps, $\sqrt{\Phi}$ is defined by taking its representation $\Phi = \exp(X)$ and then setting $\sqrt{\Phi} = \exp(X/2)$. In our case, Φ will always be an exact flow φ^t_X, in which case $\sqrt{\varphi^t_X} = \varphi^{t/2}_X$.

We now give a result concerning reversible systems, which is of use for the analysis of periodic numerical paths of reversible splitting methods.

Lemma 4.1. *Let $X \in \mathfrak{X}(\mathscr{P})$ be reversible with respect to $R \in \mathrm{Diff}(\mathscr{P})$. Assume that the set $\mathsf{U} = \{\boldsymbol{x} \in \mathscr{P}; R(\boldsymbol{x}) = \boldsymbol{x}\}$ of fix-points of R is non-empty and that $\gamma : \mathbb{R} \to \mathscr{P}$ is a solution curve of X for which there exists $t_1, t_2 \in \mathbb{R}$ with $t_1 < t_2$ such that $\gamma(t_1), \gamma(t_2) \in \mathsf{U}$. Then γ is periodic.*

Proof. For simplicity assume that $t_1 = 0$ and $t_2 > 0$, which is not a restriction. The curve $\gamma_2(t) = (R \circ \gamma)(-t)$ is also a solution curve due to reversibility. Further, since R restricted to U is the identity map we have the equalities $\gamma(t_1) = \gamma_2(t_1)$ and $\gamma(-t_2) = \gamma_2(t_2)$. Due to uniqueness of solutions the first equality implies $\gamma_2 = \gamma$, which in conjunction with the second equality implies that $\gamma(-t_2) = \gamma(t_2)$. Thus γ returns to the same point twice, so it is periodic.

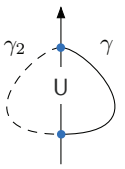

4.1 Rigid body problem

The Euler equations for the free rigid body is a Nambu–Poisson system on the phase space $\mathbb{R}^3$, equipped with the canonical Nambu–Poisson structure $\eta = \partial/\partial x_1 \wedge \partial/\partial x_2 \wedge \partial/\partial x_3$. Its two

Hamiltonians are total angular momentum $M(\boldsymbol{x}) = \sum x_i^2/2$ and kinetic energy $T(\boldsymbol{x}) = \sum x_i^2/(2I_i)$, where $I_i > 0$ are the principal moments of inertia. Thus, the governing equations are

$$\frac{\mathrm{d}F}{\mathrm{d}t} = \{M, T, F\}, \quad \forall\, F \in \mathcal{F}(\mathbb{R}^3) \tag{4.1a}$$

which explicitly reads

$$\begin{aligned} \dot{x}_1 &= a_1 x_2 x_3, \quad a_1 = (I_2 - I_3)/(I_2 I_3) \\ \dot{x}_2 &= a_2 x_3 x_1, \quad a_2 = (I_3 - I_1)/(I_3 I_1) \\ \dot{x}_3 &= a_3 x_1 x_2, \quad a_3 = (I_1 - I_2)/(I_1 I_2) \end{aligned} \tag{4.1b}$$

It is straightforward to check that the system is reversible with respect to the linear diffeomorphism $R_1 : \boldsymbol{x} \mapsto (-x_1, x_2, x_3)$, and in symmetry, also with respect to R_2, R_3 defined analogously. Thus, due to Lemma 4.1, we have the following KAM–like result for the free rigid body.

Theorem 4.1. *Let $\tilde{X}_h \in \mathfrak{X}(\mathbb{R}^3)$ depend smoothly on h such that $\tilde{X}_0 = X_{M,T} \neq 0$. Assume that $\tilde{X}_h$, for each h, is reversible with respect to R_1, R_2 and R_3. Then, for small enough h, the solution paths of $\tilde{X}_h$ are periodic.*

Proof. It is known that if γ is a solution curve of the Euler equations, then it is either an equilibrium, or it is periodic with finite period $t_e > 0$, in which case it crosses either of the planes $\mathsf{U}_\mathrm{i} = \{\boldsymbol{x} \in \mathbb{R}^3; R_i(\boldsymbol{x}) = \boldsymbol{x}\}$ every half period [14]. That is, it holds that $\gamma(t_1), \gamma(t_1 + t_e/2) \in \mathsf{U}_k$ for some $k \in \{1, 2, 3\}$ and $t_1 \in [0, t_e/2)$. Further, since $X_{M,T} \equiv 0$ is not allowed, it is known that if γ is an equilibrium, then $\gamma(t) \in \mathsf{U}_k$. Let $\tilde{\gamma}_h$ be a solution curve of $\tilde{X}_h$ and let γ be the solution curve of $X_{M,T}$ such that $\gamma(0) = \tilde{\gamma}_h(0)$. Assume first that γ is not an equilibrium. Then, for any $\delta \in (0, t_e/2)$ it holds that a continuous path between $\gamma(t_1 - \delta)$ and $\gamma(t_1 + \delta)$ must cross the plane U_k. For small enough h it holds that $\tilde{\gamma}_h(t_1 - \delta)$ and $\tilde{\gamma}_h(t_1 + \delta)$ approximates $\gamma(t_1 - \delta)$ and $\gamma(t_1 + \delta)$ well enough to also be separated by U_k. Thus, $\tilde{\gamma}_h(\tilde{t}_1) \in \mathsf{U}_1$ for some $\tilde{t}_1 \in (t_1 - \delta, t_1 + \delta)$. Likewise, $\tilde{\gamma}_h(\tilde{t}_2) \in \mathsf{U}_1$ for some $\tilde{t}_2 \in (t_1 + t_e/2 - \delta, t_1 + t_e/2 + \delta)$. Since $\tilde{X}_h$ is reversible with respect to R_1 it follows from Lemma 4.1 that $\tilde{\gamma}_h$ is periodic. If γ is an equilibrium and $\tilde{\gamma}_h$ is not, then either there exists $s > 0$ such that $\tilde{\gamma}_h(s) \notin \mathsf{U}_k$, in which case the solution curve of $X_{M,T}$ such that $\gamma(s) = \tilde{\gamma}_h(s)$ is periodic, so we are back to the first case, or $\tilde{\gamma}_h(0), \tilde{\gamma}_h(s) \in \mathsf{U}_k$, in which case the assertion follows directly from Lemma 4.1. □

The traditional perception in the literature is to view the rigid body equations (4.1) as a Poisson system, with the non-canonical Poisson tensor $\eta_M = \eta(\,\mathrm{d}M, \cdot_1, \cdot_2)$, induced by the total angular momentum (M is a Casimir, cf. [14], for this Poisson structure). We denote the corresponding bracket by $\{\cdot_1, \cdot_2\}_M$. It is clear that Diff_{η_M} is a sub-group of Diff_η. Consider the Hamiltonian splitting $T = \sum T_i$, where $T_i(\boldsymbol{x}) = x_i^2/(2I_i)$. The sub-system $\dot{F} = \{T_i, F\}_M$ does not affect x_i, i.e., $\dot{x}_i = 0$, and all the quadratic terms contain x_i. Hence, it is in essence a linear system on $\mathbb{R}^2$, and therefore explicitly integrable (since the exponential map is computable for any 2×2–matrix). A well known second order integrator is obtained by the symmetric composition

$$\Phi_h^{YT} = \varphi_{M,T_1}^h \circledcirc \varphi_{M,T_2}^h \circledcirc \varphi_{M,T_3}^h$$

This integrator has the following properties:

1. It is reversible with respect to R_1, R_2 and R_3. Thus, its modified vector field $\tilde{X}_h$ is a R_1, R_2, R_3–reversible perturbation of X, so Theorem 4.1 may be used to deduce periodic orbits of the numerical solution.

2. It is a Poisson map, i.e., $\Phi_h^{\curlyvee T} \in \mathrm{Diff}_{\eta_M}(\mathscr{P})$. This implies that its modified vector field $\tilde{X}_h$ is the Hamiltonian vector field of a modified Hamiltonian $\tilde{T}_h = T + \mathcal{O}(h^2)$, so T is nearly conserved. Further, since M is a Casimir of the Poisson structure it is exactly conserved.

Remark 4.3. One may also view the rigid body equations (4.1) as a Poisson system with the Poisson tensor $\eta_T = \eta(\cdot_1, \mathrm{d}T, \cdot_2)$, and then construct an integrator $\Phi_h^{\curlyvee M}$ by splitting of M. This integrator will exactly conserve T, and nearly conserve M.

Following our notion, we now consider Hamiltonian splitting of both M and T. To this end, let $M_i(\boldsymbol{x}) = x_i^2/2$. Since $X_{M_i,T_i} = 0$ it follows that

$$X_{M,T} = X_{M_1+M_2,T_1+T_2} + X_{M_2+M_3,T_2+T_3} + X_{M_3+M_1,T_3+T_1}$$

Each such vector field is integrable by linear extrapolation, for example,

$$\varphi^t_{M_1+M_2,T_1+T_2}(\boldsymbol{x}) = \boldsymbol{x} + tX_{M_1+M_2,T_1+T_2}(\boldsymbol{x})$$

Thus, a second order integrator is obtained by

$$\Phi_h^{\curlyvee M \curlyvee T} = \varphi^h_{M_1+M_2,T_1+T_2} \circledcirc \varphi^h_{M_2+M_3,T_2+T_3} \circledcirc \varphi^h_{M_3+M_1,T_3+T_1}$$

This integrator is computationally cheaper than $\Phi_h^{\curlyvee T}$, since computation of the exponential map, which involves evaluation of sin and cos, is not necessary. Further, it has the following properties:

1. It is reversible with respect to R_1, R_2 and R_3. Thus, its modified vector field $\tilde{X}_h$ is a R_1, R_2, R_3–reversible perturbation of $X_{M,T}$, so Theorem 4.1 may be used to deduce periodic orbits of the numerical solution.
2. It is an η–map, i.e., $\Phi_h^{\curlyvee M \curlyvee T} \in \mathrm{Diff}_\eta$, which implies $\tilde{X} \in \mathfrak{X}_\eta(\mathscr{P})$. However, $\Phi_h^{\curlyvee M \curlyvee T}$ does not correspond to a modified Nambu–Poisson system (see Remark 1.3), so there are no exactly conserved modified Hamiltonians $\tilde{M}$ and $\tilde{T}$. Nevertheless, M and T are still nearly conserved due to the periodicity of the numerical solution.

Consider now time transformation of system (4.1) into an extended Nambu–Poisson system

$$\frac{\mathrm{d}F}{\mathrm{d}\tau} = \bar{\{}M, T, G, F\bar{\}}, \quad \forall F \in \mathcal{F}(\mathbb{R}^4) \tag{4.2}$$

We have the following generalisation of Theorem 4.1.

Theorem 4.2. *Let $\tilde{X}_\epsilon \in \mathfrak{X}(\mathbb{R}^4)$ depend smoothly on ϵ such that $\tilde{X}_0 = X_{M,T,G} \neq 0$. Assume that $\tilde{X}_\epsilon$, for each ϵ, is reversible with respect to $\bar{R}_1$, $\bar{R}_2$ and $\bar{R}_3$, and that there exists $\delta > 0$ such that $\partial G/\partial \xi > \delta$. Then, for small enough ϵ, the solution paths of $\tilde{X}_\epsilon$ are periodic.*

Proof. From the definition of $\bar{R}_i$ it follows that $\bar{\mathsf{U}}_i = \{\bar{\boldsymbol{x}} \in \mathbb{R}^4; \bar{R}_i(\bar{\boldsymbol{x}}) = \bar{\boldsymbol{x}}\}$ is a hyper-plane, and that $\mathbb{R}^3 \ni \boldsymbol{x} \in \mathsf{U}_i$ implies $(\boldsymbol{x}, \xi) \in \bar{\mathsf{U}}_i$ for all $\xi \in \mathbb{R}$. Let γ be a solution curve of $X_{M,T,G}$. Since it is a time transformation of a solution curve of $X_{M,T}$ and since $\partial G/\partial \xi > \delta$ it follows that there exists $t_1 < t_2$ and $k \in \{1, 2, 3\}$ such that $\gamma(t_1), \gamma(t_2) \in \bar{\mathsf{U}}_k$. Thus, γ is periodic due to Lemma 4.1. The proof now proceeds exactly as the proof of Theorem 4.1. □

Assume G takes the splitted form $G(\bar{\boldsymbol{x}}) = G_1(\boldsymbol{x}) + G_2(\xi)$. We propose the following adaptive versions of $\Phi_h^{\curlyvee T}$ and $\Phi_h^{\curlyvee M \curlyvee T}$.

$$\Phi_\epsilon^{\curlyvee T \curlyvee G} = \varphi^\epsilon_{M,T,G_1} \circledcirc \varphi^\epsilon_{M,T_1,G_2} \circledcirc \varphi^\epsilon_{M,T_2,G_2} \circledcirc \varphi^\epsilon_{M,T_3,G_2}$$
$$\Phi_\epsilon^{\curlyvee M \curlyvee T \curlyvee G} = \varphi^\epsilon_{M,T,G_1} \circledcirc \varphi^\epsilon_{M_1+M_2,T_1+T_2,G_2} \circledcirc \varphi^\epsilon_{M_2+M_3,T_2+T_3,G_2} \circledcirc \varphi^\epsilon_{M_3+M_1,T_3+T_1,G_2}$$

Notice that all of the partial flows are explicitly integrable. In particular, $\varphi^\epsilon_{M,T,G_1}(\bar{\boldsymbol{x}}) = \bar{\boldsymbol{x}} + \epsilon X_{M,T,G_1}(\bar{\boldsymbol{x}})$. Further, it holds that

$$\varphi^\epsilon_{M,T_i,G_2}(\bar{\boldsymbol{x}}) = (\varphi^{\epsilon \frac{\partial G_2}{\partial \xi}(\xi)}_{M,T_i}(\boldsymbol{x}), 0), \quad i = 1,2,3$$

and correspondingly for $\varphi^\epsilon_{M_i,T_i,G_2}$. These integrators have the following properties:

1. They are reversible with respect to $\bar{R}_1$, $\bar{R}_2$ and $\bar{R}_3$. Thus, their modified vector fields are $\bar{R}_1, \bar{R}_2, \bar{R}_3$–reversible perturbation of $X_{M,T,G}$, so Theorem 4.2 may be used to deduce periodic orbits of the numerical solution. (Assuming $\exists \varepsilon > 0$ such that $\partial G_2/\partial \xi > \varepsilon$.)
2. They are $\bar{\eta}$–maps. However, they do not correspond to a modified Nambu–Poisson system (see Remark 1.3). Nevertheless, M, T and G are still nearly conserved due to the periodicity of the numerical solution. In fact, M is exactly conserved by $\Phi^{\curlyvee T \curlyvee G}$, since each partial flow is an η_M–map.

As an illustration, numerical simulations with $\Phi^{\curlyvee M \curlyvee T}$, $\Phi^{\curlyvee T}$, $\Phi^{\curlyvee M \curlyvee T \curlyvee G}$, and $\Phi^{\curlyvee T \curlyvee G}$ are given. The moments of inertia are $I_1 = 1/2$, $I_2 = 1$, $I_3 = 2$, and initial data are $\boldsymbol{x}_0 = (0, \cos(\theta), \sin(\theta))$, with $\theta = 0.2$, which correspond to rotation "nearly" about the unstable principle axis. For the adaptive integrators the additional Hamiltonian is $G = G_1 + G_2 = -\log(\|X_{M,T}\| + 0.01) + \log(\xi)$, so the steps become smaller as the magnitude of the vector field $X_{M,T}$ increases. The step size $h = 0.15$ is used for the non-adaptive integrators, and for the adaptive integrators ϵ is chosen to yield the same mean time step (i.e. so that the mean of $\epsilon \partial G/\partial \xi$ is h).

A comparison of solutions in the t (non-adaptive) and in the τ (adaptive) variables are given in Figure 1. Notice that the time-stretching makes the solution "smoother". Further, the numerical errors in the Hamiltonians are plotted in Figure 2. Notice that the errors are significantly smaller for the adaptive integrators.

5 Conclusions

A time transformation technique for Nambu–Poisson systems, based on extending the phase space, have been developed (Theorem 2.1). The technique is shown to preserve reversibility under mild conditions on the additional Hamiltonian function (Theorem 3.1). A family of numerical integrators based on splitting of the Nambu–Poisson Hamiltonians is suggested. In particular, a novel approach for numerical integration of the Euler equations for the free rigid body is presented. By backward error analysis, it is shown that periodicity is preserved (Theorem 4.1 and Theorem 4.2).

Acknowledgement The author is grateful to Claus Führer, Gustaf Söderlind and Sergei Silvestrov for fruitful discussions, and to Olivier Verdier for many helpful suggestions on improvement. The author would also like to thank SKF for the support given.

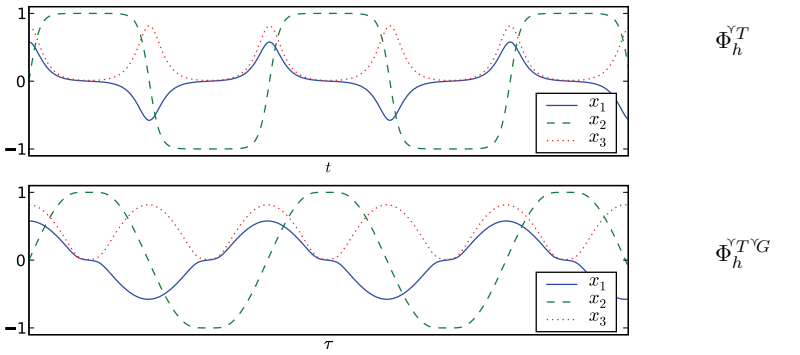

Figure 1. Solution curves for the non-adaptive integrator $\Phi^{\gamma T}$, and for the adaptive integrator $\Phi^{\gamma T \gamma G}$. Notice that the curves in the lower graph, corresponding to $\Phi^{\gamma T \gamma G}$, are "smoother". This is due to the time-stretching.

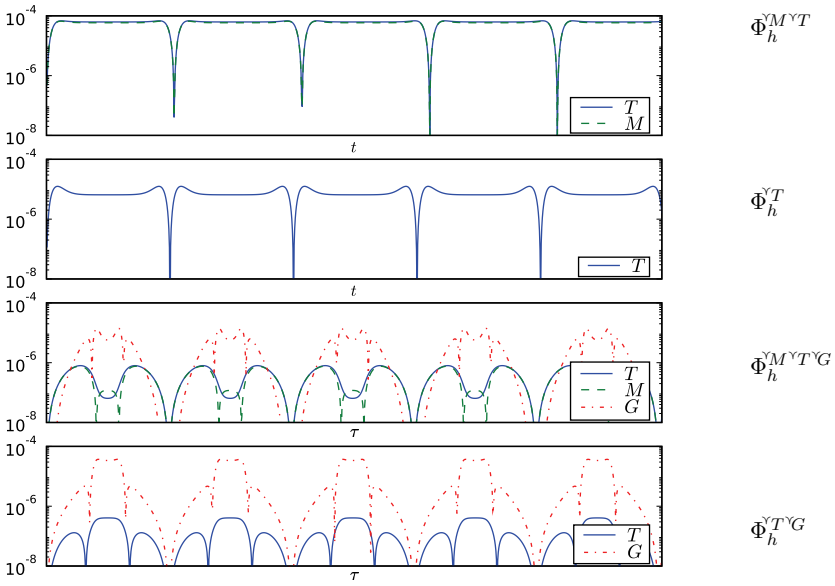

Figure 2. Absolute errors in the Hamiltonians. Notice that the errors in T (and M) are significantly smaller for the adaptive integrators. Thus, increased efficiency due to adaptivity is obtained. (Recall that $\Phi^{\gamma T}$ and $\Phi^{\gamma T \gamma G}$ conserve M up to rounding errors, whence M is not plotted for these.)

References

[1] D. Alekseevsky and P. Guha. On decomposability of Nambu-Poisson tensor. Acta Math. Univ. Comenian. (N.S.), **65** (19969, 1–9.

[2] S. Blanes and C. J. Budd. Adaptive geometric integrators for Hamiltonian problems with approximate scale invariance. SIAM J. Sci. Comput., **26** (2005), 1089–1113 (electronic).

[3] S. D. Bond and B. J. Leimkuhler. Time-transformations for reversible variable stepsize integration. Numer. Algorithms, **19** (1998), 55–71,

[4] R. Chatterjee and L. Takhtajan. Aspects of classical and quantum Nambu mechanics. Lett. Math. Phys. **37** (1996), 475–482.

[5] S. Codriansky, R. Navarro, and M. Pedroza. The Liouville condition and Nambu mechanics. J. Phys. A, **29** (1996), 1037–1044.

[6] P. Gautheron. Some remarks concerning Nambu mechanics. Lett. Math. Phys. **37** (1996),103–116.

[7] E. Hairer. Variable time step integration with symplectic methods. Appl. Numer. Math., **25** (1007), 219–227.

[8] E. Hairer, C. Lubich, and G. Wanner. *Geometric numerical integration.* Springer Series in Computational Mathematics, **31**, Springer-Verlag, Berlin, Second Ed., 2006.

[9] E. Hairer and G. Söderlind. Explicit, time reversible, adaptive step size control. SIAM J. Sci. Comput. **26** (2005), 1838–1851 (electronic).

[10] W. Huang and B. Leimkuhler. The adaptive Verlet method. SIAM J. Sci. Comput. **18** (1997), 239–256.

[11] R. Ibáñez, M. de León, J. C. Marrero, and D. Martin de Diego. Dynamics of generalized Poisson and Nambu-Poisson brackets. J. Math. Phys. **38** (1997), 2332–2344.

[12] J. S. W. Lamb and J. A. G. Roberts. Time-reversal symmetry in dynamical systems: a survey. Phys. D, **112** (1998), 1–39.

[13] G. Marmo, G. Vilasi, and A. M. Vinogradov. The local structure of n-Poisson and n-Jacobi manifolds. J. Geom. Phys. **25** (1998), 141–182.

[14] J. E. Marsden and T. S. Ratiu. *Introduction to mechanics and symmetry*, Texts in Applied Mathematics, **17**, Springer-Verlag, New York, Second Ed., 1999.

[15] R. I. McLachlan. On the numerical integration of ordinary differential equations by symmetric composition methods. SIAM J. Sci. Comput. **16** (1995),151–168.

[16] R. I. McLachlan and G. R. W. Quispel. What kinds of dynamics are there? Lie pseudogroups, dynamical systems and geometric integration. Nonlinearity, **14** (2001), 1689–1705.

[17] R. I. McLachlan and G. R. W. Quispel. Splitting methods. Acta Numer. **11** (2002), 341–434, 2002.

[18] S. Mikkola and P. Wiegert. Regularizing time transformations in symplectic and composite integration. Celestial Mech. Dynam. Astronom. **82** (2002), 375–390.

[19] K. Modin. On explicit adaptive symplectic integration of separable Hamiltonian systems. Journal of Multibody Dynamics, 2008 (to be published).

[20] K. Modin and C. Führer. Time-step adaptivity in variational integrators with application to contact problems. ZAMM Z. Angew. Math. Mech. **86** (2006), 785–794.

[21] P. Morando. Liouville condition, Nambu mechanics, and differential forms. J. Phys. A, **29** (1996), L329–L331.

[22] N. Nakanishi. On Nambu-Poisson manifolds. Rev. Math. Phys. **10** (1998), 499–510.

[23] Y. Nambu. Generalized Hamiltonian dynamics. Phys. Rev. D, **7** (1973), 2405–2412.

[24] M. Preto and S. Tremaine. A class of symplectic integrators with adaptive timestep for separable hamiltonian systems. Astron. J. **118** (1999), 2532–2541.

[25] R. Schmid. Infinite dimensional Lie groups with applications to mathematical physics. J. Geom. Symmetry Phys. **1** (2004), 54–120.

[26] D. Stoffer. Variable steps for reversible integration methods. Computing, **55** (1995), 1–22.

[27] L. Takhtajan. On foundation of the generalized Nambu mechanics. Comm. Math. Phys. **160** (1994), 295–315.

[28] I. Vaisman. A survey on Nambu-Poisson brackets. Acta Math. Univ. Comenian. (N.S.), **68** (1999), 213–241.

[29] I. Vaisman. Nambu-Lie groups. J. Lie Theory, **10** (2000), 181–194.

Received September 10, 2008
Revised October 07, 2008

Paper V

Klas Modin, Dag Fritzson and Claus Führer.
Proceedings of the 48th Scandinavian Conference on Simulation and Modeling (SIMS 2007).
30-31 October, 2007, Göteborg (Särö), Sweden

Semiexplicit numerical integration by splitting with application to dynamic multibody problems with contacts

Klas Modin and Dag Fritzson

SKF Engineering Research Centre
MDC, RKs–2
SE–415 50 Göteborg, Sweden
E–mail: Klas.Modin@na.lu.se, Dag.Fritzson@skf.com

Claus Führer

Centre for Mathematical Sciences
Box 118, SE–221 00 Lund, Sweden
E–mail: claus@maths.lth.se

October 7, 2008

Numerical integration is considered for second order differential equations on the form

$$\ddot{q} = A(q, \dot{q}, t) + B(q, \dot{q}, t)\,,$$

where A is significantly more expensive to evaluate than B, and B is stiff (highly oscillatory) in comparison with A. Examples of such problem are multibody problem with contact forces acting between bodies, and constraints formulated as penalty forces.

Based on the splitting $A + B$ of the acceleration field, a numerical integration algorithm, which is explicit in the A–part and implicit in the B–part, is suggested. Consistency and linear stability analysis of the proposed method is carried out.

Numerical examples with the proposed method is carried out for two simple test problems, and for a complex multibody model of a rotating ball bearing. Comparison with conventional implicit methods is given for each example. The results indicate that the proposed method is more efficient, in terms of number of evaluations of A, at the same accuracy level.

Contents

1. Introduction

We are interested in the numerical time integration of dynamic multibody systems. In particular, problems where bodies frequently come in contact with each other, which is modelled by complex force laws. The application we have in mind is simulation of rolling bearings, where contacts between bodies are present. Our aim is to design a numerical integrator that is particularly efficient for such problems.

In Section 2, a characterization of the governing equations is given. The objective is twofold: (i) to pin-point where the computational cost is high; (ii) to estimate typical frequencies in the solution. The specific character of the governing equations is then used as a basis in Section 3 in order to design a more efficient integrator. Further, in Section 4 the proposed integrator is analyzed in terms of consistency and linear stability. In Section 5 we discuss issues concerned with adaptive time-stepping. Lastly, in Section 6, we give numerical test examples, both for simple test problems and for a fully complex rolling bearing problem.

2. Characterization of the governing equations

In this section we give an overview of the formulation, and a characterization, of the governing differential equations that are to be numerically integrated. There are, of course, a number of choices on how to formulate the equations of motion for multibody systems. Primarily, the so called "floating frame of reference" is what we have in mind. In particular, the formulation used in the multibody simulation software BEAST, which is a tool for detailed transient analysis of rolling bearings and other machine

elements, developed and maintained by SKF (www.skf.com). For a full specification of the governing equations, see [Nak06]. In this paper we consider only issues that are essential for the proposed integrator.

Let $\mathcal{Q} = \mathbb{R}^d$ be the configuration space of the multibody system. Further, let $\boldsymbol{q} \in \mathcal{Q}$ denote the position coordinates. For rigid systems these are the centre of mass and the orientation of each body, relative to a fixed global coordinate system in Euclidean 3–space. In the case of elasiticity, generalized coordinates describing the deflection field of each body are also included in $\boldsymbol{q}$. The governing equations are on the form

$$M(\boldsymbol{q},\dot{\boldsymbol{q}})\ddot{\boldsymbol{q}} = F(\boldsymbol{q},\dot{\boldsymbol{q}},t)\,, \qquad \boldsymbol{q}(0) = \boldsymbol{q}_0\,, \qquad \dot{\boldsymbol{q}}(0) = \dot{\boldsymbol{q}}_0\,, \tag{1}$$

where the mass matrix $M(\boldsymbol{q},\dot{\boldsymbol{q}})$ is a symmetric positive definite $d \times d$–matrix, and the force field $F(\boldsymbol{q},\dot{\boldsymbol{q}},t)$ is a vector valued map corresponding to the forces acting on the system. Time is denoted t. Notice that (1) is a second order ordinary differential equation (ODE).

Constraints are taken into account by penalty force laws. Thus, we do not utilize the standard Lagrangian multiplier formulation, which is typically used for constrained mechanical systems. Notice that the penalty formulation implies that (1) is highly stiff. Thus, an implicit numerical integrator must be used.

Remark. The integrator suggested in this paper could easily be extended to governing equations formulated as a differential algebraic system using Lagrangian multipliers.

2.1. Computational costs

Solving (1) numerically with a standard ODE solver basically involves the following computations in order to evaluate the vector field:

- Compute the inverse of the mass matrix. This is a cheap operation, as the mass matrix is block diagonal (one block per body).
- Compute the constraint forces, which is also cheap.
- Compute "simple" non-stiff forces such as gravity and Coriolis forces.
- Compute contact forces. This task is heavily dominating the computational cost. Evaluation of each contact involves searching for intersecting surfaces. In the case of rolling bearings, the surface geometries of the bodies are highly complex. Further, for very detailed contact models (as in BEAST), tribological issues, such as oil film thickness in the contact, are also taken into account. See [SF01] for details on advanced contact modelling.

In order to be able to separate the computationally intensive force evaluations from less costly evaluations, we rewrite (1) as

$$M(\boldsymbol{q},\dot{\boldsymbol{q}})\ddot{\boldsymbol{q}} = F^A(\boldsymbol{q},\dot{\boldsymbol{q}},t) + F^B(\boldsymbol{q},\dot{\boldsymbol{q}},t)\,, \tag{2}$$

where F^A are the contact forces plus "simple" non-stiff forces (from now on we refer to F^A as contact forces), and F^B are the constraint penalty forces. Multiplying from the left with the inverse of the mass matrix we get a second order ODE written on standard form

$$\ddot{\boldsymbol{q}} = A(\boldsymbol{q},\dot{\boldsymbol{q}},t) + B(\boldsymbol{q},\dot{\boldsymbol{q}},t) \quad \text{or shorter} \quad \ddot{\boldsymbol{q}} = C(\boldsymbol{q},\dot{\boldsymbol{q}},t)\,. \tag{3}$$

The maps A and B correspond to accelerations due to contact forces and constraint forces respectively. $C = A + B$ is the total acceleration field. The field A is much more expensive to compute than B. This "splitting formulation" of the governing equations will be utilized by the integrator algorithm described in Section 3.

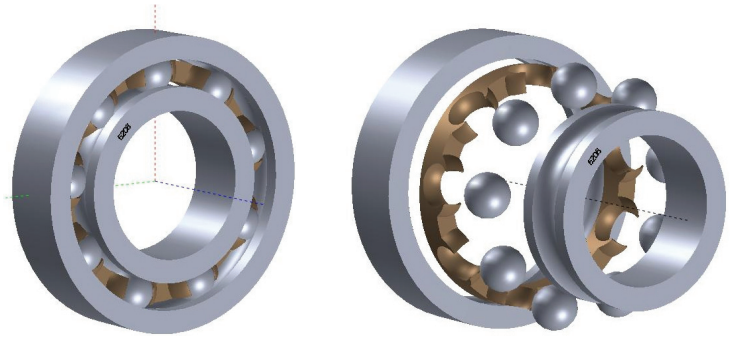

Figure 1: A common ball bearing. To the right in exploded view. The bodies in the model are: (1) an outer ring; (2) a cage; (3) nine balls; (4) an inner ring. All elements are steel, except the cage which is plastic.

Notice that (3) is a non-autonomous differential equation, i.e., the right hand side depends explicitly on time t. From now on we rewrite the governing equations as an autonomous first order system, evolving on the extended phase space $\mathscr{P} = T\mathscr{Q} \times \mathbb{R} = \mathbb{R}^{2d+1}$, equiped with coordinates $z = (q, \dot{q}, t)$. That is, we write (3) as

$$\frac{\mathrm{d}}{\mathrm{d}t}\begin{pmatrix} q \\ \dot{q} \\ t \end{pmatrix} = \begin{pmatrix} \dot{q} \\ A(q,\dot{q},t) + B(q,\dot{q},t) \\ 1 \end{pmatrix} \quad \text{or shorter} \quad \dot{z} = X(z)\,. \tag{4}$$

The phase flow corresponding to (4) is denoted φ^h. That is, φ^h is a map $\mathscr{P} \to \mathscr{P}$, depending on the time step length h, such that $\varphi^h(q(t), \dot{q}(t), t) = (q(t+h), \dot{q}(t+h), t+h)$.

2.2. Estimated frequencies

Our next objective is to estimate the frequencies, or time scales, in the system due to A and B. In order to do so we consider a simplified model of a ball bearing, see Figure 1.

We begin with typical frequencies due to contact forces, i.e., due to A. The stiffness in a steel–steel contact (e.g. between a ball and the outer ring) is typically about $k = 10^8\,\mathrm{N/m}$. The damping and friction forces are small, so we neglect them in this simple analysis. The mass of a ball is about $m = 0.01\,\mathrm{kg}$. Thus, a typical translational frequency is about $(\sqrt{k/m})/(2\pi) \approx 1.6 \cdot 10^4\,\mathrm{Hz}$. The smallest moment of inertia of the outer ring is about $J = 3 \cdot 10^{-5}\,\mathrm{kg \cdot m^2}$ and its radius about $3 \cdot 10^{-2}\,\mathrm{m}$. This gives a typical rotational frequency of about $5 \cdot 10^4\,\mathrm{Hz}$. From experience with the BEAST software, using a standard implicit ODE solver, it is known that the time step length, for bearings like in Figure 1, typically is about $10^{-6}\,\mathrm{s}$. This time step is small enough to fully capture the dynamics of A.

In order to get an accurate result, the stiffness (and damping) of the constraint forces must be set much higher than the stiffness of the "real physical" forces. From our point of view, it means that the time scales of B must be much smaller than those of A. For the bearing case described it is suitable to choose the stiffness and damping of the penalty forces so that the frequencies of B are about $10^7\,\mathrm{Hz}$. As the time step $10^{-6}\,\mathrm{s}$ is not small enough to resolve such frequencies, it is essential to use an implicit integrator.

3. Integrator algorithm

From the previous section it is clear that the governing equations are stiff due to constraint forces, so for the time step lengths we have in mind an implicit integrator is needed in order to achieve stability. From an efficiency point of view, an implicit integrator is, per time step, more expensive than an explicit dito, because at each step a non–linear root finding problem needs to be solved iteratively. In particular, this implies that A and B are evaluated several times per time step. Furthermore, the Jacobian needs to be computed for an implicit method (which is severely expensive for A in our case), as it is used by the root finding algorithm (typically some variant of Newton's method).

The frequency analysis of the previous section indicates that the dynamics of A can be resolved accuratelly with an explicit integrator for the time step lengths we have in mind. However, it is not so for B. One possibility is of course to choose a much smaller time step, but that would be inefficient, as to many time steps are needed.

Our approach is to treat A explicitly and B implicitly. The notion is that B is "responsible" for the stiff character of the system, so in order to have stability for long time steps it is enough if only this part is handled implicitly. The idea is that the number of evaluations of A should be on par with that of explicit methods, whereas B can be evaluted more frequently without any significant increase in the computational cost.

An obvious possibility is to use so called splitting methods (see [MQ02]). That is, to consider an explicit method Φ_h^A for the equation $\ddot{\boldsymbol{q}} = A(\boldsymbol{q}, \dot{\boldsymbol{q}}, t)$ and an implicit method Φ_h^B for $\ddot{\boldsymbol{q}} = B(\boldsymbol{q}, \dot{\boldsymbol{q}}, t)$, and then utilized a composition of the two methods, e.g. $\Phi_h^A \circ \Phi_h^B$ or $\Phi_{h/2}^B \circ \Phi_h^A \circ \Phi_{h/2}^B$. However, this approach is not so good in our case. Indeed, as Φ_h^A does not take constraint forces into account, the solution would at each step drift away a little from the constraint manifold, and then be "forced back" towards it by Φ_h^B. As Φ_h^B does not exactly project onto the constraint manifold, high frequency $\mathcal{O}(h)$ oscillations would thus appear in the solution.

We suggest the following discretization of the governing equations (4)

$$\begin{aligned} \boldsymbol{q}_{n+1} &= \boldsymbol{q}_n + h\dot{\boldsymbol{q}}_n + \frac{h^2}{2}\Big(A_{n+\alpha} + B_{n+\beta}\Big) \\ \dot{\boldsymbol{q}}_{n+1} &= \dot{\boldsymbol{q}}_n + h\Big(A_{n+\alpha} + B_{n+\beta}\Big) \\ t_{n+1} &= t_n + h\,, \end{aligned} \tag{5}$$

where $\alpha, \beta \in [0, 1]$ are method parameters and

$$\begin{aligned} A_{n+\alpha} &= A(\boldsymbol{q}_n + h\alpha\dot{\boldsymbol{q}}_n, \dot{\boldsymbol{q}}_n, t_n + \alpha h) \\ B_{n+\beta} &= B\big((1-\beta)\boldsymbol{z}_n + \beta\boldsymbol{z}_{n+1}\big)\,, \quad \boldsymbol{z}_n = (\boldsymbol{q}_n, \dot{\boldsymbol{q}}_n, t_n)\,. \end{aligned}$$

Notice that $A_{n+\alpha}$ is independent of $\boldsymbol{q}_{n+1}$ and $\dot{\boldsymbol{q}}_{n+1}$ for all α. Thus, it only needs to be evaluated once per time step, and the Jacobian of A is not needed. This is what we mean by "treating A explicitly".

The method (5) is a blend of the Störmer–Verlet method, the explicit Euler method, and the implicit midpoint rule. The correspondence is as follows.

Condition	**Method**
$B = 0$, $\alpha = 1/2$, and A independent of $\dot{\boldsymbol{q}}$	Störmer–Verlet
$B = 0$ and A independent of $\boldsymbol{q}$	explicit Euler (for the $\dot{\boldsymbol{q}}$ part)
$A = 0$ and $\beta = 1/2$	implicit midpoint rule

4. Consistency and linear stability analysis

In this section we analyse the order of consistency and the linear stability of the proposed method (5). We begin with the consistency analysis. Next, the stability analysis, which is split into two parts. First the explicit component of the algorithm is analysed separately, i.e. the case $B = 0$. Based on these results, stability of the full algorithm, with constraint forces present, is thereafter analysed.

4.1. Order of consistency

Let $\Phi_h : \mathscr{P} \to \mathscr{P}$ be the numerical flow of (5), i.e., the map defined by

$$\Phi_h(\boldsymbol{q}_n, \dot{\boldsymbol{q}}_n, t_n) = (\boldsymbol{q}_{n+1}, \dot{\boldsymbol{q}}_{n+1}, t_{n+1}) .$$

The local error map is given by $E_h = \Phi_h - \varphi^h$. Consistency of Φ_h with respect to φ^h means that $E_h(\boldsymbol{z}) = \mathcal{O}(h^2)$ as $h \to 0$ for all $\boldsymbol{z} \in \mathscr{P}$. Concering the principle term of E_h we have the following result:

Lemma 1. *The $\boldsymbol{q}$, $\dot{\boldsymbol{q}}$ and t components of the local error map E_h fulfills*

$$E_h(\boldsymbol{z}) = \begin{pmatrix} \frac{1}{6}h^3\Big((3\alpha-1)\big(\partial_q A(\boldsymbol{z})\dot{\boldsymbol{q}} + \partial_t A(\boldsymbol{z})\big) - \partial_{\dot{q}} A(\boldsymbol{z})C(\boldsymbol{z}) + (3\beta-1)\partial_z B(\boldsymbol{z})X(\boldsymbol{z})\Big) + \mathcal{O}(h^4) \\ \frac{1}{2}h^2\Big((2\alpha-1)\big(\partial_q A(\boldsymbol{z})\dot{\boldsymbol{q}} + \partial_t A(\boldsymbol{z})\big) - \partial_{\dot{q}} A(\boldsymbol{z})C(\boldsymbol{z}) + (2\beta-1)\partial_z B(\boldsymbol{z})X(\boldsymbol{z})\Big) + \mathcal{O}(h^3) \\ 0 \end{pmatrix} .$$

Proof. Compare Taylor expansions in h of $\Phi_h(\boldsymbol{z})$ and $\varphi^h(\boldsymbol{z})$. □

Using the lemma we immediatelly obtain the following result:

Theorem 2. *The method Φ_h, defined by* (5)*, has the following order of consistency properties.*

- *It is consistent for all α, β.*
- *It is second order accurate in position variables $\boldsymbol{q}$ for all α, β.*
- *If $\alpha = \beta = 1/2$ and A is independent of $\dot{\boldsymbol{q}}$, then it is second order accurate in all variables.*

Remark. In our application, the friction and damping in the contacts are very small in comparison to the stiffness. That is, $||\partial_{\dot{q}} A(\boldsymbol{z})||$ is small in comparison to $||\partial_q A(\boldsymbol{z})||$. Thus, we have "almost" second order accuracy for $\alpha = \beta = 1/2$.

4.2. Stability analysis when $B = 0$

In absence of constraint forces, i.e., when $B = 0$, the method Φ_h is fully explicit. Thus, it has a bounded stability region in terms of the step size h. We carry out a linear stability analysis for the scalar test equation given by

$$\ddot{q} = A(q, \dot{q}) = -kq - c\dot{q} , \qquad k, c \in \mathbb{R} . \tag{6}$$

Recall that stability of the method Φ_h means that $\lim_{n\to\infty} \Phi_h^n(\boldsymbol{z})$ is bounded. The result is as follows.

Theorem 3. *The stability region of the method* (5) *applied to* (6) *(with $B = 0$) is given by*

$$\Omega = \Big\{(hc, h^2k) \in \mathbb{R}^2 \setminus \{(0,0), (2-4\alpha, 4)\} \; ; \; h^2k \geq 0, hc \leq 2 - \alpha h^2 k, hc \geq (1/2 - \alpha)h^2 k\Big\} . \tag{7}$$

See Figure 2 for an illustration.

Proof. The numerical flow map Φ_h is linear for the test equation (6), i.e., it can be written

$$\Phi_h(q,\dot{q}) = R\begin{pmatrix} q \\ \dot{q} \end{pmatrix}, \qquad \text{with} \quad R = R(h,k,c) \in \mathbb{R}^{2\times 2}. \tag{8}$$

Thus, $\lim_{n\to\infty} \Phi_h^n(q,\dot{q}) = \lim_{n\to\infty} R^n \begin{pmatrix} q \\ \dot{q} \end{pmatrix}$. This expression is bounded for all $(q,\dot{q})$ if and only if the eigenvalues of R satisfy the root condition, i.e., they lie on or within the unit circle and if on the unit circle they are simple. Written out, the characteristic equation $\det(R - \mathrm{Id}\lambda) = 0$ is

$$1 - hc + \frac{1}{2}h^2k(1-2\alpha) - \left(2 - hc - \frac{1}{2}h^2k(1+2\alpha)\right)\lambda + \lambda^2 = 0. \tag{9}$$

The solutions, i.e., the two eigenvalues, are

$$\lambda_\pm = 1 - \frac{hc}{2} - \frac{h^2k(1+2\alpha)}{4} \pm \frac{1}{4}\sqrt{\left(2hc + h^2k(1+2\alpha)\right)^2 - 16h^2k}. \tag{10}$$

The eigenvalues are equal (non-simple) and lie on the unit circle for $(hc, h^2k) \subset \{(0,0),(2-4\alpha,4)\}$. They are unequal (simple) and and one of them lie on the unit circle at $\partial\overline{\Omega}\setminus\{(0,0),(2-4\alpha,4)\}$. Furthermore, inside Ω they are both strictly inside the unit circle, and outside Ω at least one of them is strictly outside the unit circle. □

From (10) in the proof of Theorem 3 we get the following result, which is a discrete analog to what is known as critical damping.

Corollary 4. *The numerical solution is oscillatory in*

$$\Omega^{osc} = \left\{(hc, h^2k) \in \Omega;\ hc < 2h\sqrt{k} - \frac{1}{2}h^2k(1+2\alpha)\right\}$$

and non-oscillatory in $\Omega \setminus \Omega^{osc}$. *See Figure 2 for an illustration.*

Remark. The oscillation condition (critical damping) for the exact flow φ^h of (6) is given by

$$\omega^{osc} = \left\{(hc, h^2k);\ hc < 2h\sqrt{k}\right\}.$$

Notice that for $\alpha > -1/2$ we always have $\Omega^{osc} \subset \omega^{osc}$. This means that critical damping in the numerical flow is "reached too fast" as c is increased from zero. Curiously, the choice $\alpha = -1/2$ gives exactly the correct critical damping.

4.3. Full stability analysis

We now extend the analysis to the linear test equation

$$\ddot{q} = A(q,\dot{q}) + B(q,\dot{q}) = -k_A q - c_A\dot{q} - k_B q - c_B\dot{q}, \tag{11}$$

with $A(q,\dot{q}) = -k_A q - c_A\dot{q}$ and $B(q,\dot{q}) = -k_B q - c_B\dot{q}$. This test equation is then discretized by the proposed scheme (5). Again, the numerical flow map is linear, i.e.,

$$\Phi_h(q,\dot{q}) = S\begin{pmatrix} q \\ \dot{q} \end{pmatrix}, \qquad \text{with} \quad S = S(h,k_A,c_A,k_B,c_B) \in \mathbb{R}^{2\times 2}. \tag{12}$$

Hence, our objective is to study the magnitude of the eigenvalues of the matrix S. The following result connects the stability analysis carried out in the previous section (the case $B = 0$) to the current case.

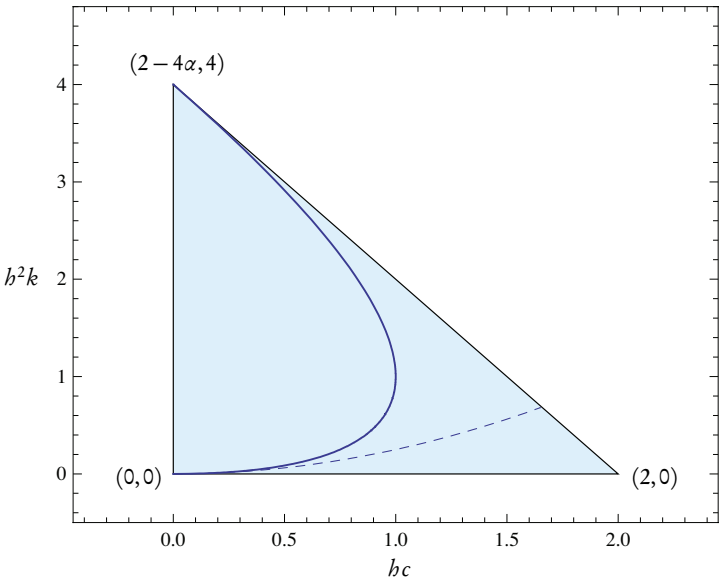

Figure 2: Stability region of the method (5) applied to (6) illustrated in the (hc, h^2k)–plane. The region is triangular, with corners marked. The full drawn curve within the region gives the "critical damping" condition, i.e., to the left of this curve the numerical solution is oscillatory and to the right it is non–oscillatory. The dashed curve gives the critical damping condition of the exact flow.

4. Consistency and linear stability analysis

Lemma 5. *The transformation*

$$hc \quad \longleftrightarrow \quad \frac{2h(c_A + c_B)}{2 + 2\beta hc_B + \beta h^2 k_B} \tag{13a}$$

$$h^2 k \quad \longleftrightarrow \quad \frac{2h^2(k_A + k_B)}{2 + 2\beta hc_B + \beta h^2 k_B} \tag{13b}$$

$$\alpha \quad \longleftrightarrow \quad \frac{\alpha h^2 k_A + \beta h^2 k_B}{h^2 k_A + h^2 k_B} \tag{13c}$$

takes the characteristic equation (9) *into the characteristic equation* $\det(S - \mathrm{Id}\lambda) = 0$.

Proof. Substitute (hc, h^2k, α) in (9) by the transformation (13). The resulting equation coincides with the characteristic equation $\det(S - \mathrm{Id}\lambda) = 0$. □

From Theorem 3 we know for which (hc, h^2k, α) the eigenvalues of R in (8) fulfill the root condition. Thus, using Lemma 5, we can investigate the root condition for the eigenvalues of S in (12). The following result, which asserts that the stability of the "explicit part" is not affected by the "implicit part", is then obtained:

Theorem 6. *For $\beta \geq 1/2$ the method* (5) *applied to* (11) *is stable for all $k_B, c_B \geq 0$ if $(hc_A, h^2k_A) \in \Omega$.*

Proof. From Theorem 3 it follows that the root condition is fulfilled for the roots of (9) if

(i) $h^2k \geq 0$,

(ii) $hc + \alpha h^2 k \leq 2$,

(iii) $(1/2 - \alpha)h^2k - hc \leq 0$.

Using Lemma 5, the root condition for the roots of $\det(S - \mathrm{Id}\lambda) = 0$ are fulfilled if the conditions obtained by substituting (13) in (i)–(iii) are fulfilled. Thus, our objective is to investigate (i)–(iii) after the substitution (13).

(i) Trivial because (13b) is always non-negative, so the condition is always true.

(ii) After substitution the condition becomes

$$\frac{2hc_A + 2\alpha h^2 k_A + 2hc_B + 2\beta h^2 k_B}{2 + 2\beta hc_B + \beta h^2 k_B} \leq 2 .$$

For $\beta \geq 1/2$ the left hand side is a decreasing function of both c_B and k_B. Thus, the left hand side is maximal when $c_B = k_B = 0$, which corresponds to the case $B = 0$.

(iii) After substitution the condition becomes

$$\frac{h^2 k_A(1 - 2\alpha) - 2hc_A + h^2 k_B(1 - 2\beta) - 2hc_B}{2 + 2\beta hc_B + \beta h^2 k_B} \leq 0 .$$

Again, for $\beta \geq 1/2$ the left hand side is a decreasing function of both c_B and k_B, and the maximum at $c_B = k_B = 0$ corresponds to the case $B = 0$. □

Remark. The stability result in Theorem 6 is the best possible, because for $B = 0$ it replicates Theorem 3, and for $A = 0$ it gives unconditional stability (cooresponding exactly to the classical θ–method with $\theta = \beta$).

5. Adaptivity

In order to increase the efficiency of the integration process it is important to introduce adaptive time stepping. There are various ways of doing this. It is out of scope of this paper to discuss any of them in full detail, but we mention two techniques.

The classical approach is to estimate the local error l^{err} at each time step, and then to consider the control objective $l^{err} \approx tol$ for some user specified tolerance level tol, see [Söd02, Söd03] for details.

Another approach, which is typically used in conjunction with geometric integration, is to introduce a Sundman transformation of the governing equations, which is a dynamic time transformation. Let s be a strictly positive real valued function on the phase space $\mathscr{P}$, called a scaling function, and introduce a new independent variable τ defined dynamically by $\mathrm{d}/\mathrm{d}\tau = s(\boldsymbol{z})\,\mathrm{d}/\mathrm{d}t$. The governing equations (4) then transform into

$$\frac{\mathrm{d}\boldsymbol{z}}{\mathrm{d}\tau} = s(\boldsymbol{z})X(\boldsymbol{z})\,. \tag{14}$$

Solutions to (14) correspond to time stretched solutions of (4). Thus, equidistant steps ε in the τ–domain correspond to variable steps $h = h(\boldsymbol{z}) = s(\boldsymbol{z})\varepsilon$ in the physical time domain. The easiest way to use this approach in conjunction with the proposed method (5) is to set $h = s(\boldsymbol{z}_n)\varepsilon$ at each step $n \to n+1$. For other, more intricate, techniques that also conserve the geometric properties of the flow (e.g. energy for conservative systems), see [MF06, HS05, HLW06].

5.1. Choice of control objective

As mentioned above, in classical ODE solvers the local error is estimated at each time step and is used as step size control objective. We suggest another choice based instead on the stability condition.

In Section 4 we found that for A only dependent on $\boldsymbol{q}$ and t (i.e. no damping), the linear stability condition is $h^2\sigma(\partial A(\boldsymbol{z})/\partial \boldsymbol{q}) \leq 4$. Thus, if an estimate $\sigma^{est} \approx \sigma(\partial_{\boldsymbol{q}} A(\boldsymbol{z}))$ is available, then a feasible step size control objective is $h^2\sigma^{est} \approx tol \leq 4$.

For the proposed algorithm (5), an estimate of $h\alpha\partial_{\boldsymbol{q}} A(\boldsymbol{z}_n)\dot{\boldsymbol{q}}$ is given by $A_{n+\alpha} - A_n$. Thus, the quantity

$$\sigma^{est} = \frac{||A_{n+\alpha} - A_n||}{h\alpha||\dot{\boldsymbol{q}}||} \tag{15}$$

gives an estimate of the stiffness in the direction of the flow. Notice that (15) is a function of $\boldsymbol{z}_n$, i.e., $\sigma^{est} = \sigma^{est}(\boldsymbol{z})$ is a function on the phase space $\mathscr{P}$. Thus, the corresponding scaling function is given by $s(\boldsymbol{z}) = 1/\sqrt{\sigma^{est}(\boldsymbol{z})}$. Hence, the Sundman transformation technique (14) may be used in conjunction with this control objective. Furthermore, from Lemma 1 it is evident that for $\alpha \neq 1/2$ this choice corresponds to keeping the principle relative local error term constant for velocity variables.

6. Numerical examples

In this section we present numerical examples of the proposed algorithm (5) applied to: (1) a simple linear problem consisting of two harmonic oscillators; (2) a non-linear pendulum problem in Cartesian coordinates; and (3) a complex multibody ball bearing problem. The last example is carried out in the multibody environment BEAST, where the method has been implemented.

6.1. Harmonic oscillators

The problem describes two particles, both with mass 1, moving on the real line. Between the two particles there is a linear spring with stiffness 10^3 and damping 10^2. One of the particles is attached to

a spring with stiffness 1 and no damping. The governing equations are

$$\ddot{q} = -\begin{pmatrix} 1 & 0 \\ 0 & 0 \end{pmatrix} q - 10^3 \begin{pmatrix} 1 & -1 \\ -1 & 1 \end{pmatrix} q - 10^2 \begin{pmatrix} 1 & -1 \\ -1 & 1 \end{pmatrix} \dot{q} \,.$$

In terms of (3), we split the acceleration field so that the first term corresponds to $A(z)$, and the two last terms to $B(z)$. Thus, A corresponds to the weak spring, and B to the stiff spring "constraining" the two particles to stick together. We are interested in resolving the dynamics in A, but not that in B. The frequencies in the system are $1/(4\pi)$ Hz (due to the weak spring) and $(1/\pi) \cdot 10^3$ Hz (due to the stiff spring). As initial data we choose $q_0 = (1.0, 1.1)$ and $\dot{q}_0 = (0, 0)$.

Numerical simulation with the method (5) is carried out for the constant step size $h = 1$, and method parameters $\alpha = 1/2$ and $\beta = 0.8$. A comparison is given with the classical θ–method, with $\theta = 1/2$ and $\theta = 0.8$. This method is fully implicit in both A and B, and thus requires many more evaluations of A (which we "pretend" to be expensive).

The results in Figure 3 show that, although the θ–method is more expensive per time step, it is less accurate. This is due to the fact that $\alpha = 1/2$ corresponds to a symplectic integrator for the A–part (the explicit part), which is known to have superior accuracy for conservative systems. The θ–method with $\theta = 1/2$ (i.e. the implicit midpoint rule) is also symplectic, but with this choice the highly oscillatory dynamics is not damped out correctly.

6.2. Non-linear pendulum

The problem is a pendulum expressed in Cartesian coordinates $q = (q^x, q^y)$. The length and mass of the pendulum is 1. Thus, a constraint is given by $||q||^2 - 1 = 0$. This constraint is modeled by as stiff spring. The governing equations are

$$\ddot{q} = g - 10^4(||q||^2 - 1)q \,,$$

where the gravity is given by $g = (0, -1)$. We choose A as the first term and B as the second term.

Initial conditions are given by $q_0 = (1.01, 0)$ and $\dot{q}_0 = (0, 0)$. Numerical simulation is carried out for the constant step size $h = 0.01$, and method parameters $\alpha = 1/2$ and $\beta = 0.6$. A comparison is given with the θ–method, with $\theta = 1/2$ and $\theta = 0.6$.

The plots in Figure 4 show the error in the variable q^x. It is small for the $\theta = 1/2$ method, but the solution there contains high oscillations due to the constraint forces, which are not damped out correctly (as in the previous example). Figure 5 shows the constraint error, i.e., the quantity $||q||^2 - 1$. Furthermore, these small oscillations cause the Newton solver to require significantly more iterations, which means more evaluations of A (which we pretend to be expensive).

6.3. Complex ball bearing

This example consists of the ball bearing model illustrated in Figure 1. The outer ring is held fixed, and the inner ring is rotated with 10^4 revolutions per minute. Further, the inner ring is loaded axially with a constant force of 10^3 N.

Simulations of the system is carried out within the software package BEAST with: (i) the proposed integrator with $\alpha = 1/2$, $\beta = 0.8$ and constant step size $h = 10^{-6}$ s; (ii) a standard implicit BDF–solver with adaptive time steps (CVODE, see [Hin]). The plots in Figure 6 show: the contact forces between the first ball and the outer ring; between the first ball and the cage; and the angular velocity of the cage. The results are nearly identical. Since these variables are highly sensitive (especially contact forces on the cage) high similarity between the two simulations indicate that the accuracy is about the same.

Statistics from the two simulations are given in the table below.

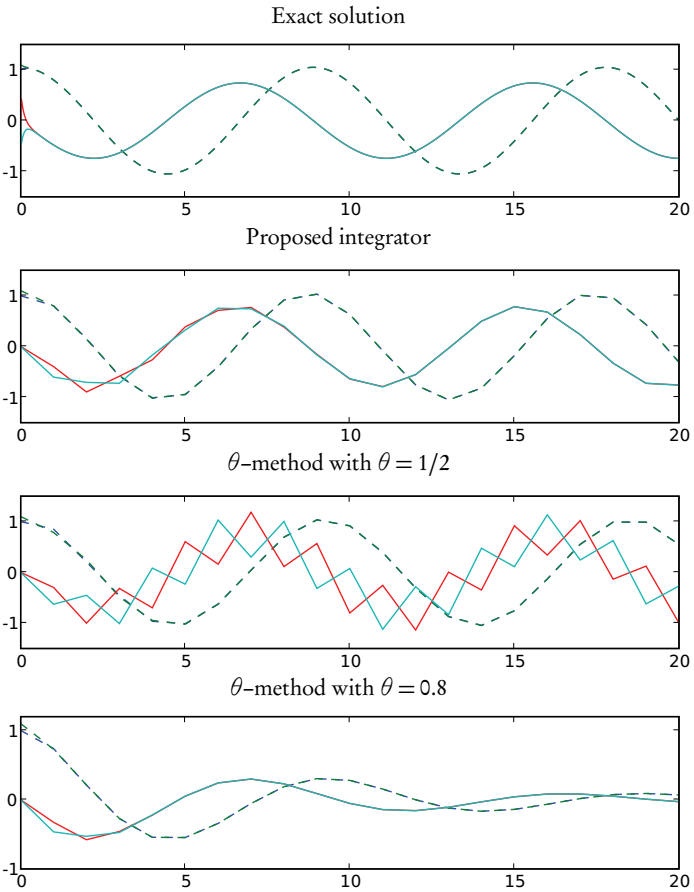

Figure 3: Numerical results for the test problem in Section 6.1. The full drawn curves are the position variables $\boldsymbol{q}$ and the dashed curves are the velocity variables $\dot{\boldsymbol{q}}$. The upper graph shows the exact solution. Notice that the θ method gives a less accurate result than the proposed method (both for $\theta = 1/2$ and $\theta = 0.8$), even though it is more expensive in terms of evaluations of A.

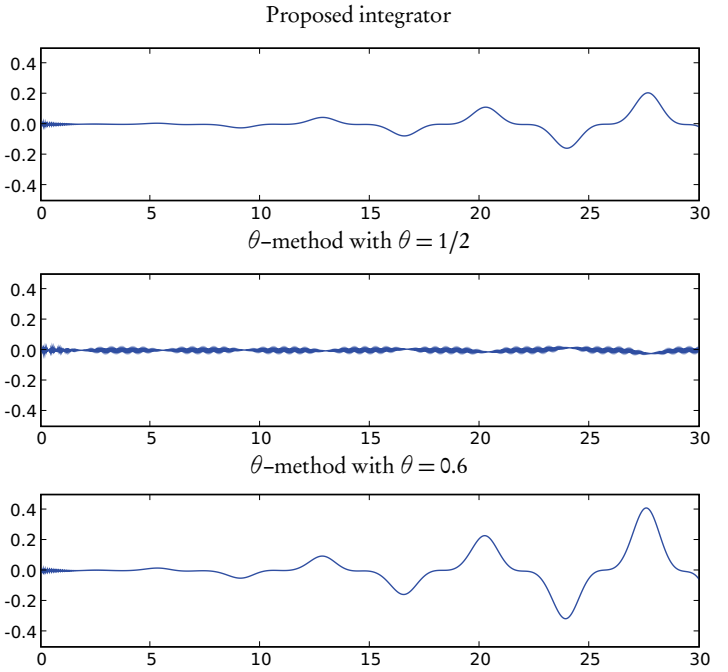

Figure 4: Numerical results for the test problem in Section 6.2. Global error in the q^x variable. Notice that, although the error is small for the $\theta = 1/2$ method, the solution is highly oscillatory.

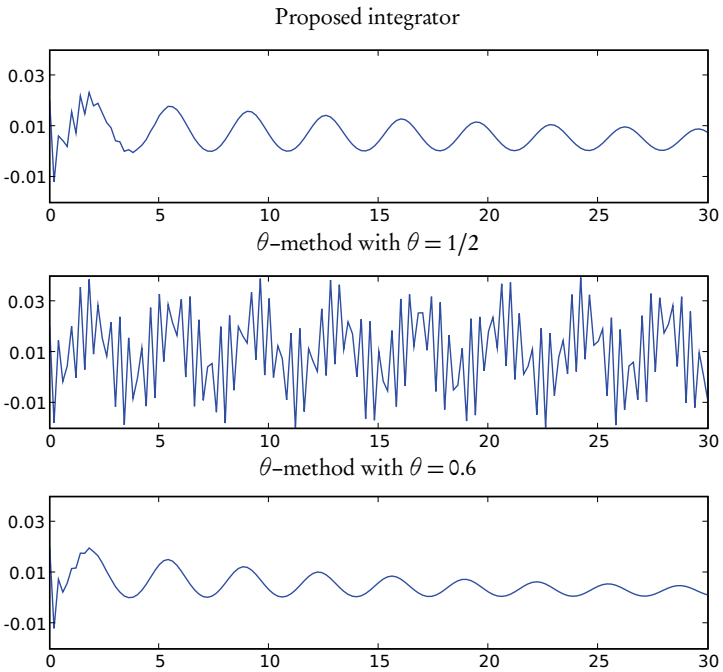

Figure 5: Numerical results for the test problem in Section 6.2. Error in the constraint $||q|| - 1$.

	mean h	force evaluations
BDF–solver	$6.8 \cdot 10^{-7}$ s	1588[1]
proposed method	$1 \cdot 10^{-6}$ s	600

Thus, we gain a factor of about $1588/600 \approx 2.6$ in efficiency. We estimate that the gain will increase if the proposed solver is implemented with adaptive time steps. Further, for rigid models a Jacobian evaluation is relatively cheap (12 force evaluations are needed). With flexible bodies it is much more expensive ($12+2n_f$ force evaluations with n_f number of flexible states), so the potential efficiency gain for models with flexible bodies is promising.

7. Conclusions

A new numerical integrator specifically designed for problems of the type described in Section 2 (e.g. multibody problems with contact forces between bodies) have been proposed. Contrary to standard methods for such problems, the proposed integrator requires only one evaluation of the contact forces per time step, and no contact Jacobians.

Consistency and stability analysis of the proposed integrator have been carried out, and a control objective for adaptive step size implementations has been proposed, based on the stability condition.

Numerical examples show that the proposed integrator is more efficient (in terms of number of contact force evaluations) in comparison with standard implicit integrators.

[1] 1288 force evaluations from iterations plus 25 Jacobian evaluations. Each Jacobian require 12 force evaluation, so in total $1288 + 25 \cdot 12 = 1588$.

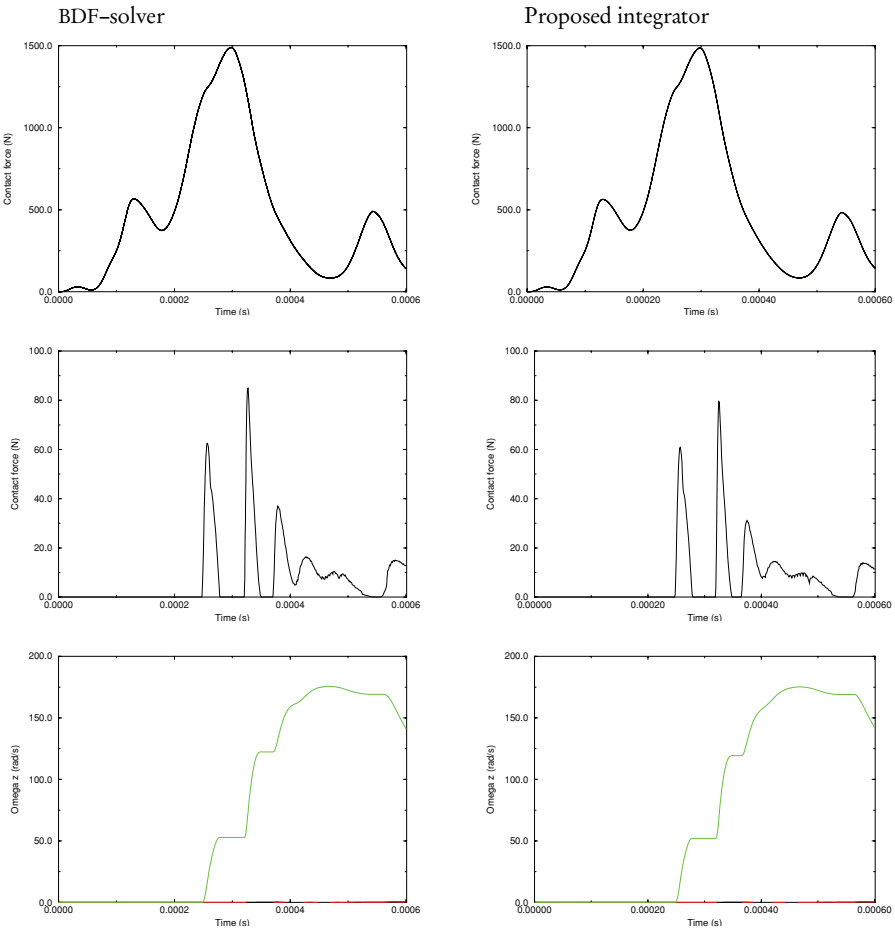

Figure 6: Numerical results for the test problem in Section 6.3. In the left column a standard adaptive BDF–solver is used. In the right column the proposed method is used. The first row is the contact force between one of the balls and the outer ring. The second row is the contact force between one of the balls and the cage. The third row is the angular velocity of the cage.

References

[Hin] A. Hindmarsh. *CVODE open-source software*. `www.llnl.gov/CASC/sundials/`.

[HLW06] Ernst Hairer, Christian Lubich, and Gerhard Wanner. *Geometric numerical integration*, volume 31 of *Springer Series in Computational Mathematics*. Springer-Verlag, Berlin, second edition, 2006. Structure-preserving algorithms for ordinary differential equations.

[HS05] Ernst Hairer and Gustaf Söderlind. Explicit, time reversible, adaptive step size control. *SIAM J. Sci. Comput.*, 26(6):1838–1851 (electronic), 2005.

[MF06] Klas Modin and Claus Führer. Time-step adaptivity in variational integrators with application to contact problems. *ZAMM Z. Angew. Math. Mech.*, 86(10):785–794, 2006.

[MQ02] Robert I. McLachlan and G. Reinout W. Quispel. Splitting methods. *Acta Numer.*, 11:341–434, 2002.

[Nak06] I. Nakhimovski. *Contributions to the Modeling and Simulation of Mechanical Systems with Detailed Contact Analyses*. PhD thesis, LinkÃűpings Universitet, LinkÃűping, 2006.

[SF01] L-E Stacke and D. Fritzson. Dynamical behaviour of rolling bearings: simulations and experiments. *Proc. Instn. Mech. Engrs.*, 215:499–508, 2001.

[Söd02] Gustaf Söderlind. Automatic control and adaptive time-stepping. *Numer. Algorithms*, 31(1-4):281–310, 2002. Numerical methods for ordinary differential equations (Auckland, 2001).

[Söd03] Gustaf Söderlind. Digital filters in adaptive time-stepping. *ACM Trans. Math. Software*, 29(1):1–26, 2003.